Dispersion relations and low – energy meson - meson interactions

Carrotte, John Brewster

DISPERSION RELATIONS AND LOW - ENERGY MESON - MESON INTERACTIONS

by

John Brewster Carrotte

A thesis presented for the degree of Doctor of Philosophy of the University of Durham

July 1972.

Mathematics Department
University of Durham

CONTENTS

CONTENTS

PREFACE

The work presented in this thesis was carried out in the Department of Mathematics at the University of Durham during the period October 1969 to July 1972, under the supervision of Dr. R.C. Johnson. The author wishes to express his sincere thanks to Dr. Johnson for his continual guidance, patience and encouragement at all stages of this research.

The work in this thesis has not been submitted for any degree in this or any other University. It is based essentially on one paper by the author, and two papers by the author in collaboration with Dr. R.C. Johnson, together with some unpublished work by the author. No claim of originality is made on chapter one. Chapter two contains work done by the author and Dr. R.C. Johnson. Most of chapters three, four, five and six are claimed to be original.

The author would like to thank Mrs. C. Kitching for her skilful typing of this thesis, and the Science Research Council for a Research Studentship.

ABSTRACT

This thesis deals with some general work on the use of inverse amplitude dispersion relations to describe low-energy $\pi\pi$ and πK scattering, and how the sub-threshold amplitudes may then be used to describe non-leptonic decays.

In chapter one we introduce the ideas which form the background to the structure of meson-meson scattering.

In chapter two we investigate a four parameter family of solutions to the $\pi\pi$ partial-wave dispersion relations using the inverse amplitude method assuming elastic unitarity. The S-waves have sub-threshold zeros consistent with the Adler condition and inelastic effects are estimated and found to be small below the rho-meson mass.

In chapter three we analytically continue the sub-threshold $\pi\pi$ amplitude found previously to fit the structure of the Dalitz plot in the non-leptonic decays $K \to 3\pi$ and $\eta \to 3\pi$.

In chapter four we review the unitary effective-range expansions which have been used to describe $\pi\pi$ scattering, and we examine a new unitary effective-range expansion which we use to describe the S-waves of πK scattering giving some estimate of the left-hand cut contributions to the amplitude.

In chapter five we extend these amplitudes by making a careful analysis of the left-hand cut and circle cut contributions to the π K partial-wave dispersion relations using the inverse amplitude method.

Finally in chapter six we investigate how the η and its

associated SU(3) generalization, the δ (962), fit into the overall picture we are able to conclude from our calculations.

CHAPTER 1.

INTRODUCTION

1.1 S-matrix approach

A complete knowledge of the S-matrix (1) is the ultimate aim of hadron physics. The S-matrix approach directly links theory and experiment; all experimental data is immediately related to the scattering matrix. In principle all the matrix elements should be obtainable from experiment, but in practice only those with two initial particles are directly accessible, when further the target is either a proton or a compound nucleus. The details of other interesting processes can be explored, however, by exploiting some of the general properties of the S-matrix. Current evidence suggests that S-matrix elements possess properties of analyticity, unitarity and crossing symmetry, and in this thesis we use these three principles (together with various physical assumptions and approximations) to study the low-energy interaction of the lightest pseudoscalar mesons:- pions and kaons.

The $\pi\pi$ and πK processes we study are, of course, not directly accessible to experiment. However, because they involve the lightest and simplest mesons which are freely produced in collisions and decays, they have an immediate and considerable effect on other processes which are directly measurable in detail. For example, the πK interaction plays an important role in processes involving kaons, such as KN scattering. The force of longest range comes from the exchange of a pion pair in the isotopic spin state $I = 0$ (2). Such an exchange takes place through the reaction.

$$\pi\pi \rightarrow K\bar{K} \rightarrow N\bar{N}. \qquad (1.1)$$

A knowledge of the $\pi\pi$, πK, and πN interactions is thus necessary to determine this process. Moreover their property of kinematical

simplicity makes $\pi\pi$ and πK systems well suited to the testing and development of dynamical ideas, free of complications.

In the rest of this chapter we briefly state the main ideas which will later be used in calculations and comparisons with experiments. This is terse and descriptive, with the detailed technicalities confined to a series of appendices. We conclude this introductory chapter with a discussion of the Veneziano model, which has had notable success in describing $\pi\pi$ and πK processes and with which we compare our results.

1.2 Kinematics

Appendix A sets out in detail the usual s,t,u kinematical variables which we use and defines notation, normalization, isospin crossing matrices, phase space factors etc. These results are entirely standard.

1.3 Experiments

Appendix B describes how we derive our knowledge of the amplitudes for $\pi\pi$ and πK scattering from high energy peripheral meson production using the ideas of Chew, Low and Goebel (3). Figure (1.1) is a diagrammatic representation of how we extract the $\pi\pi$ amplitudes, and figure (1.2) shows the "up-down" ambiguity in the phase shifts which results from the extrapolation procedure.

1.4 Rigorous constraints and sum rules

The $\pi\pi$ system was the first to which the considerations of unitarity and analyticity were applied (4), because it was recognized that this system has simple features, namely:

(i) Complete crossing symmetry.

(ii) Stability of the particles and absence of unphysical cuts

and anomalous thresholds due to the small mass of the pion.

Many people have since been searching for the solution to the problem of finding a class of functions A(s,t,u) compatible with crossing, analyticity and unitarity, and describing the $\pi\pi \to \pi\pi$ amplitude. In particular the main areas of research are:

(i) Finding the minimum input in addition to the above constraints to completely determine the low energy amplitude

(ii) Are current algebra constraints compatible with unitarity and if so what is their extrapolation to the resonance region?

Although a unique amplitude has not yet been found, the class of functions A(s,t,u) is severely restricted by the rigorous analyticity constraints developed by Martin et al. (5), and also by the crossing sum rules developed by Balachandran and Nuyts (6) and by Roskies (7). In appendix C we rederive some of the earlier constraints found by Jin and Martin (5) and also five of the crossing sum rules found by Roskies et al. (6-9).

1.5 Soft meson theory

Any model that predicts $\pi\pi$ and πK phase shifts from a dispersion relation has to be able to give some prediction for the subtraction term in the dispersion relation, which is usually the value of the amplitude at some point below threshold. The most successful models so far have been based on current algebra and the hypothesis of partially conserved axial-vector current (PCAC). These models give good predictions for the S-wave scattering lengths, and the amplitudes are analytic and crossing symmetric but not unitary. Because they are parameter free we rederive in appendix

D the models of Weinberg (10) and Griffith (11) for $\pi\pi$ and πK scattering respectively as their results will be used in later chapters. We also give there a simple derivation of one of the most powerful constraints on meson-meson scattering - the Adler consistency relations (12).

1.6 Veneziano model

The current algebra results depend on the idea of single meson dominance. It is now believed that there is a series of particles, equally spaced in $(\text{mass})^2$ with each spin and set of internal quantum numbers e.g. In addition to the ρ there should be ρ', ρ'' etc. This belief comes not from experiment (where the ρ' and ρ'' have not yet been observed) but from the widespread success in strong interaction phenomenology which has followed from the Veneziano model (15) which assumes the existence of linear Regge trajectories with equally spaced daughters. Thus instead of a factor

$$\frac{g1}{M_\rho^2 - S} \tag{1.2}$$

in calculations we should have something like

$$\frac{g1}{M_\rho^2 - S} \times \frac{g2}{M_{\rho'}^2 - S} \times \frac{g3}{M_{\rho''}^2 - S} \times \text{----} \tag{1.3}$$

which is equivalent to the use of the Γ function

$$\Gamma(1 - \alpha(s)) \tag{1.4}$$

where in the case we are considering $\alpha(s)$ is the ρ Regge trajectory. The Veneziano amplitude $V_{xy}(s,t)$ is defined by

$$V_{xy}(s,t) = \frac{\Gamma(1-\alpha_x(s))\ \Gamma(1-\alpha_y(t))}{\Gamma(1-\alpha_x(s)-\alpha_y(t))} \qquad (1.5)$$

The invariant amplitude A(s,t,u) for $\pi\pi$ scattering is given by

$$A(s,t,u) = \beta(V_{\rho\rho}(s,t) + V_{\rho\rho}(s,u) - V_{\rho\rho}(t,u)) \qquad (1.6)$$

and that for $\pi K \to \pi K$ is given by

$$A^{\pm}(s,t,u) = \gamma(V_{K^*\rho}(s,t) \pm V_{K^*\rho}(u,t)) \qquad (1.7)$$

where β and γ are normalization constants, $\alpha_\rho(s)$ is the exchange degenerate linear $\rho - f - A_2 - \omega$ trajectory, and $\alpha_{K^*}(s)$ is the exchange degenrate linear $K^*(890) - K^{**}(1420)$ trajectory.

If we now just consider the $\pi\pi \to \pi\pi$ amplitude then the single Veneziano term has many properties in agreement with current algebra (16).

(i) It satisfies the Adler consistency condition as equation (1.5) has a factor $\alpha_\rho(s) + \alpha_\rho(t) - 1$ and this is zero when

$$\alpha_\rho(\mu^2) = \tfrac{1}{2} \qquad (1.8)$$

which agrees with the phenomenological ρ Regge trajectory.

(ii) The Veneziano amplitude assumes the existence of an I = 0 S-wave resonance in $\pi\pi$ scattering (σ) and an I = $\frac{1}{2}$ S-wave resonance in $K\pi$ scattering (κ) as they are the first daughters of the ρ and $K^*(890)$ respectively. It predictsthe equality of the ρ and σ, and $K^*(890)$ and κ masses, and also the following relation for the ratio of the widths:

$$\frac{\Gamma(\rho)}{\Gamma(\sigma)} = \frac{2}{9} \qquad (1.9)$$

Both of these predictions are in agreement with current algebra (17).

(iii) The scattering lengths are within 10% of those predicted by Weinberg (10).

(iv) If we assume soft-kaon PCAC we get the obvious generalization of (1.8)

$$\alpha_{K^*}(m^2) = \tfrac{1}{2} \tag{1.10}$$

and we obtain the two SU(6) sum rules

$$m^2_{K^*} - m^2 = m^2_\rho - \mu^2 \tag{1.11}$$

$$m^2_{A_1} - m^2_\rho = m^2_\rho - \mu^2 \tag{1.12}$$

If $\mu = 0$ then (1.12) agrees with the deduction of Weinberg (17)

(v) When we take one of the external pions off mass-shell to a large positive mass, we consider the 3π decay of a particle withe the same quantum numbers as the pion. This will have the same Regge trajectory as $\pi\pi$ scattering so the Veneziano form can only differ by some overall constant. With a single Veneziano term we can then predict everything except the total decay rate. A single term expansion gives good fits to the $K \to 3\pi$ and $\eta \to 3\pi$ Dalitz plots. This is discussed further in chapter three.

The basic model as stated above is not unitary as all the poles appear as poles on the real axis. Since unitarity requires Regge trajectories to become complex above threshold the simplest phenomenological prescription has been to add imaginary parts to the α's above threshold and leave them unchanged below. However, not only does this introduce ancestors and violate crossing and unitarity, but it violates unitarity badly in that resonances such as the ρ and σ get equal widths although they have different couplings. Note also that as the I = 2 channel is exotic the I = 2 amplitude stays

real. Lovelace's K-matrix technique (18) partly overcomes these difficulties.

For a partial wave projection of the Veneziano formula V_l we write

$$A_l(s) = V_l(s) / (1 + \rho_l(s)\, V_l(s)) \qquad (1.13)$$

where $$\mathrm{Im}\rho_l(s) = -2k/\sqrt{s}. \qquad (1.14)$$

This form satisfies elastic unitarity and the poles move off the real axis with finite widths. Phase shifts may now be predicted for meson-meson scattering and figures (1.3) and (1.4) show the results for $\pi\pi \to \pi\pi$ and $\pi K \to \pi K$ processes. It can be seen that both S-waves favour the "~~down——up~~" "up - down" solution.

The above equations (1.13) and (1.14) do not put any constraint on $\mathrm{Re}\,\rho_l(s)$ and the equations as written above have lost their simple crossing symmetry at the expense of gaining elastic unitarity. Several models (19) have been proposed for $\mathrm{Re}\,\rho_l(s)$ giving it some analyticity on the left and right hand unitarity cuts, and using the crossing sum rules of Roskies (7) to regain crossing symmetry in some global sense. The resultant phase shifts are still in agreement with those of figures (1.3) and (1.4).

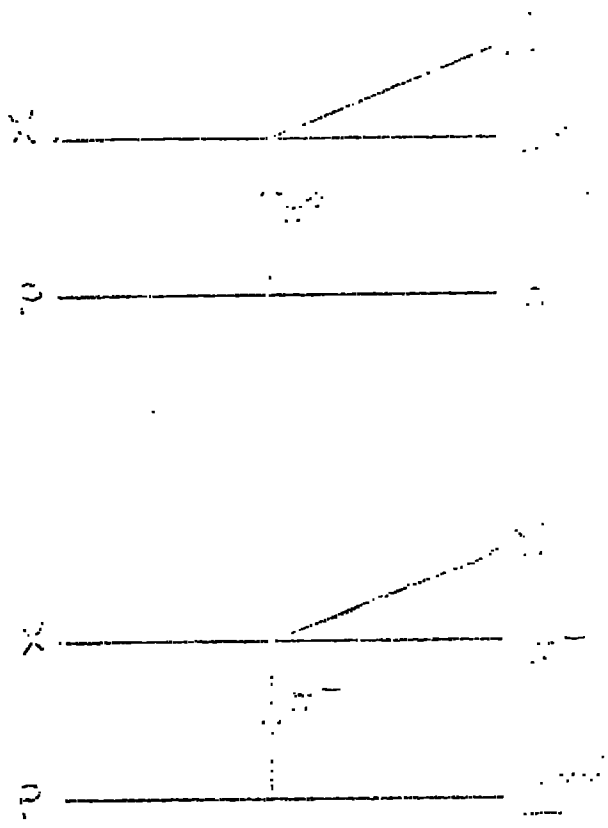

Fig. 1.1 Pion-exchange processes discussed in the text.

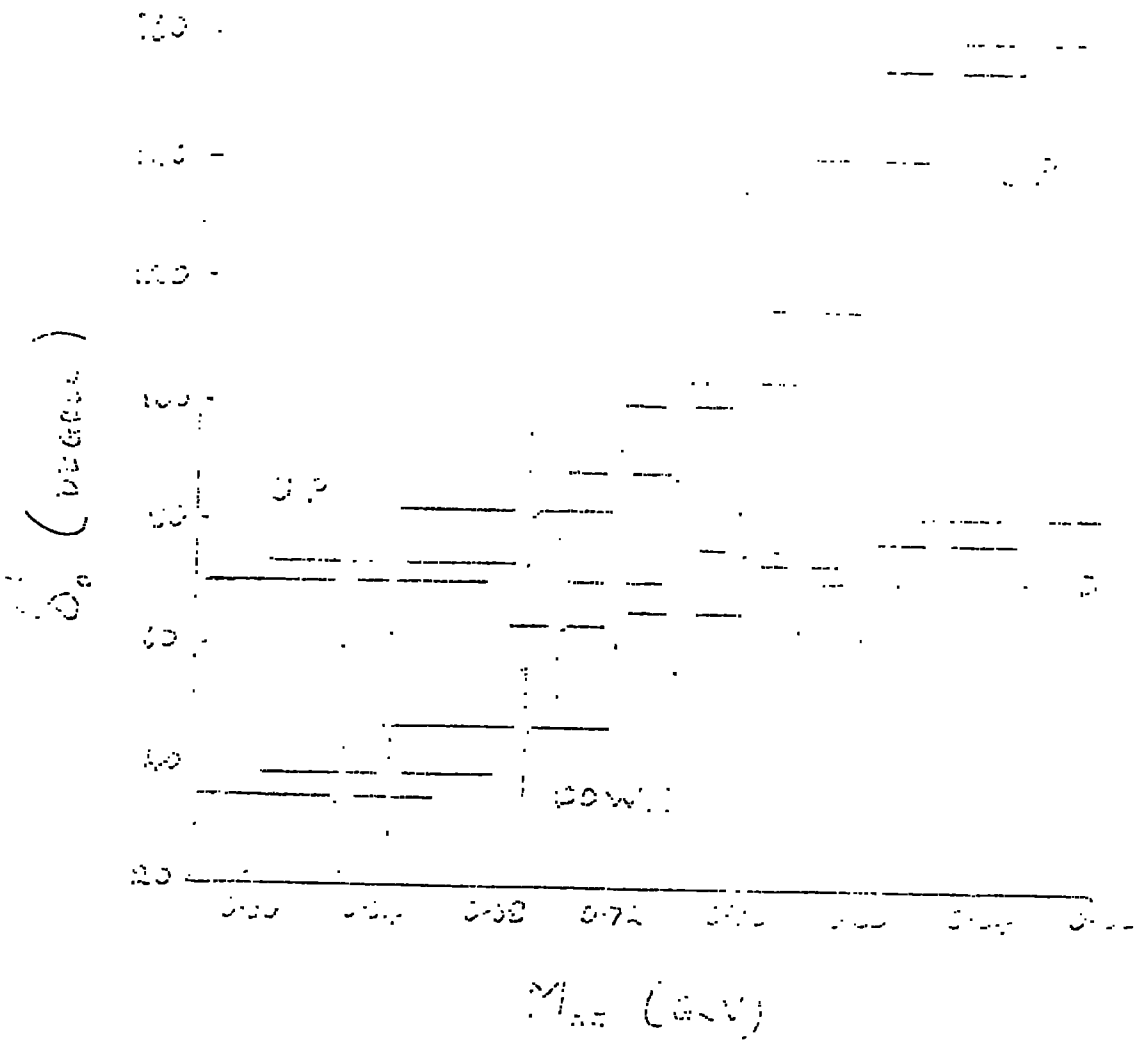

Fig. 1.2 Experimental I = 0 S-wave phase shifts showing the "up-down" ambiguity.

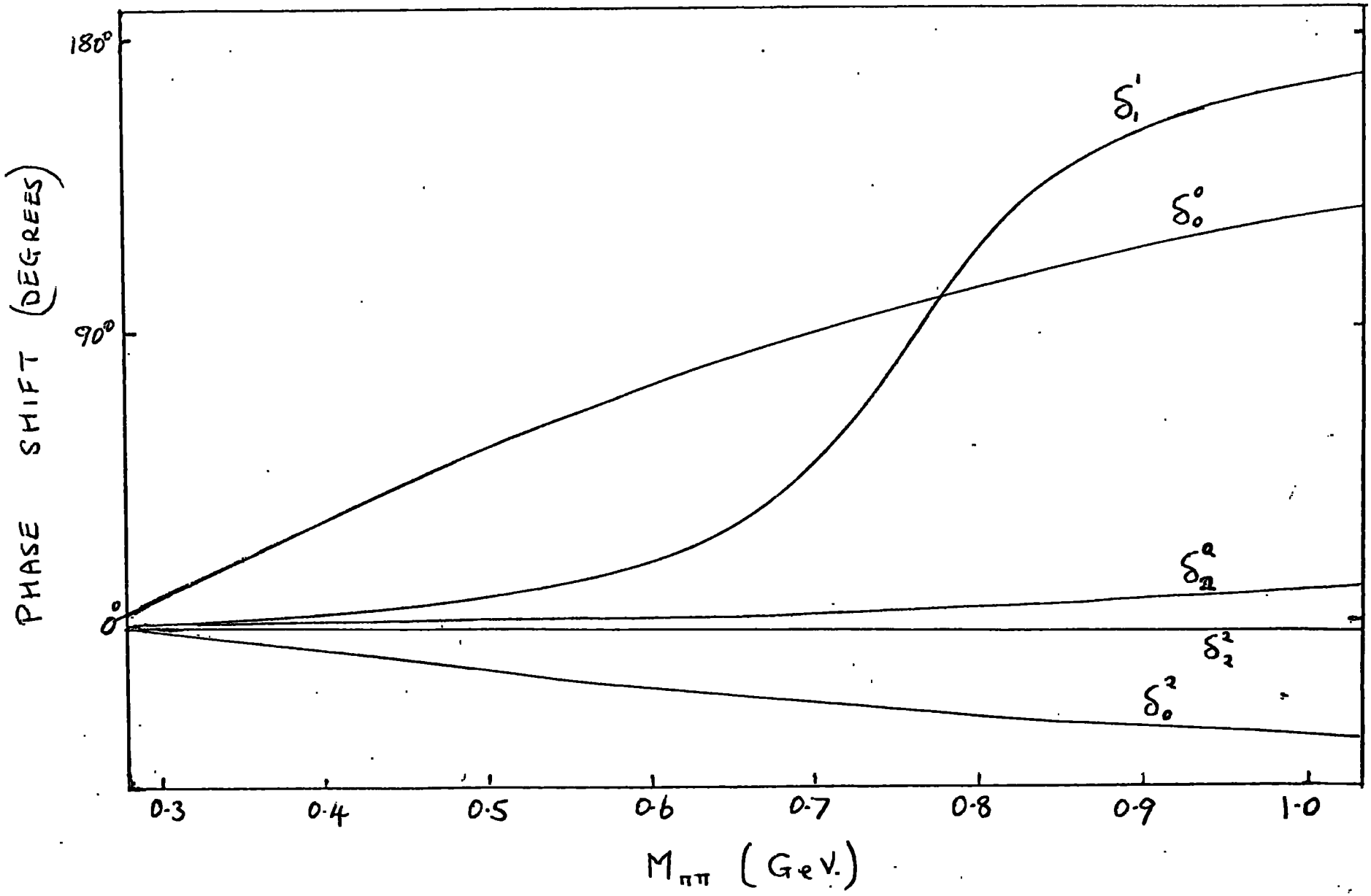

Fig. 1.3 $\pi\pi$ phase shifts predicted by a unitarized Veneziano theory.

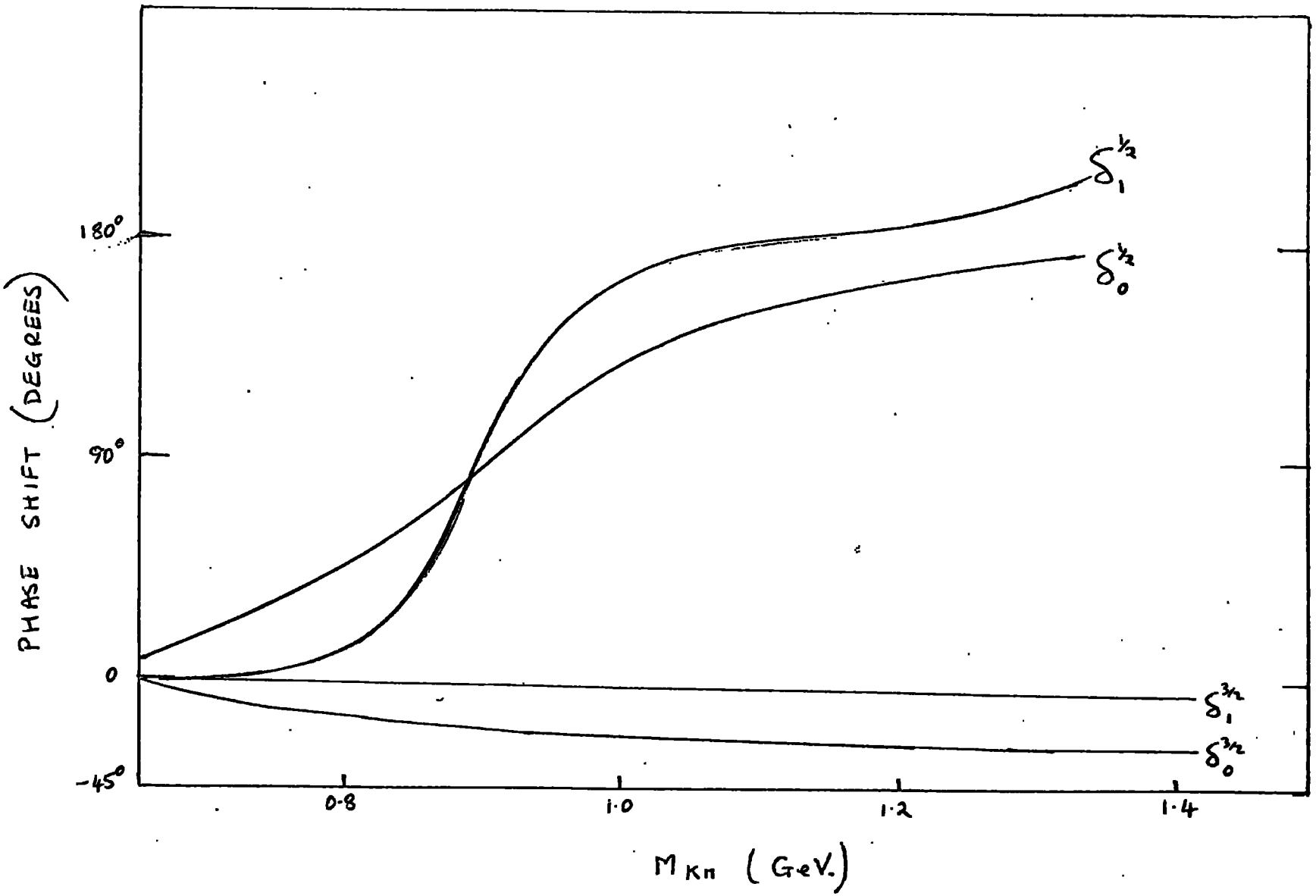

Fig. I.4 Kπ phase shifts predicted by a unitarized Veneziano theory.

CHAPTER 2

LOW-ENERGY $\pi\pi$ SCATTERING

2.1 Introduction

It is a common feature of all low-energy $\pi\pi$ models, which satisfy analyticity, unitarity and crossing symmetry (e.g. (20, 21)) and allow a resonating P-wave, that they give S-wave scattering lengths in close agreement with current algebra. In contrast the work of Atkinson and Kupsch (22) has shown us that there are on infinity of functions which satisfy the fundamental requirements, and so in principle we might expect to find models with wide ranges of values of S-wave scattering lengths. Dilley (23) has indeed found, using a parameterization that allows him to extend his amplitude above threshold (24), that there exists a large number of solutions for the $\pi\pi$ S-wave amplitude in the low energy region. (Similar results have also been found by Ader et al (25) for πK scattering). His solutions fall into two distinct classes:

(i) The S-wave dominant type originally studied by Chew, Mandelstam and Noyes (26) and which were found by them to give only a small P-wave amplitude.

(ii) The P-wave dominant type obtained by most axiomatic models. Within this class current algebra S-wave scattering lengths are favoured.

The relationship between $\pi\pi$ models which incorporate the existence of the rho-meson and those which incorporate current algebra input is explained by Dilley's results as his second class of S-wave amplitudes are characterised by having zeros below threshold. It is easy to see how this is related to the physical requirements of a resonating P-wave; for whilst the P-waves have kinematic zeros at threshold, the S-waves are in principle only bounded by unitarity which gives

$$\sqrt{s}/2k \geq \left| A_0^I(s) \right|^2 \qquad (2.1)$$

Thus we would expect the S-wave to dominate the whole scattering amplitude in the low energy region. However we know that if the S-waves do dominate we can have no rho resonance (26), but, of course, the converse is not obvious i.e. It may be possible to have large P-waves and large S-waves.

Since kinematics and unitarity alone do not allow the P-waves to dominate, we are forced to introduce dynamical zeros into these partial wave amplitudes in order to guarantee the existence of the Pennington and Pond (27) have shown that such zeros which must be present in physical $\pi\pi$ S-waves are identical with those implied by the Adler consistency condition.

Most of the results that favour the "up" solution above the ρ mass are of the type where a model for the total $\pi\pi$ mass spectrum is assumed as input to the calculation e.g., the Veneziano model input in the work of Tryon (28) and the Regge pole model with unitarity cuts of Moffat et al. (29). Their final amplitudes can be made to give current algebra scattering lengths, and satisfy all the constraint equations and crossing sum rules below threshold; however, it seems to us that one of the main objectives in scattering is to determine the mass spectrum in the energy region below 1 GeV., given only that the P-wave is ρ dominated, and D - and higher waves are small. Assuming the existence of the σ near the ρ will always generate phase shifts of the conventional Breit-Wigner "down-up" type, and thus these models loose a lot of their predictive power.

In this chapter we present a simple model for the $\pi\pi$ interaction

in the region $\sqrt{s} \leq 1$ GeV. (30), using inverse amplitude dispersion relations, and by not assuming any mass spectrum for the S-waves we are able to investigate the existence of the σ and its relationship with the ρ

The approach leads to a four parameter family of crossing-symmetric and unitary S-, P- and D- wave amplitudes. While the four parameters may be varied to study within a single framework the properties of a large class of models, in the present work we concentrate entirely on calculating amplitudes which on the one hand satisfy as closely as possible all the general theoretical constraints which have recently been discovered (e.g. (31)), and which on the other interpolate available experimental data to give a detailed picture of the low-energy region.

A central dynamical assumption is the existence of the ρ meson at its physical mass. Its width is (essentially) one of the available variable parameters. No attempt is made to explain (or bootstrap) this particle.

In addition there are four major physical approximations:

(i) only S-, P-, and D-waves contribute in the region of interest, $\sqrt{s} \leq 1$ GeV.

(ii) the S-wave scattering lengths are small.

(iii) elastic unitarity holds for $\sqrt{s} \leq 1$ GeV,

(iv) the left hand cuts of the partial-wave amplitudes can be estimated directly from the crossed-channel partial-wave series.

Of these, both (i) and (iii) appear to be supported by all analyses of peripheral pion production (20, 21). However, we cannot disregard the fact that through analyticity and crossing both

higher partial waves and absorptive effects in the region $\sqrt{s} \gtrsim 1$ GeV can influence significantly the lower waves in $\sqrt{s} \leq 1$ GeV. Such possibilities are considered in detail in the numerical calculations.

The approximation of small S-wave scattering length (ii) is perhaps the most restrictive. However, it is suggested by most current theoretical models (10, 23, 32), and indeed has positive experimental support, as we describe below. It should be noted, however, that in the original work of Weinberg we have the choice between saying that small scattering lengths imply the Weinberg linear expansion is valid, or vice versa, which was the way the model was originally proposed. This dichotomy has now been solved by recent experimental data.

The fourth approximation allows the use of crossing to close the calculational system of integral equations. It is equivalent to disregarding the presence of the third double spectral function, which is at least consistent with the ideas of exchange degeneracy (33). In practice, the partial-wave dispersion relations are subtracted and rapidly convergent, and hence insensitive to details of the distant left-hand cut. Our ignorance of this region is absorbed into subtraction constants.

The next section describes in detail the construction of the inverse amplitude dispersion relations for $\ell \leq 2$ (34), and describes how they are solved when subtraction constants and pole terms (amplitude zeros) are specified. This is the place where the four variable parameters enter, according to a subtraction scheme relying on assumption (ii) above - that the thresholds are weak.

The partial waves in the Mandelstam triangle (s, t, u all positive) are linked together by an approximate representation in terms of a crossing - symmetric quadratic polynomial expression, which parameterizes the subthreshold amplitudes in terms of four independent real coefficients. These may be taken to be the P-wave scattering length, the two S-wave scattering lengths, and the Chew-Mandelstam coupling constant (4). Choosing values of these quantities fixes the dispersion-relation subtraction constants, and determines the amplitude zeros (which lead to pole-terms).

Therefore, the output phase shifts are expressed through subtractions in terms of the ρ-meson mass and four low-energy parameters, and connected in a controllable and explicitly crossing-symmetric way to the size, shape and zero-structure of the subthreshold amplitudes.

The input parameters (including extra phenomenological inelastic terms, and higher partial waves) may be varied to seek satisfaction of detailed analyticity and crossing constraints, and to obtain agreement with various pieces of experimental information. In the process, the self-consistency of the model can be checked, (details are given in section 3).

The numerical results presented in section 4 show that there are solutions to the model which satisfy all but one of the desirable constraints and properties - this in itself is not trivial. Moreover, the range of possible acceptable solutions is quite narrow and agrees rather well with the results of related but substantially different approaches.

The principal feature of the results is the strong preference

for a resonant isoscalar S-wave - a super broad σ- with the phase shift choosing a down behaviour above the 90^0 position. This is true even when inelasticity (expected to be strong in this wave about 1 GeV.) is taken into account (see section 5).

2.2 Method

The first part of this section describesthe inverse-amplitude dispersion relations (34), and the second gives details of the polynomial amplitudes which tie them together.

A. Dispersion Relations.

The analytic properties of $A^I_\ell(s)$ in the s-plane are well known (4). Defining $B^I_\ell(s) = (A^I_\ell(s))^{-1}$, on the right-hand cut elastic unitarity reads

$$\text{Im } B^I_\ell(s) = -\rho(s) \tag{2.2}$$

where $\rho(s) = ((s-4\mu^2)/s)^{\frac{1}{2}}$. Then a dispersion relation for $B^I_\ell(s)$ may be written

$$B^I_\ell(s) = H(s) - H(s_0) + B^I_\ell(s_0) + L^I_\ell(s) + P^I_\ell(s) + R^I_\ell(s) \tag{2.3}$$

where a subtraction is made at $s = s_0$ (which may depend on I and ℓ).

The advantage of this expression is that from (2.2) the elastic right-hand cut contribution H can be evaluated once and for all in closed form independent of I and ℓ;

$$H(s) = \frac{1}{\pi}\int_{4\mu^2}^{\infty} \frac{-\rho(s')\,ds'}{(s'-s)}$$

$$= \frac{1}{\pi}\rho(s)\ln\left(\frac{\rho(s)+1}{\rho(s)-1}\right), \qquad s \geq 4\mu^2 \tag{2.4}$$

For $s \leq 4$ ^{2}, H is evaluated by encircling the branch-points anticlockwise.

Of the other terms in (2.3) $H(s_0)$ and $B(s_0)$ are subtraction constants, and the left-hand cut contribution is

$$L^I_\ell(s) = -\frac{(s-s_0)}{\pi} \int_{-\infty}^{0} \frac{\mathrm{Im} A^I_\ell(s')}{|A^I_\ell(s')|^2} \frac{ds'}{(s'-s)\ (s'-s_0)} \qquad (2.5)$$

Possible poles of $B^I_\ell(s)$ (zeros of A (s) are represented by $P^I_\ell(s)$, which for one simple pole at $s = s_p$, has the form

$$\frac{(s-s_0)\ c}{(s-s_p)\ (s_p-s_0)}$$

where $$c = \left[\frac{dA}{ds}(s) \Big|_{s=s_p} \right]^{-1}$$

The inelastic part of the right-hand cut contributes

$$R^I_\ell(s) = -\frac{(s-s_0)}{\pi} \int_{S_{in}}^{\infty} \frac{r^I_\ell(s')\ \rho(s')\ ds'}{(s'-s)\ (s'-s_0)} \qquad (2.6)$$

where $r^I_\ell(s)$ is the ratio of inelastic to elastic partial-wave cross - sections and from equations (A33) and (A34) is

$$r^I_\ell(s) = \frac{1-(\eta^I_\ell)^2}{|\eta^I_\ell \exp(2\delta^I_\ell) - 1|^2} \qquad (2.7)$$

with $\sqrt{s_{in}} \geq 1$ GeV (assumption (iii)).

There are fivepartial waves in the model, and the amplitudes are calculated interatively, as follows.

The first step is the specification of each value of so, $B^I_l(s_0)$, $P^I_l(s)$ and $R^I_l(s)$. Then with an initial choice of $L^I_l(s)$ (zero is convenient, but other choices lead to the same result) $B^I_l(s)$ may be calculated for s ranging from some left-hand cutoff $-\Lambda$ to a convenient right-hand point, ($\sqrt{s} \approx 1$ GeV), and $A^I_l(s)$ constructed by inversion.

Now a better approximation to the amplitude is calculated by using an estimate of $L^I_l(s)$ obtained from (2.5) by integrating over a left-hand discontinuity given by crossing (4) (assumption (iv)):

$$\mathrm{Im}\,A^I_l(s) = \frac{1}{4\mu^2-s}\int_{4\mu^2-s}^{4\mu^2} P_l\left(1+\frac{2t}{s-4\mu^2}\right)\sum_{I'=0}^{2}\beta_{II'}\sum_{l'=0}^{2}(2l'+1)\,P_{l'}\left(1+\frac{2s}{t-4\mu^2}\right)\mathrm{Im}\,A^{I'}_{l'}(t)\,dt$$

$$+(-1)^{I+I'}\frac{1}{4\mu^2-s}\int_{4\mu^2-s}^{4\mu^2} P_l\left(-1-\frac{2u}{s-4\mu^2}\right)\sum_{I'=0}^{2}\beta_{II'}\sum_{l'=0}^{2}(2l'+1)\,P_{l'}\left(-1-\frac{2s}{u-4\mu^2}\right)\mathrm{Im}\,A^{I'}_{l'}(u)\,du$$

We can combine these two expressions into one by noting that $P_l(-z) = (-1)^l P_l(z)$ and hence the second expression is equal to the first except for a factor $(-1)^{I+I'+l+l'}$ but as we have Bose statistics $I + l$ is even and hence we obtain

$$\mathrm{Im}\,A^I_l(s) = \frac{2}{4\mu^2-s}\int_{4\mu^2-s}^{4\mu^2} P_l\left(1+\frac{2t}{s-4\mu^2}\right)\sum_{I'=0}^{2}\beta_{II'}\sum_{l'=0}^{2}(2l'+1)\,P_{l'}\left(1+\frac{2s}{t-4\mu^2}\right)\mathrm{Im}\,A^{I'}_{l'}(t)\,dt \qquad (2.8)$$

The imaginary part of $A^I_l(s)$ for $s \geq 4\mu^2$ is needed in (2.8) and the real part of $A^I_l(s)$ for $s \leq 0$ is needed in (2.5); both are given by the previous estimates. The integral in (2.5) is cut off at $s = -\Lambda$, and for $s \leq -\Lambda$ we assume

$$\mathrm{Im}\,B^I_l(s) = \mathrm{Im}\,B^I_l(-\Lambda) \times (s/-\Lambda)^{\alpha} \qquad (2.9)$$

The results for the phase shifts for $s \leq 50\mu^2$ (where they are most likely to be reliable) are insensitive to the precise values

of Λ and α, provided $\alpha \leq 0$ and $\Lambda \geqslant 25$ [2]. For all the results quoted here $\alpha = 0$.

This straightforward iterative application of crossing symmetry is repeated until two successive cycles agree. Convergence is easy to prove, and in practice further changes are small after 4 or 5 cycles and neglible after about 10.

Thus by application of crossing, analyticity and unitarity (which is explicit at each stage) output amplitudes are produced depending on the chosen input values for s_0, $B^I_\ell(s_0)$, $P^I_\ell(s)$ and $R^I_\ell(s)$. This is where the approximate polynomial amplitudes are used.

B. Polynomial Amplitudes

It is convenient to use the standard Chew-Mandelstam invariant amplitude $A(s,t,u)$ symmetric under the interchange $t \leftrightarrow u$ and related to the s - channel isospin amplitudes by equations (A22 - 24)

$$\begin{aligned} A^0 &= 3A(s,t,u) + A(t,s,u) + A(u,s,t) \\ A^1 &= A(t,s,u) - A(u,s,t) \\ A^2 &= A(t,s,u) + A(u,s,t) \end{aligned} \qquad (2.10)$$

Neglecting the threshold branch points (assumption (ii)) and partial waves with $\ell \geqslant 2$ (assumption (i)), we may write quite generally

$$A(s,t,u) = a + b\,(t+u) + ctu + d(t+u)^2 \qquad (2.11)$$

This is an explicitly crossing-symmetric S-, P- and D-wave description of the $\pi\pi$ interaction at and below threshold in terms of four real coefficients. If provides a four-parameter subtraction scheme for the inverse-amplitude partial-wave dispersion relations, and specifies any pole terms $P^I_\ell(s)$ to be inserted below

threshold, and at threshold for $l \geq 0$. In the first category we have in mind especially zeros of the S-waves below threshold; the second category is the usual angular momentum zeros.

Instead of the constants a, b, c, d it is more convenient to parametrise the subthreshold amplitudes in terms of the following four alternative independent quantities:

(i) the ratio of isoscalar and isotensor S-wave scattering lengths, $R = a_0/a_2$;

(ii) the t - channel isovector combination of scattering lengths, $L = (2a_0 - 5a_2)/6$;

(iii) the P-wave scattering length, $a_1 = 4 \left.\frac{dA^1}{ds}\right|_{\substack{s = 4\mu^2 \\ t = u = 0}}$;

(iv) the Chew-Mandelstam coupling constant $\lambda = -A^2(s=t=u=4\mu^2/3)/2$

These quantities are more convenient for direct comparison with experiment, and with other models.

We record here the relation between a,b,c,d and R, L, a_1, λ :

$$R = \frac{5a + 8\mu^2 b + 32\mu^2 d}{2a + 8\mu^2 b + 32\mu^2 d} \qquad (2.12)$$

$$L = -4\mu^2 (b + 4\mu^2 d) \qquad (2.13)$$

$$a_1 = -4 (b + 4\mu^2 c + 8\mu^2 d)/3 \qquad (2.14)$$

$$\lambda = - (a + 8\mu^2 b/3 + 16\mu^2 (c + 4d)/9) \qquad (2.15)$$

Note that we have of course (10) equation (D33)

$$L = 3\mu^2 a_1 + \text{D-wave corrections} \qquad (2.16)$$

2.3 Constraints

The inverse amplitude is extremely convenient for implementing unitarity and for enforcing some parts of the desirable properties of analyticity and crossing symmetry. However, it suffers from two theoretical drawbacks - that it may in fact lead to important violations of both crossing symmetry and analyticity.

First the analyticity properties of $A^I_\ell(s)$ may be unacceptable because either $B^I_\ell(s)$ constructed from (2.3) has physical-sheet zeros that give ghost-poles in the amplitudes, or else conversely $A^I_\ell(s)$ has important zeros left out of $P^I_\ell(s)$, (or perhaps both).

Second, crossing is necessarily violated on the left-hand cut - not simply through uncritical use of (2.8) but because $\mathrm{Re}A^I_\ell(s)$ calculated dispersively does not agree with that calculated from crossing, (via a subtracted Froissart-Gribov projection).

As far as ghosts are concerned, their presence is obvious when they appear as antiresonances (i.e. close to the physical part of the real axis) because then the phase shift plunges downward through $-\pi/2$. The omission of other zeros of $A^I_\ell(s)$ from $P^I_\ell(s)$ (apart from those specified by the polynomial amplitudes) is justified only on grounds of simplicity and agreement with experiment. The violations of crossing we expect to have minimal effects on the physical phase shiftsbecause, firstly the partial wave amplitudes are constrained below threshold ($0 \leq s \leq 4\mu^2$) to match quite closely an explicit crossing-symmetric amproximation, and secondly the iterative calculations are very stable and rapidly convergent.

However, stringent checks are possible of the degree to which our calculated amplitudes possess acceptable properties of analyticity,

crossing symmetry and unitarity, because these desirable attributes have a multitude of rigorously proven consequences (sum rules, inequalities, bounds etc.) whose satisfaction can be tested.

The rest of this section occupies two main parts. The first enumerates some of these theoretical constraints which we apply to $\pi\pi$ amplitudes, and the second considers the possible range of phenomenological values which can be assigned to the four polynomial parameters R, L, a_1, and λ. There is also some discussion of the question of inelasticity and of higher partial waves ($l \geq 2$).

Our philosophy regarding the various kinds of constraints is that the phenomenological results give some idea of the values of the input quantities and an estimate of reasonable limits of variation, while the theoretical constraints are to be imposed on the output amplitudes (if possible) by adjustment of input parameters within their allowed range.

A Rigorous Theorems

The rigorous theoretical results fall into two classes: sum rules from crossing alone that are sufficient as well as necessary, and inequalities and bounds combining also analyticity and unitarity. The latter are merely necessary conditions, but their power to rule out otherwise apparently plausible models isconsiderable (e.g. (35)).

The crossing sum rules are the five involving only S- and P-waves given in Appendix C.

Sum rules involving D-waves and higher are not examined in

detail because the predicted sizes of the amplitudes for $l \geq 2$ are uniformly small, and their effects via crossing on the larger and more interesting S- and P-waves are entirely neglible (see section 4).

In all cases, the S- and P-waves obey equations (C35, 37, 39, 43, 45) accurately, and we are confident that the violations of crossing symmetry can be disregarded in practice.

Of the many constraints that follow from the additional properties of analyticity and unitarity (positivity), historically the first to be established were the geometrical inequalities of Martin (5) and of Common (36), lately extended by Auberson et al.(37). These apply to partial-wave amplitudes for $s \in (0, 4\mu^2)$.

There is also a large class of more recently discovered integral inequalities (31, 38, 39), of which the most useful seem to be those derived and tested by Yen and Roskies (39). These authors find inequalities involving integrals over the physical partial-wave amplitudes ($s > 4\mu^2$), and by comparison with previously known results and by the explicit testing of some models, the new constraints as they apply to the $\pi^0 \pi^0 \to \pi^0 \pi^0$ S-wave amplitude are shown to be more restrictive than those found before.

These present calculations proceed by building in at the outset satisfaction of the simplest of the geometrical inequalities (5, 36, 37) by imposing them explicitly on the subtraction polynomial amplitudes. Then the output amplitudes are checked for detailed satisfaction of the geometrical constraints and of the most restrictive neutral-pion S-wave Yen-Roskies conditions. Note

incidentally that the detailed check of the geometrical constraints is a valuable test of the consistency with analyticity and unitarity of the polynomial approximation.

The constraints built into the polynomial amplitudes (and thus to a good approximation into the partial-wave amplitudes) are the simple inequalities applying to the $\pi^0 \pi^0 \to \pi^0 \pi^0$ S-wave amplitude $f_0^{00}(s)$ defined in Appendix C. In addition to the ones proved there (C7, 11, 18, 26) we also have the following additional constraints.

$$\frac{df_0^{00}(s)}{ds} < 0 \qquad 0 \leq s \leq 1.05^2 \qquad (2.17)$$

$$\frac{d^2 f^{00}}{ds^2} > 0 \qquad 0 \leq s \leq 1.7^2 \qquad (2.18)$$

$$f_0^{00}(4\mu^2) > -4 \qquad (2.19)$$

$$4\mu^2 \int_0 (A_0^0(s) - 4A_0^2(s))\, ds \leq 6\mu^2 A_0^2(0) \qquad (2.20)$$

and $F_0^{00}(s)$ has a unique minimum in the region (41)

$$1.127^2 \leq s \leq 1.697^2 \qquad (2.21)$$

Within the framework of the quadratic polynomial approximation this and all the other simple subthreshold geometrical S-wave constraints (5, 36, 37, 40 - 42) are satisfied if and only if the D-wave $\pi^0 \pi^0$ scattering length is positive, (a condition of course required by the validity of the Froissart-Gribov projection for $l = 2$, plus positivity).

Therefore there is an inequality connecting the quadratic coefficients in (2.11), namely

$$c < 2d. \qquad (2.22)$$

Translated into a relation between scattering lengths and the

Chew-Mandelstam coupling constant we have

$$a_0 + 2a_2 + 9\lambda > 0 \qquad (2.23)$$

Note that a_1 (which essentially controls the ρ width) is not constrained because the P-wave does not contribute to $\pi^0\pi^0 \to \pi^0\pi^0$ scattering.

The constraints of Yen and Roskies (39) which we use may be expressed as follows. Define first the following moments of the $\pi^0\pi^0 \to \pi^0\pi^0$ S-wave amplitude below threshold:

$$A_{20} = \frac{1}{256\mu^6}\left\langle (4\mu^2 - s)\,(10s^2 - 32\mu^2 s + 16\mu^4)\, f_0^{00}(s)\right\rangle \qquad (2.24)$$

$$A_{30} = \frac{1}{1024\mu^8}\left\langle (4\mu^2 - s)\,(35s^3 - 180\mu^2 s^2 + 240\mu^4 s - 64\mu^6)\, f_0^{00}(s)\right\rangle \qquad (2.25)$$

$$A_{40} = \frac{1}{4096\mu^{10}}\left\langle (4\mu^2 - s)\,(126s^4 - 896\mu^2 s^3 + 2016\mu^4 s^2 - 1536\mu^6 s + 256\mu^8)\, f_0^{00}(s)\right\rangle \qquad (2.26)$$

where $\langle\text{---}\rangle$ denotes $\int_0^{4\mu^2}(\text{---})\,ds$. Introduce also the three quantities

$$C_l = (-1)^l \frac{1}{2(l+1)\pi\mu^2}\int_{4\mu^2}^{\infty} \mathrm{Im} f_0^{00}(s)\left(Q_l(z) - Q_{l+1}(z)\right) ds$$

$$(l = 2,3,4) \qquad (2.27)$$

where $z = s/2\mu^2 - 1$ and $Q_l(z)$ is the second - kind Legendre function. Note that (2.27) involves the absorptive part of $f_0^{00}(s)$ in the physical region, and the convergence of the integrals is rapid, s^{-3} or faster. (They can be cut off safely at $s = 50\mu^2$). Then:

$$A_{20} > \frac{5}{2}\, C_2 > 0 \qquad (2.28)$$

and $(x, y) \in D$ where $x = \dfrac{5A_{30}}{2A_{20}}$, $y = \dfrac{5A_{40}}{7A_{20}}$ (2.29)

$(x^o, y^o) \in D_o$ where $x = \dfrac{-C_3}{C_2}$, $y = \dfrac{C_4}{C_2}$ (2.30)

$(\bar{x}, \bar{y}) \in \bar{D}$ where $\bar{x} = \dfrac{x-px^o}{1-p}$, $\bar{y} = \dfrac{y-py^o}{1-p}$ (2.31)

with $p = \dfrac{5C_2}{2A_{20}}$

The three regions D, Do and $\bar{D}$ are shown in figure (2.1), and it has been shown that these restrictions are almost optimum (and almost sufficient). Like Yen and Roskies, we find (2.31) to be in practice the most exacting constraint. It is particularly interesting because it relates amplitudes above threshold (via x^o, y^o) to those below threshold (via x, y).

It is vital to stress the origin of the results (2.28 - 2.31) (39). They include not only the assumption that the S-waves have positive imaginary parts above threshold, but also they rely heavily on positivity in higher partial waves, including $l \geqslant 2$ (which is relevant via crossing). Therefore, although the present model does not include explicitly scattering in F, G, H —— waves, its lower partial waves are constrained to obey at least some of the stronger consequences of belonging to physically fully realistic $\pi\pi$ amplitudes $A^I(s,t,u)$ where there is some scattering (however small) in all angular momentum states.

We note the relevance of the above comment to any model with a finite number of partial waves (43). Even though the model may be

exactly crossing-symmetric have all its physical absorptive parts positive, and have correct analytic properties, its S-wave amplitudes may still violate the consequences of positivity in higher (neglected) angular momenta, unless these are explicitly enforced.

In the calculations described in section 4, constraints (2.23) and (2.28 - 2.31) are demonstrated to lead to a fairly narrow range of acceptable solutions to their model, happily including the physical ones.

B. Phenomenological Information

All the experimental inferences are rather indirect, but some more so than others.

From peripheral pion production ($\pi N \to \pi\pi N$ with π exchange) broad features of the two S-wave amplitudes in the region of the meson can be deduced from study of interference patterns (20, 21). It is currently accepted that both amplitudes have neglible inelasticity in this region, and while the isoscalar phase shift is large (probably resonating), the isotensor phase shift is much smaller and negative, attaining a value of perhaps -10° to -20° at $s = m_\rho^2$.

Also from analysis of production data it is observed that the onset of significant inelasticity into e.g. 4π, $K\bar{K}$ etc. is at about $\sqrt{s} = 1$ GeV, and the results are consistent with small contributions from partial waves with $l > 2$ in the elastic region.

Closer to threshold, recent determinations have been made from

peripheral production of the ratio R of S-wave scattering lengths.

Gutay et al. (44) have studied the forward - backward $\pi^+ \pi^-$ asymmetry in $\pi^- p \to \pi^+ \pi^- n$, and by making a model for the off-shell $\pi\pi$ amplitude (including the Adler consistency condition (12)) they deduce

$$R \approx -3.2. \qquad (2.32)$$

C line at al. (45) have found a similar value from study of the charged branching ratios $R_1 = \sigma(\pi^0 \pi^0)/\sigma(\pi^+ \pi^+)$ and $R_2 = \sigma(\pi^0 \pi^0)/\sigma(\pi^+ \pi^-)$ near threshold. After correcting for small P- and D-waves effects the two ratios give consistent values for R of

$$R = -3.2 \pm 1.1. \qquad (2.33)$$

Especially in view of the fact that these two determinations rely on different assumptions, their agreement with each other, and with the usual current algebra result (10)

$$R = -3.5 \qquad (2.34)$$

is impressive. Note the (perhaps not surprising) consistency with the apparent behaviour of the phase shifts at higher energies.

There are also predictions for both L and a_1.

The value of L can be calculated from an unsubtracted forward dispersion relation for the combination of amplitudes corresponding to pure I = 1 in the t - channel. Convergence follows from the Pomeranchuk theorem, and Regge ρ exchange gives an estimate of high energy contributions.

Both Olsson (46) and Morgan and Shaw (47) have considered this sum rule in detail and agree on a "universal value."

$$L \approx 0.10 \qquad (2.35)$$

The "universality" refers to the fact that the value does not depend on which of the alternative experimental S-wave phase shifts solutions are used in the calculation. Note that (2.35) agrees well with the Weinberg $SU(2) \otimes SU(2)$ current algebra prediction (10), and taken together with (2.32 - 2.34) is the main piece of evidence for the assumption (ii) underlying the polynomial approximation - weakness of S-wave thresholds (as gauged by the size of the scattering lengths).

The value of a_1 can be calculated also from a dispersion relation. This was done several years ago by Olsson (48) with the result

$$a_1 \approx (0.03 - 0.04)\mu^{-2} \qquad (2.36)$$

This number is not sensitive to S-wave contributions, and is in quite good agreement with a simple-minded linear effective - range extrapolation from the ρ meson, mass 765 MeV, width about 125 MeV. In the next section the numerical results are seen to justify the extrapolation in detail.

Note that the sum rule (2.16) is satisfied with (appropriately) small D-wave corrections. In fact the D-wave corrections can be calculated from a sum rule which has a rigorous foundation, and which converges quickly (49). Using phenomenologically - based estimates of the low partial waves the agreement of the numbers (2.35) and (2.36) with the sum rule (2.16) is found to be very satisfactory.

The consistency of the number (2.35) calculated from current algebra with the scattering length (2.36) obtained from ρ dominance has been remarked upon before (50) in connection with the KSRF relation (51).

There do not seem to be any direct estimates of the value of the fourth parameter of the polynomial amplitude, namely the Chew-Mandelstam coupling constant λ . However its size may be expected to be close to the current algebra estimate ($\lambda = -0.007$) since R, L and a_1 are approximately equal to Weinberg's values and the D-wave corrections, (though important in principle) are small.

There are also bounds on λ . One is that in terms of a_0 and a_2 (or R and L) following from the Martin geometrical constraints applied to the polynomial amplitude, i.e. eq. (2.23). With $L \approx 0.10$ and $R \approx -3.5$ we have

$$\lambda > -0.008. \qquad (2.37)$$

The second bound is the phenomenological are derived by Shaw (52). It involves integrals over physical phase shifts, and with reasonable phenomenological estimates leads to

$$\lambda < 0.10 \qquad (2.38)$$

In summary, there are fairly good indications of the values of three of the four polynomial amplitude parameters, (R, L and a_1), while the fourth (λ) is at least bounded. All are slightly adjustable (if necessary) to seek satisfaction of the rigorous theorems.

Besides the four polynomial coefficients, the inelastic terms $R_l^I(s)$ in (2.3) need to be specified. The simplest approximation, and

the one usually made, is $R_l^I(s) = 0$, perhaps on the grounds that s_{in} is too large for the term to be significant. This is not necessarily true, especially in the I = 0 S-wave (which is probably the most interesting channel). Here the isoscalar $K\bar{K}$ threshold opens at $\sqrt{s} \approx 950$ MeV and is expected to have a large contribution to the ratio $r_0^0(s)$ (eq (2.7)) of S-wave I = 0 inelastic to elastic cross-sections because of the presence of the S* effect.

In the numerical calculations estimates of $R_l^I(s)$ are made, using information both from Hoangs analysis of the S* effect (53) and from the Toronto - Wisconsin phase shifts for $\sqrt{s} \leq 1.4$ GeV. (54).

The I = 2 amplitudes stay fairly elastic in the region 1.0 - 1.4 GeV as several of the two-body channels that open up do not couple to I = 2 e.g. $K\bar{K}$, $\pi\omega$, $N\bar{N}$.

Rather surprisingly, although the inelastic effects are individually large, their effects on the phase shifts for $s < m_\rho^2$ are quite small because of cancellations between direct - channel contributions and contributions from the crossed-channels via $L_l^I(s)$. There is then possible justification for simply neglecting inelasticity below the ρ.

The model as formulated neglects the existence of higher partial waves ($l > 2$) - except, of course, in the rigorous constraints discussed above - and in fact as already mentioned the numerical sizes of predicted D-waves and higher are extremely small.

Some consistency checks can be made by inserting by hand contributions from higher resonances (f^0, g etc.) and studying their effects both on the D, F waves etc. as well as in the S- and P- waves.

As the next section discusses in detail the effects are exceedingly small.

2.4 Results

The subtraction point s_o is fixed at the $\frac{4}{3}\mu^2$ (symmetry point) in all but the P-wave where the ρ meson is inserted through a subtraction at $s_o = m_\rho^2 = (765\text{MeV})^2$ with $B_1^1(m_\rho^2) = 0$.

The choice of subthreshold subtraction point is made well away from the physical branch-point at $s = 4\mu^2$ so that the approximation of weak thresholds can be tested and its possible inconsistency can be detected by comparison of polynomial and dispersion-relation threshold S-wave amplitudes.

The range of parameter values investigated in detail is $R = -3.2 \pm 1.1$, $L = 0.08 \pm 0.04$ and $a_1 = (0.03 \pm 0.01)\mu^{-2}$ with λ chosen in accordance with the geometrical inequality (2.23). We find that in any attempt to construct solutions with (2.23) violated, one of the predicted D-waves at least contains ghosts (the phase shifts violates Wigner's Theorem), and if the violation is more than slight, the S_2 wave also has a ghost. Conversely, if (2.23) is satisfied there are no obvious ghosts below $\sqrt{s} = 1$ GeV in any of the partial waves.

For the above range of values of R, L and a_1 it also turns out that satisfaction of (2.23) by a good margin (i.e. replacing the right-hand side by 0.06), and the consequent imposition of the rigorous geometrical constraints on the polynomial amplitudes leads to the satisfaction of the same constraints on the calculated output amplitudes, If (2.23) is only marginally obeyed, some constraints are violated by the computed amplitudes, and at the same time the S_2 phase

shift shows signs of a ghost above the upper end of the energy range - the phase shift is large and negative and steeply falling at about 1 GeV.

Satisfaction of the geometrical constraints in fact is correlated with the agreement of the two versions of the amplitude below threshold. In the acceptable cases the polynomial approximation is accurate and the calculational assumptions are consistent. Figure (2.2) illustrates the agreement between the polynomial and calculated $\pi^0\pi^0$ S-wave below threshold in a favoured case.

Satisfaction of (2.23) above is however not very restrictive (λ is bound only on one side) and a wide range of possibilities are allowed. There are some general features in common, nevertheless, namely as large positive S_0 phase shift and a smaller S_2 phase shift, a very symmetric P-wave (ρ) resonance, and extremely small D-waves. The general agreement with the peripheral production implications is already evident.

As remarked in the previous section, the crossing sum rules are always accurately satisfied. Furthermore, the crossing sum rules and all the other constraints investigated, (especially those on the larger output S- and P-waves) are unaffected by the contributions of the D-wave phase shifts, because they are so small ($< 5^\circ$). If the calculation is modified so that cross-channel D-waves amplitudes are ignored on the left hand cut, the S and P wave amplitudes are changed by at most 1%, which is neglible. This is true in all the calculations made here, including cases where the contribution of the f^0 (1260) meson (in the D wave) is inserted by hand with Γ = 150 MeV. This resohance contributes significantly

only to the distant left-hand cut, which is damped by the subtraction.

The detailed behaviour of the P-wave phase shift in all cases (whether or not inelasticity is included) is controlled mainly by the value chosen for a_1. This parameter determines the width of the ρ resonance in the output phase shift, approximately according to the simple effective-range extrapolation formula (50).

$$A_1^1(s) = k^2 a_1 ((1 - k^2/q^2) - i k^2 a_1 \rho)^{-1} \qquad (2.39)$$

where $4q^2 = M^2 - 4\mu^2$, M is the ρ meson mass and

$$\rho = ((s - 4\mu^2)/s)^{\frac{1}{2}} \qquad (2.40)$$

with $a_1 = M^2 \Gamma/8q^5$ (2.41)

Figure (2.3) shows the remarkable linearity of the P-wave effective - range plot for a typical set of parameters. Thus there is detailed dynamical justification for the rho-dominance derivations of the KSRF formula referred to in section 3 (50), and we confirm the results found previously (48), The value $a_1 = 0.04\mu^{-2}$ determines a reasonable physical value of $\Gamma \approx 125$ MeV.

The range of possible solutions allowed by (2.23) and the crossing sum rules is considerably narrowed by imposition of the Yen-Roskies constraints (2.28 - 2.31). In fact, these constraints are so strong that they cannot be completely satisfied, but an attempt to minimise the violations determines not only λ but also preferred values for the other two parameters L and R, and consequently leads to an almost complete determination of the two S-wave amplitudes.

The theoretically most satisfactory amplitudes which we have found (with no inelastic terms, i.e. $R_l^I = 0$) is shown in figure (2.4). This solution obeys all the constraints (2.28 - 2.31)except for a

small violation of (2.31). (See figure 2.1) This is a measure of the severity of the approximation of neglecting $l \geq 3$ partial waves, and perhaps would be improved if for example the polynomial subtraction amplitudes included cubic and higher terms.

The main features of the results in figure (2.4) are (i) a large S_0 phase shift, passing through $\pi/2$ near $\sqrt{s}$ = 540 MeV. and of the "down" type above the ρ mass; (ii) the S_2 phase shift much smaller, falling to about -12^0 at $\sqrt{s}$ = 1 GeV.

There is a distinct correlation between the point where the S_0 phase shift passes $\pi/2$ and the size of the S_2 phase shift - the higher the former, the larger the latter. If S_0 resonates at $s = m_\rho^2$ then the S_2 phase shift falls to about -15^0 at s = 1GeV. However this possibility (included in figure (2.4) does violate (2.30) as well as (2.31) - see figure (2.1).

All the solutions which come close to satisfying (2.28 - 2.31) have zeros in the S_0 and S_2 amplitudes for $s \in (0, 4\mu^2)$ (at $s^{(0)}$ and $s^{(2)}$ respectively). These may be identified as on-shell manifestations of the Adler zeros (12) demanded by PCAC - not because they are at the Weinberg positions (10) ($s^{(0)} = 0.5\mu^2$, $s^{(2)} = 2\mu^2$) but because they satisfy the Pennington-Pond sum rule (27).

$$4\, s^{(0)} + 5\, s^{(2)} = 12\mu^2 \qquad (2.42)$$

This result (2.42) is more general than Weinberg's, which relies on a linear off-shell extrapolation in s,t,u.

The actual zero positions for the two solutions of figure (2.4) are very close at

$$\begin{aligned} s^{(0)} &= 1.5\mu^2 \\ s^{(2)} &\doteq 1.2\mu^2 \end{aligned} \qquad (2.43)$$

It is interesting to note that the solutions with λ chosen relative to R and L so as to satisfy (2.23) only marginally have $s^{(0)} \approx 0.8\mu^2$ and $s^{(2)} \approx 1.7\mu^2$, closer to the current algebra positions, and the output phase shifts are similar to those of Brown and Goble (55)

showing evidence of an important ghost in the S_2 channel.

Note that the theoretically best solution of figure (2.4) agrees very well with the central solution in the range found by Le Guillou, Morel and Navelet (56), who constructed amplitudes satisfying constraints similar to those used here. The parameterisation and iteration methods of Le Guillou et al. are very different from ours, but the very close agreement between the results suggests that possibly all low energy $\pi\pi$ models which obey these consequences of analyticity etc. should give the same predictions.

2.5 Inelastic effects

Although our model is strictly a low energy model and no strong predictions can be made near 1 GeV. we do predict that the phase shift stays near 90° above the ρ mass. This is in agreement with the results obtained by the Berkeley group (57) from analyses of the reactions

$$\begin{aligned} \pi^+ p &\to \pi^+ \ \pi^- \ \Delta^{++} \\ \pi^+ p &\to K^+ \ K^- \ \Delta^{++} \end{aligned} \qquad (2.44)$$

at 7 GeV/C, as experimentally the S-P interference term passes through zero near 980 MeV. If we assume ρ dominance of the P-wave then $\delta_1^1 \simeq 150^\circ$ and thus from equation (B5) we have $\delta_0^0 \simeq 60^\circ$ or 180°. The cross section data shows that the S-wave must be at its maximum value near 950 MeV ($\delta_0^0 \simeq 90^\circ$) and drop to a minimum at 980 MeV ($\delta_0^0 \simeq 180^\circ$).

Morgan (58) has also analysed the $\pi\pi$ phase shifts near the $K\bar{K}$ threshold using a K-matrix formalism. His two solutions smoothly join up with either the "up" or "down" branch of the data of Baton et al. (59) at 800 MeV. The opening up of the $K\bar{K}$ channel will make the inelasticity η_0^0 decrease above 2m as $(s - 4m^2)^{\frac{1}{2}}$ and with

this decrease we will get a large rapid increase of δ_0^0 near 995 MeV. For both solutions he found the I = 0 S-wave has a zero near the $K\bar{K}$ threshold. The solution joining the "down" branch at 800 MeV. has the $\pi^+ \pi^-$ mass spectrum showing a sharp drop just before the $K\bar{K}$ threshold. The "up" solution, however, cannot have this behaviour as the amplitude is near the bottom of the Argand diagram over all this energy range. Preliminary data (60, 61) does seem to prefer the "down" branch below 850 MeV.

Further support for this explanation of the $\pi\pi \to K\bar{K}$ threshold is given by Hoang (53) who fits the cross-section data for $\pi^+ \pi^- \to K^+ K^-$ with a bound state pole of the $K\bar{K}$ system (S*) with mass 957 MeV.

It is interesting to note that the Lovelace-Veneziano formula also has a zero at 915 MeV. due to the S*, although in this model the S* only couples weakly to $K\bar{K}$.

Against this evidence we have the work of Johnson and Bennett (62) who do a phenomenological analysis of $\pi\pi \to \pi\pi$ scattering using a generalised effective-range expansion for the S-waves based on inverse amplitude dispersion relations. They get $\delta_0^0 \approx 180^\circ$ near 1 GeV, but they also find the cross-section ratio $r_0^0(s)$ is a factor of four larger than the peak value in the 1.1 GeV region calculated from Hoang's result. This discrepancy is probably due to the fact that they do not put in any physical sheet amplitude zero near 1 GeV, and so if the I=0 S-wave is as heavily absorbed as they predict, then we would expect more absorption in the I=2 S-wave even though it couples to fewer channels.

To investigate the effects of inelasticity, the experimental results of Oh et al.(54) were used. These give information on $r_l^I(s)$ for $\sqrt{s}$ between 1.0 and 1.4 GeV. There are two possibilities for the S_0 channel: one has $\eta_0^0 \approx 0.5$ at 1050 MeV and δ_0^0 of the "down" type above the ρ, whilst the other has $\eta_0^0 \approx 0$ at 1050 MeV and δ_0^0 is of the "up" type above the ρ. The values for $r_l^I(s)$ derived and used here are given in figure (2.5). In the absence of any other information it was assumed that the valuesof $r_l^I(s)$ for $\sqrt{s} \geq 1.4$ GeV. are constant and equal to the values at $\sqrt{s} = 1.4$ GeV.

After integration to give $R_l^I(s)$, the size of this term turns out to be of the same order of magnitude as H(s) (see figure (2.6)) and thus would seem to have a large effect on the phase shift. However, there is also a change in $L_l^I(s)$ from crossed-channel absorption, which is for $s < m_\rho^2$ opposite in sign and about the same in magnitude and the net result in all the partial waves up to the resonance region is a change of less than 5% in the phase shift see figure (2.7). This is true whichever of the two possibilities for $r_0^0(s)$ is used. Although the inelastic effects do increase the phase-shifts above the ρ they do so smoothly and not sharply as experiment suggests (57). The only way for our model to obtain a zero near the $K\bar{K}$ threshold would be to insert it as a dynamical zero.

The result of including inelastic effects, which was not entirely anticipated, provides justification for the usual practice of neglecting absorption in calculating the low energy phase shifts.

Because of the small net influence of these phenomenological absorption contributions near threshold and the rapid convergence of the integrals in (2.27), satisfaction of the rigorous theorems of section 3 is not affected, and so the optimum predictions for the S- and P-waves remain of the form shown in figure (2.7).

2.6 Conclusions

We have described a simple and flexible model for the low-energy $\pi\pi$ interaction, and investigated some of its solutions. We have concentrated on finding amplitudes that are theoretically as satisfactory as possible and which give good agreement with experiment. It is not neceasarily trivial that this is possible.

The numerical predictions of amplitudes and phase shifts are in full accord with the results of the most ambitious of other calculations that aim from different points of view of satisfaction of the rigorous consequences of analyticity, crossing-symmetry, and unitarity. In particular we note the strong similarity between our predicted S-wave phase shifts and those of Le Guillou, Morel, and Navelet (56). Like these authors, we favour the existence of a broad σ (or ε) resonance just below the ρ in mass, and predict that the S_0 phase shift above the resonance is of the "down" type.

Below threshold both S-wave amplitudes have simple zeros, not in the Weinberg current algebra positions but slightly displaced in reasonable agreement with the favoured results of a recent phenomenological analysis (62). The zero-positions obey a general relation first emphasised by Pennington and Pond, and therefore they are on-shell manifestations of the Adler condition. The extrapolation

to zero pion mass is significantly non-linear, because the simplest Martin geometrical constraints demand non-linearity even on-shell.

We have discussed the effects on the phase shifts below $\sqrt{s} \approx 1$GeV of inelasticity at higher energies. The phase shifts are affected in two ways via analyticity and crossing, one contribution coming from direct-channel thresholds, the other from the crossed-channel through the left-hand cut term. Somewhat surprisingly with inelastic effects calculated from available experimental analyses, we have found for $\sqrt{s} < m_\rho$ almost complete cancellation between the two terms, which individually are large. This perhaps provides some justification for the hitherto general practice of ignoring absorption altogether.

We are not able to make firm claims of uniqueness for the favoured solution. However, in view of the work of Dilley (23) and others (e.g. (47)) the existence of physically and theoretically acceptable amplitudes of a radically different kind for $\sqrt{s} < 400$MeV seems highly unlikely.

Furthermore the possibility of bootstrap solutions in the old-fashioned sense has not yet been properly explored. We are not optimistic about this possibility unless further assumptions are injected as the left-hand cut contributions to the amplitudes are small, and so inserting the ρ into the left hand cut for the I = 0 S-wave will not generate enough force to create the σ and vice versa. This is in agreement with the recent result of Tryon (63) who has done a phenomenological analysis of the distant left-hand cut, and concludes the forces present are not strong enough to generate the ρ and in fact are only able to make $\delta_1' \approx 20^\circ$ at the ρ meson mass.

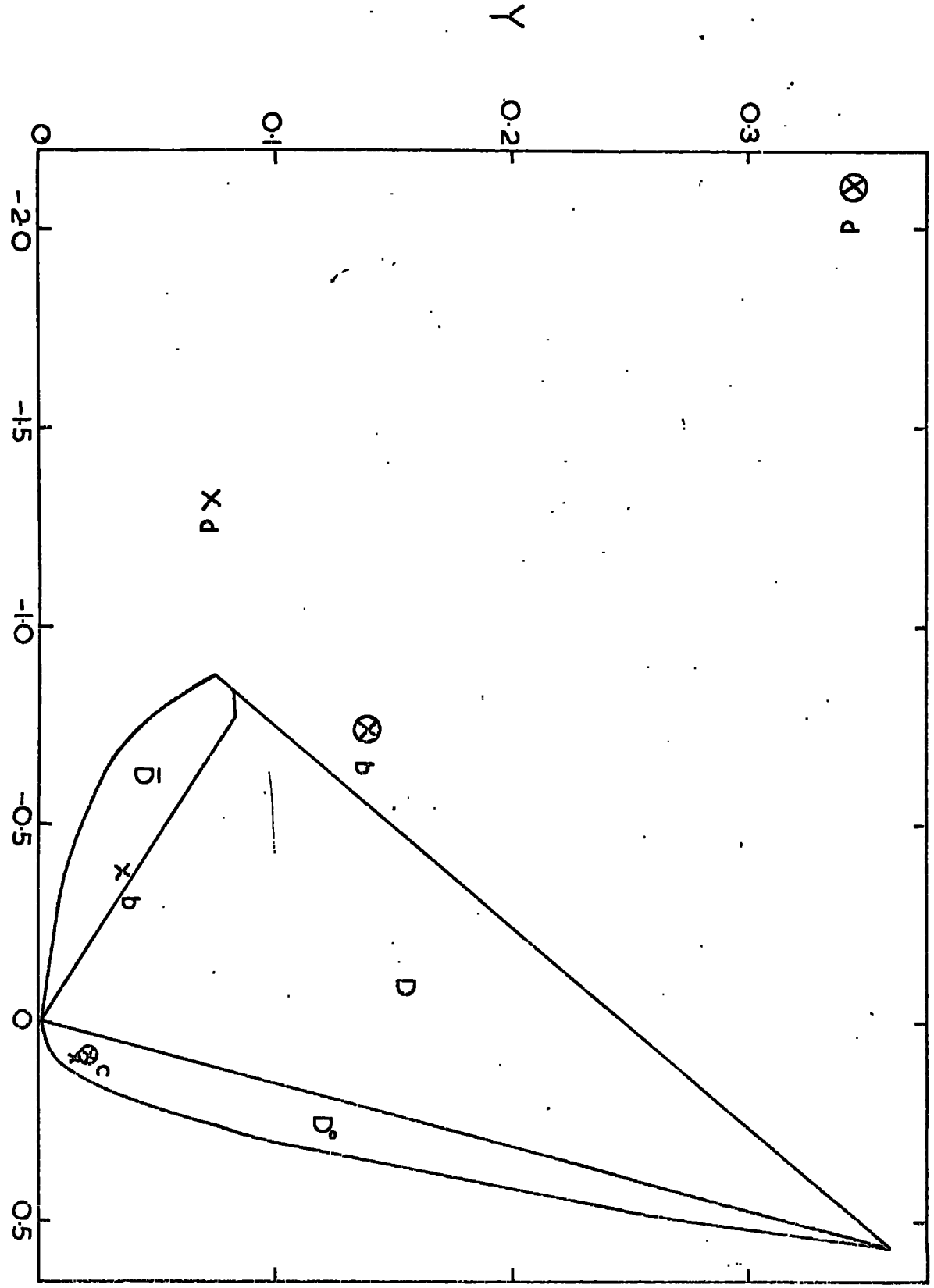

Fig. 2.1 D, D_o, $\overline{D}$ regions with D the convex hull of D_o and $\overline{D}$. The points are those of the best solution (×) and the second solution of fig.2.4 (⊗), to the equations (2.29), (2.30) and (2.31) .

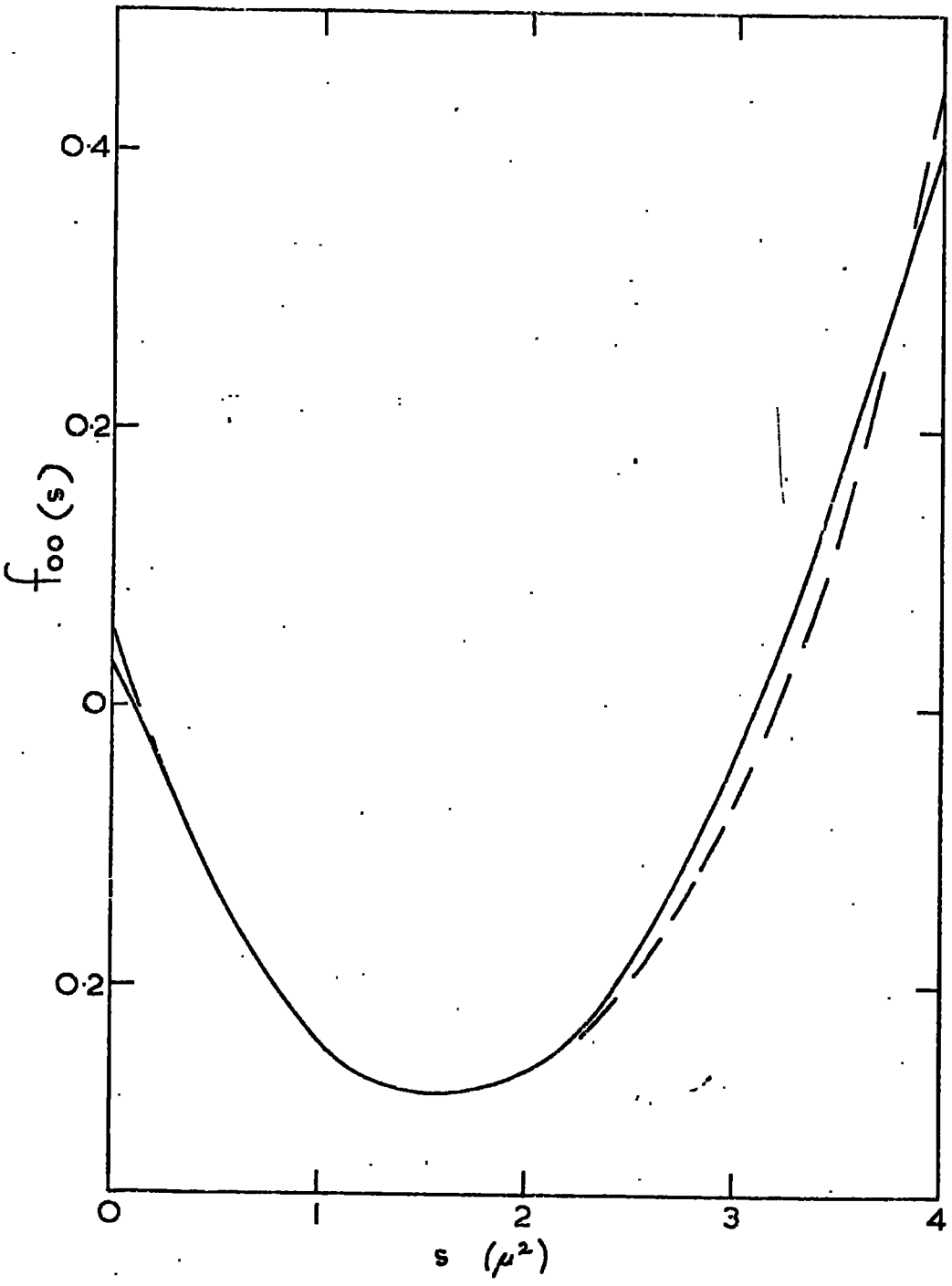

Fig. 2.2 f(s), $0 \leq s \leq 4\mu^2$ for the polynomial amplitude (solid line) and the calculated amplitude (dashed line) for the best solution.

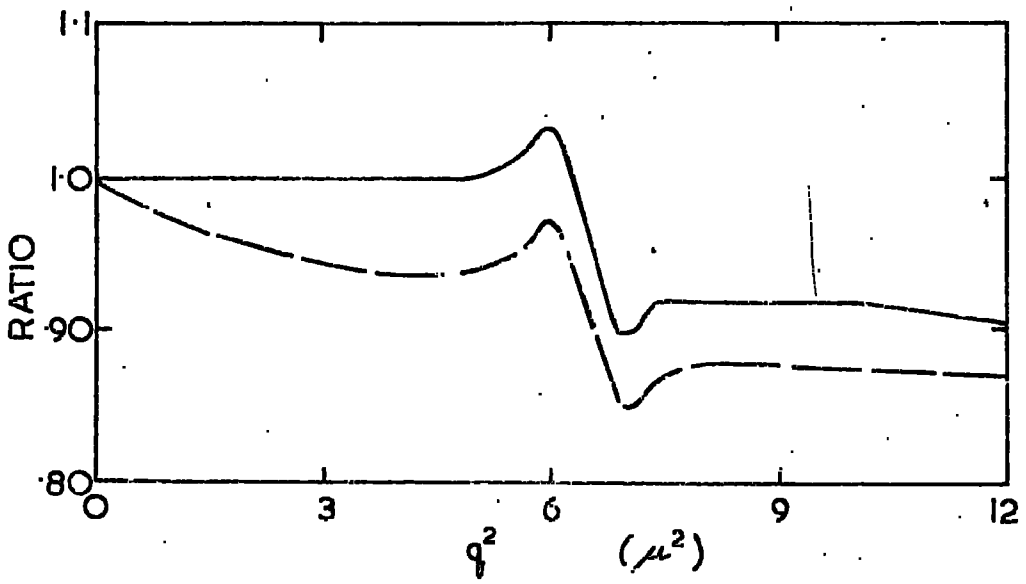

Fig. 2.3 I = 1 P-wave effective range ratio = $a_1 q^2 \rho \cot\delta/(1 - q^2/k^2)$. Input (i.e. with $L_1^1 = 0$) is dashed line, output is solid line.

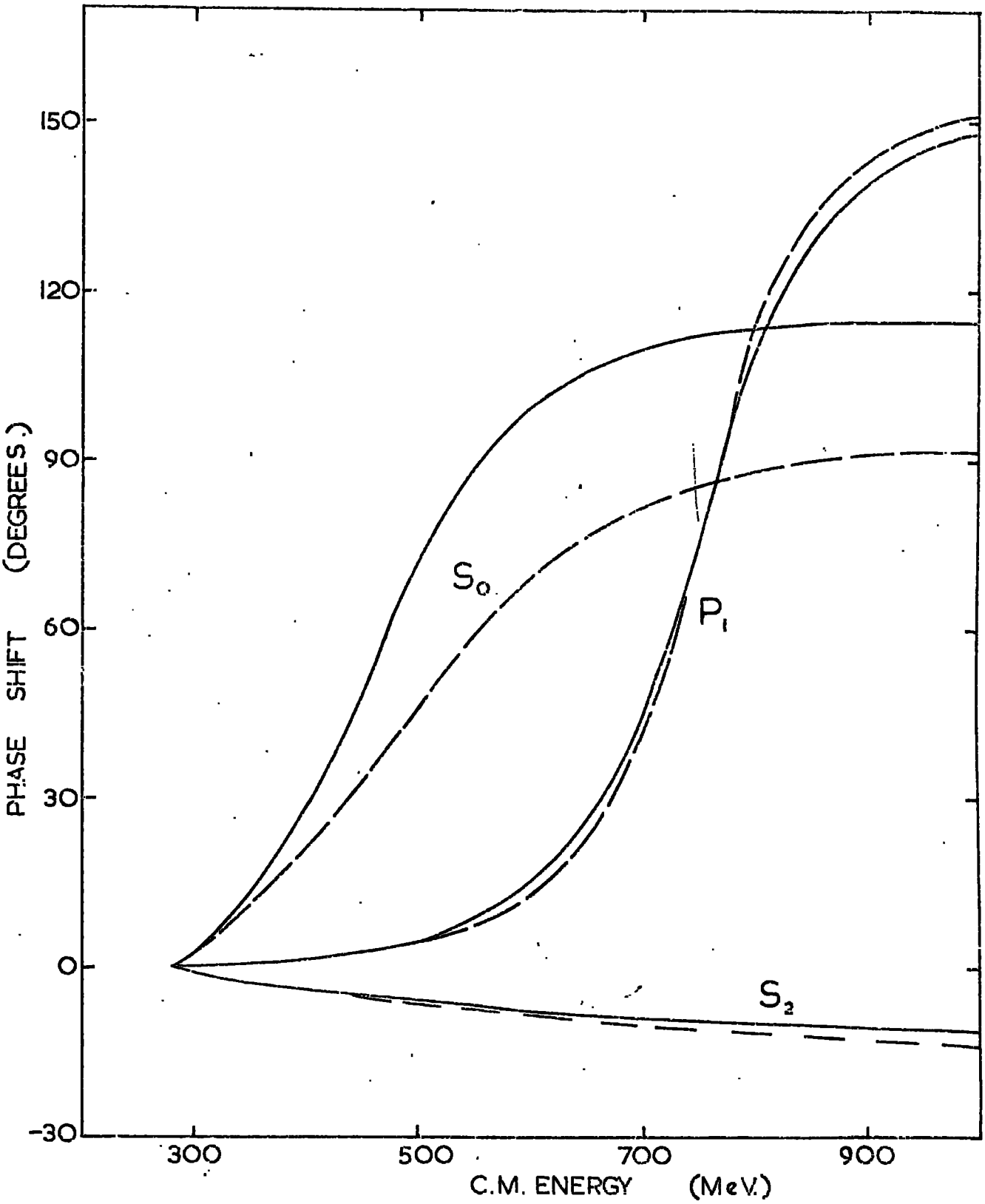

Fig. 2.4 S and P waves for best solution (λ = 0.004, R = -2.9, L = 0.085, a_1 = 0.04) - solid line, and the solution with the σ under the ρ (λ = 0.001, R = -2.9, L = 0.09, a_1 = 0.035) - dashed line. The D-waves are very small.

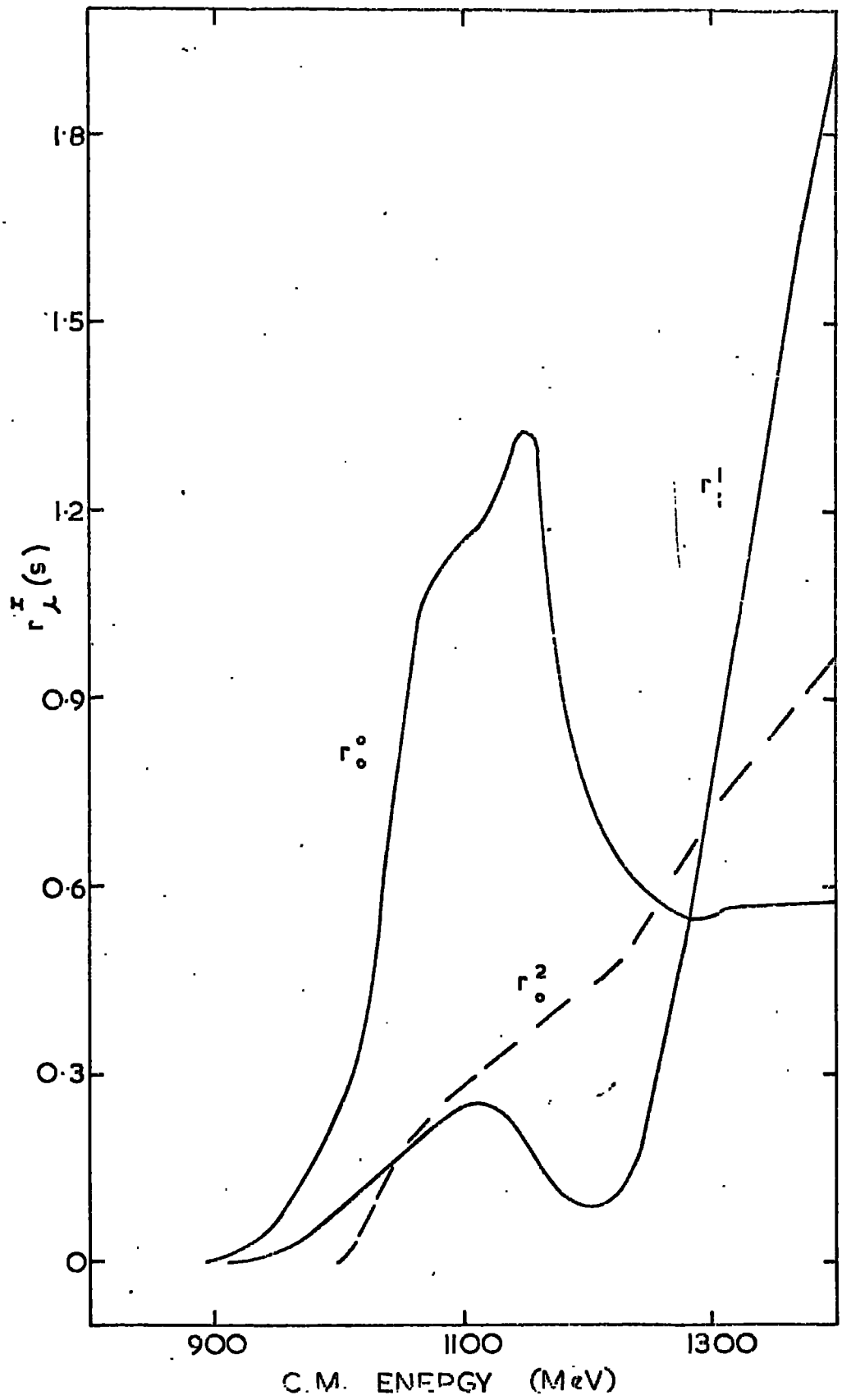

Fig. 2.5 $r_\ell^I(s)$ used, from Refs. (53) and (54).

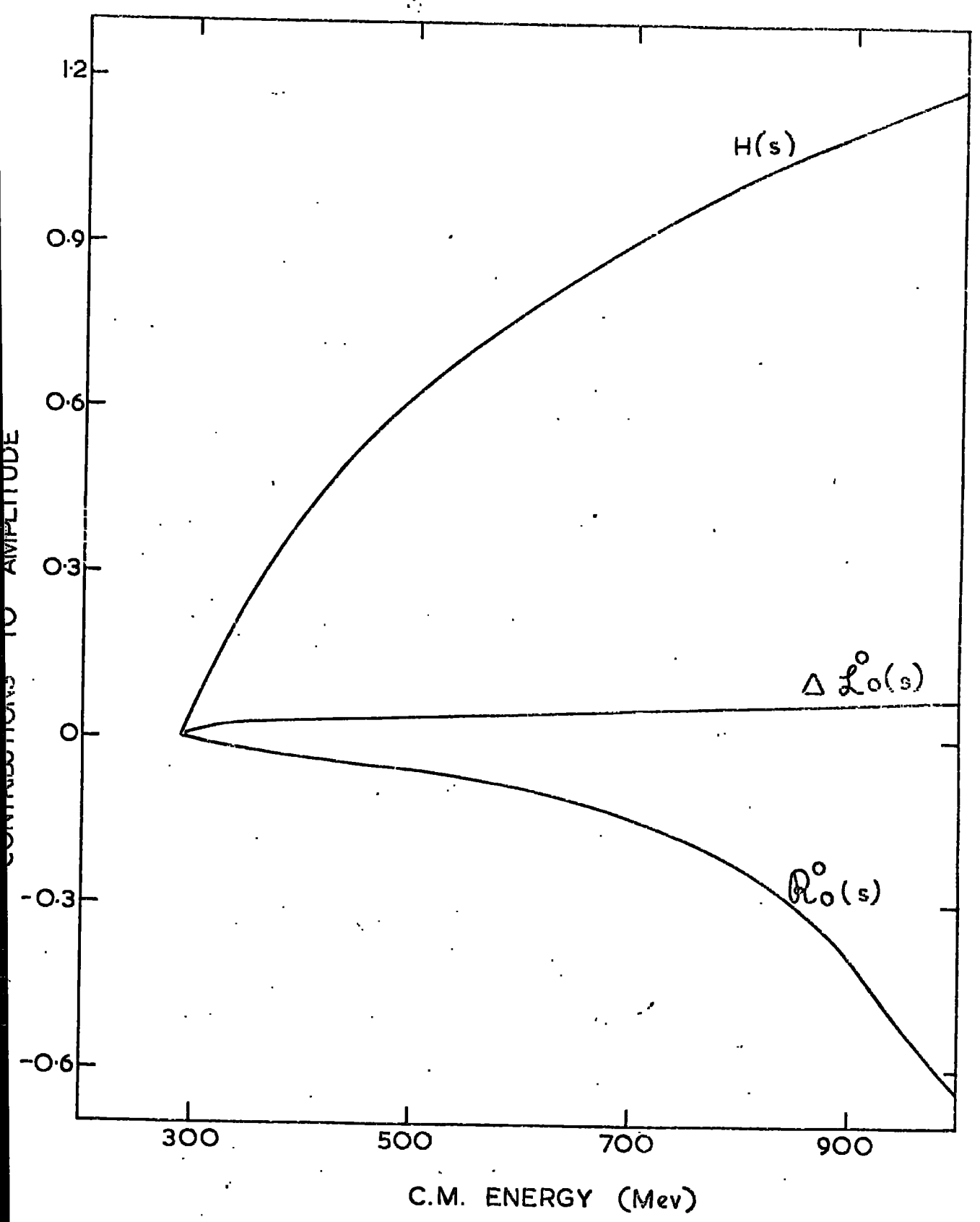

Fig. 2.6 $R_0^0(s)$, H(s) and change in $L_0^0(s)$ for $4\mu^2 \leq s \leq 50\mu^2$ and best solution.

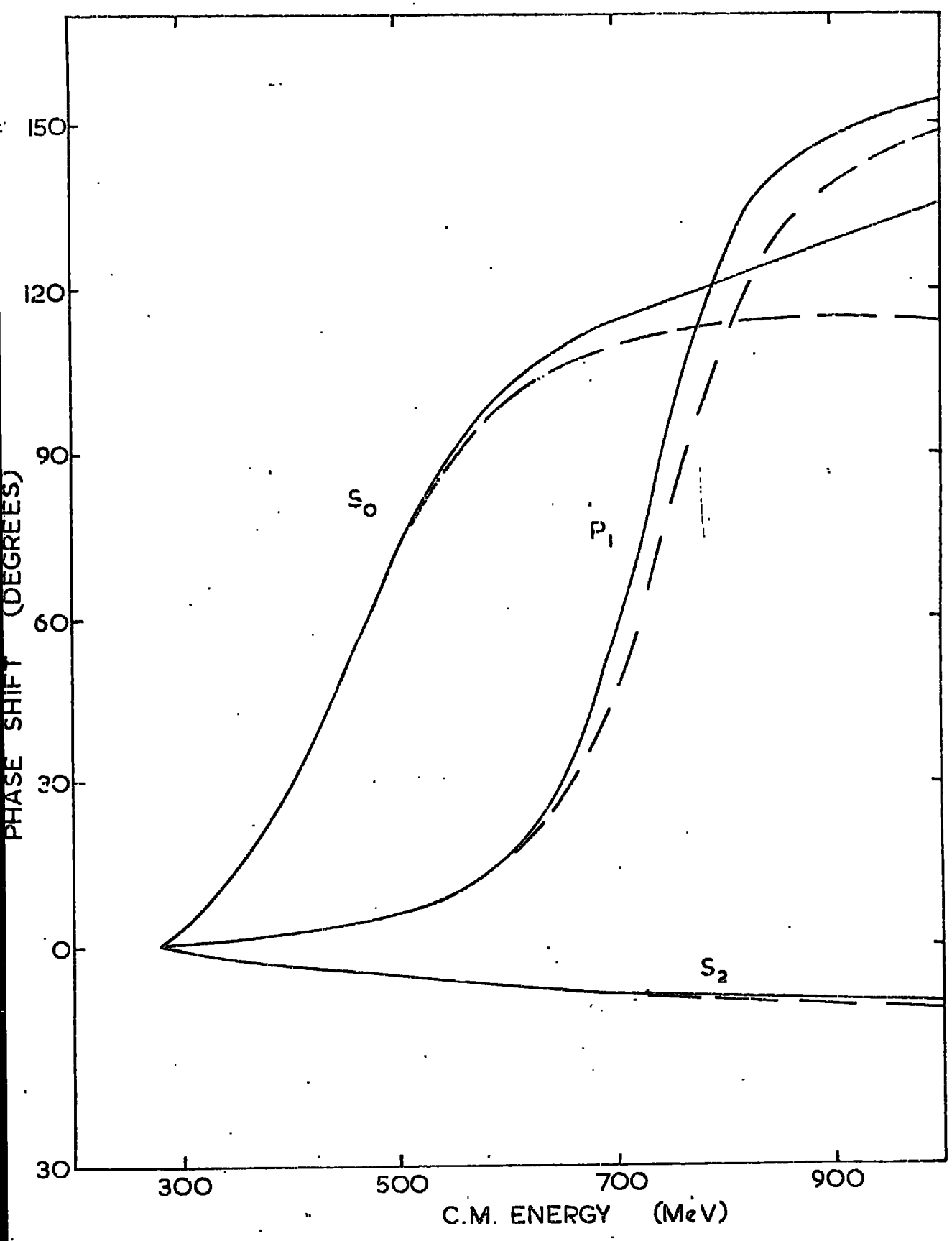

Fig. 2.7 Best solution S and P waves with (solid line) and without (dashed line) inelasticity.

CHAPTER 3.

NON - LEPTONIC DECAYS

3.1 Introduction

In this chapter we use our understanding of on - shell $\pi\pi$ scattering to investigate a simple model of the non-leptonic decays $K, \eta \rightarrow 3\pi$

The basic physical assumption is that in both processes the non-strong interaction is relatively structureless and responsible only for the transition from the initial K or η to a massive "pion" which decays strongly to three pions. Then all the structure in the decay matrix element is due to the hadronic final state interaction - $\pi\pi$ scattering with one pion off-shell (figure (3.1) gives diagrammatic illustration). This is perhaps the simplest possible model of these decays, giving a natural explanation of their rather similar Dalitz plot distributions.

Current algebra techniques have been applied to non-leptonic decays, and although soft-pion methods have been applied to $K \rightarrow 3\pi$ with great success (64), they have not been as successful when applied to the phenomenologically similar $\eta \rightarrow 3\pi$ decay as it has been shown by Sutherland (65) that if we impose current algebra constraints on a linear matrix element for $\eta \rightarrow 3\pi$ decay then the matrix elements must be identically zero and thus the decay is forbidden.

In the next section we give a parameterization for the decay, then we present our model for the description of the decays and the results we obtain, and compare them with other phenomenological analyses. Next we discuss the current algebra predictions and the effect of higher order terms in the parameterizations, and we

conclude with a discussion of the structure of our model and of the Lovelace-Veneziano model.

3.2 Parameterization

The theory of the analysis of the structurein three-pion decays was developed by Weinberg (66). The matrix element for the decay is expanded as a power series in the coordinates of the Dalitz plot:

$$X = \sqrt{3}\,(T_1 - T_2)/Q, \qquad (3.1)$$
$$Y = (3T_3 - Q)/Q,$$

where T_i are the pion kinetic energies, T_3 referring to the odd pion and $T_1 + T_2 + T_3 = Q = m - 3\mu$, where m is either the K or η mass. The matrix element for the decay is now given by:

$$|M|^2 \propto 1 + \alpha_1 \frac{QY}{m} + \alpha_2 \left(\frac{QY}{m}\right)^2 + \alpha_3 \left(\frac{QX}{m}\right)^2 + \cdots \qquad (3.2)$$

The constant of proportionality is just given by the phase-space integral for the Dalitz plot. Note that we have assumed the decays are C invariant as otherwise there would be left-right asymmetry in the Dalitz plot, and terms linear in X would be needed to describe this.

To relate the Weinberg variables X, Y to the Mandelstam variables s, t, u we go to the rest frame of the kaon and from figure (3.1) we have the total pion energies E_i given by

$$E_3 = (\mu^2 + m^2 - s)/2m, \qquad (3.3)$$
$$E_1 = (\mu^2 + m^2 - t)/2m,$$
$$E_2 = (\mu^2 + m^2 - u)/2m.$$

The kinetic energy of each particle is given by

$$T_i = E_i - m_i,$$

and thus
$$T_3 = ((\mu - m)^2 - s)/2m, \qquad (3.5)$$
$$T_1 = ((\mu - m)) - t)/2m,$$
$$T_2 = ((\mu - m)^2 - u)/2m,$$

hence
$$\frac{QY}{m} = (m^2 + 3\mu^2 - 3s)/2m^2, \qquad (3.6)$$
$$\frac{QX}{m} = \sqrt{3}(t-u)/2m^2$$

3.3 Model

Our model is to analytically continue our $\pi\pi$ subthreshold amplitude and take one of the external pions off mass-shell and put its four-momentum equal to either the K- or η - mass.

The calculation of the matrix element proceeds by assuming pion-pole dominance (16, 67) as illustrated in figure (3.1). From this we are able to write the amplitude for the decay of particle m_d (p_d) to pions $\pi_a(p_a)$, $\pi_b(p_b)$, $\pi_c(p_c)$ proportional to

$$\frac{\lambda_d}{\mu_d^2 - m_d^2} M_{d\to abc} \qquad (3.7)$$

where λ_d is the electromagnetic coupling constant for η decay and the weak coupling constant for K decay, and

$$M_{d\to abc} = \delta_{dc}\delta_{ab}A(s,t,u) + \delta_{db}\delta_{ac}A(t,s,u) + \delta_{da}\delta_{cb}A(u,t,s) \qquad (3.8)$$

is the invariant amplitude for the scattering of $dc\to ab$ pions in which c is crossed into the final state and pion d is off mass-shell (68). From (2.11) A(s,t,u) is given off-shell by

$$A(s,t,u) = a+bs + c(t+u) + d(t^2+u^2) + es(t+u) + fs^2 + gtu. \qquad (3.9)$$

When we are on-shell these seven parameters reduce to four which are conveniently given in terms of the four experimental parameters

λ, R, L and a_1 (see section (2.2B)). To find the other three equations needed to determine the parameters we use the soft-pion techniques of Weinberg given in Appendix D. When $s = t = u = \mu^2$ $A(s,t,u) = 0$, and hence

$$a + b\mu^2 + 2c\mu^2 + 2d\mu^4 + 2e\mu^4 + f\mu^4 + g\mu^4 = 0 \qquad (3.10)$$

When we take 2 pions off-shell simultaneously (D17) and (D19) give

$$a + b\mu^2 + c\mu^2 + d\mu^4 + e\mu^4 + f\mu^4 = 0, \qquad (3.11)$$

$$2b - 2c - 4d\mu^2 + 4f\mu^2 = \frac{1}{16\pi f_\pi^2} = \frac{L}{2\mu^2} . \qquad (3.12)$$

The other four equations come from putting (3.9) on-shell and then using equations (2.12 - 2.15). We thus determine our seven parameters in terms of λ, R, L and a_1.

The K^0 $(\eta^0) \to \pi^+ \pi^- \pi^0$ amplitude is now given by the $\pi^0 \pi^0 \to \pi^+ \pi^-$ amplitude, which is just $A(s,t,u)$, which we rearrange as

$$A(s,t,u) = B_1 + B_2 \frac{QY}{m} + B_3\left(\frac{QY}{m}\right)^2 + B_4\left(\frac{QX}{m}\right)^2 ,$$

$$= B_1\left(1 + R_1 \frac{QY}{m} + R_2\left(\frac{QY}{m}\right)^2 + R_3\left(\frac{QX}{m}\right)^2\right), \qquad (3.13)$$

where

$$\begin{aligned} B_1 &= a + (b+2c)(m^2+3)/3 + (m^2+3)^2 (f+2e+2d+g)/9, \\ B_2 &= m^2 (2(c-b)/3 + (m^2+3)(4d + 2g - 4f - 2e)/9), \\ B_3 &= m^4 (4f - 4e + 2d + g)/9, \\ B_4 &= m^4 (2d-g)/3. \end{aligned} \qquad (3.14)$$

The matrix element for the decay is $|M|^2$ and so we have

$$|M|^2 \propto 1 + 2R_1 \frac{QY}{m} + \left(\frac{QY}{m}\right)^2 (R_1^2 + 2R_2) + \left(\frac{QX}{m}\right)^2 2R_3 + \left(\frac{QY}{m}\right)^3 2R_1R_2$$

$$+\left(\frac{Q}{m}\right)^3 X^2Y\ 2R_1R_3 + \left(\frac{QY}{m}\right)^4 R_2^2 + \left(\frac{QX}{m}\right)^4 R_3^2 + \left(\frac{Q}{m}\right)^4 X^2Y^2\ 2R_2\ R_3. \qquad (3.15)$$

Similarly for $K^o\ (\eta^o) \to 3\pi^o$ the matrix element is proportional to

$$\left| 3B_1 + \frac{3(B_3 + B_4)}{2} (X^2+Y^2) \left(\frac{Q}{m}\right)^2 \right|^2 \qquad (3.16)$$

and for charged kaon decay $K^{\pm} \to \pi^{\pm}\ \pi^{\pm}\ \pi^{\mp}$ we have

$$\left| 2B_1 - B_2 \frac{QY}{m} + \frac{1}{2} (B_3 + 3B_4) \left(\frac{QY}{m}\right)^2 + \frac{1}{2} (3B_3 + B_4) \left(\frac{QX}{m}\right)^2 \right|^2 \qquad (3.17)$$

3.4 Results

The range of the four parameter valuesis as in chapter 2, namely: $R = -3.2 \pm 1.1$, $L = 0.08 \pm 0.04$, $a_1 = (0.03 \pm 0.01)\mu^{-2}$ with λ chosen in accordance with the geometrical inequality (2.23). Experimentally it is found that the matrix element only has a very small Y^2 dependence and thus our solutions must have $2R_2 \approx -R_1^2$ or at least $R_2 < 0$. The X^2 dependence is also neglible on all experiments up to date and this imposes the constraint that $R_3 \approx 0$.

A global analysis of the $K_L^o \to \pi^+\pi^-\pi^o$ data by Murphy (69) suggests that R_1 lies in the range -2.5 to -2.6. If we fit the data of Albrow et al. (70) and put $R_1 = -2.56$ then the minimum value of R_2 compatible with the constraints on λ, R, L and a_1 is -0.17, and then $R_3 = 0.32$. It is interesting to note that whenever we have a solution with R_1 and R_2 negative then R_3 is always small with $|R_3| < 0.9$. Thus having fitted the Y dependence we always predict the X^2 dependence to be small. Given our values for R_1, R_2 and R_3 figure (3.2) is a fit to the data of Albrow showing a linear fit and also the effect of quadratic terms. We find cubic and higher order terms have no effect that can be shown on the scale

of our figure.

The data of Albrow et al. (70) obviously requires a large cubic dependence in Y to account for the behaviour of the matrix element at either end of the spectrum, and Albrow's fit does indeed have the coefficient of $(QY/m)^3$ as about 50. However, it should be remembered that any systematic errors in the experiment could be more important at the ends of the energy spectrum, and the cubic terms may be spurious. Indeed the data of Buchanan et al. (71), although giving a rather low value for R_1, is perfectly compatible with a linear fit; and data from Ford et al. (72) on $K^{\pm} \to \pi^{\pm} \pi^{\pm} \pi^{\mp}$ and Mast et al. (73) on $K^{\pm} \to \pi^- \pi^- \pi^+$ are also compatible with no X dependence and a linear Y dependence.

To calculate the $\eta \to 3\pi$ decay matrix elements we just take the parameter values given by the best fit to the $K \to 3\pi$ process and simply change the K-mass to the η -mass in the computer programme Taking the fit shown in figure (3.2) our new values for the ratios are: $R_1 = -2.7$, $R_2 = -0.21$, $R_3 = 0.41$, and figure (3.3) shows the linear fit and also the effect of higher order terms. Again we find that the effect of cubic terms in Y is neglible and there is no significant X dependence. However, the quadratic terms in Y do have a bigger effect than in the K-decay results. When we compare our prediction for the η -decay rate with recent experimental results we find the agreement is not as good as the K decay results, although it is non-trivial that we are able to get agreement within 15%.

The average value of R_1 from recent experimental results agrees with that of Cnops et al. (74), namely $R_1 \approx -2.2$, and this implies that the value of R_1 for η -decay should be less than that

for K - decay. We find, however, that for all our solutions where $R_1 < 0$ the value for η -decay is always greater than the corresponding value for K-decay. The effect of the quadratic terms is also larger in η -decay as besides R_2 being bigger in numerical value, the multiplicative factor (Q/m) is 0.245 for η -decay whilst it is only 0.15 for K-decay. This larger value of Q/m for η -decay will also mean the series expansion in X and Y will converge more slowly than the corresponding one for K-decay and thus we might expect quadratic and higher order terms to be more important.

3.5 Current Algebra predictions

From the commutation relations for the axial charge with the weak interaction Hamiltonian we discover various simple relations for the matrix elements for $K \to 3\pi$ at the points where one of the final state pions has zero four-momentum (75). For K^+ decay these results are:

$$M(K^+ \to \pi^+ \pi^+ \pi^- ; q_{\pi^-} = 0) = M(K^+ \to \pi^0 \pi^0 \pi^+; q_{\pi^0} = 0) = 0,$$
$$M(K^+ \to \pi^+ \pi^+ \pi^- ; q_{\pi^+} = 0) = \frac{-1}{2f_\pi} M(K^0 \to \pi^+ \pi^-),$$
$$M(K^+ \to \pi^0 \pi^0 \pi^+; q_{\pi^+} = 0) = \frac{-1}{2f_\pi} M(K^0 \to \pi^0 \pi^0). \qquad (3.18)$$

In a similar fashion the commutation relations between the axial charges and the electromagnetic Hamiltonian lead to the result that the matrix element for $\eta \to 3\pi$ vanishes at each of the soft pion points (75):

$$M(\eta \to \pi^+ \pi^- \pi^0 ; q_{\pi^0} = 0) = M(\eta \to \pi^+ \pi^- \pi^0; q_{\pi^0} = 0) = 0,$$
$$M(\eta \to 3\pi^0; q_{\pi^0} = 0) = 0. \qquad (3.19)$$

The extrapolated matrix elements for $K \to 3\pi$ decay obtained from linear fits are compatible with the current algebra predications to within the experimental errors. The η -decay results in the

linear model, however, fail to show the zero in the $\eta \to \pi^+ \pi^- \pi^0$ matrix element at the soft-pion point for the odd pion (π^0). Similarly, in the linear model, the $\eta \to 3\pi^0$ amplitude is constant as can be seen from (3.16) and thus cannot show the current algebra zero. We are thus led to the conclusion that, especially in η -decay the higher order structure, neglected in the linear model, could be important.

3.6 Higher order spectrum

In chapter 2 we found we required at least a quadratic polynomial to describe the sub-threshold $\pi\pi$ amplitudes, in order to satisfy all the crossing sum rules and analyticity constraints. It is now clear that a similar amplitude is required if we are going to be able to fit the $\eta \to 3\pi$ decay amplitudes to the current algebra constraints. A quadratic $\pi\pi$ amplitude will enable us to expand the matrix element for the decays up to quartic terms in X and Y. Phenomenological analyses have been done (75) including third order terms in the matrix element and, although the errors for the extrapolated cubic spectrum are, expectedly, larger than those for the linear model, the extrapolated $\eta \to 3\pi$ amplitudes can be made completely compatible with all the soft-pion zeros.

If we now look at the $K \to 3\pi$ results we see the uncertainty in the higher order terms reflected in the large errors. Even so, the inclusion of the extra terms has tended to make the agreement with current algebra worse than in the linear model - in complete contrast to $\eta \to 3\pi$ where the agreement improved considerably.

Although the current algebra constraints make very strong predictions it should be pointed out that the matrix element

expansion is not strictly valid at the soft-pion points. For instance in $K^- \to \pi^- \pi^- \pi^+$ at the point when the odd pion has zero energy we have $T_3 = -\mu$, $s = \mu^2 + m^2$, $t=u=\mu^2$ and hence

$$\frac{QY}{m} = -1, \quad \text{and } X = 0 \qquad (3.20)$$

Similarly at the other soft-pion points:

$$\frac{QY}{m} = \frac{1}{2}, \qquad \frac{QX}{m}^2 = \frac{3}{4} \qquad (3.21)$$

We obtain the same result for $\eta \to \pi^+ \pi^- \pi^0$, and for $\eta \to 3\pi^0$ at $q_{\pi^0} = 0$ we have:

$$\frac{Q}{m}^2 (X^2 + Y^2) = 1, \qquad \frac{Q}{m}^3 (Y^3 - 3X^2 Y) = -1. \qquad (3.22)$$

In the absence of a definite model in which R_1, R_2, R_3 etc. themselves fall off reasonably fast, therefore, expansion (3.13) need not converge at the odd-pion zero-momentum points, and may converge only slowly at the other soft-pion points.

We have seen that the current algebra predictions are very difficult to satisfy for η -decay. In section (3.1) we discussed Sutherland's results (65) for η -decay and the only way round this paradox is to assume that whilst linear terms fit K-decay perfectly well, quadratic and cubic terms are essential for η decay to satisfy the current algebra constraints. This conclusion is thus in agreement with that of the previous chapter, in that any process involving two or more pions can be described by an amplitude which is at least quadratic in the usual s,t,u variables.

3.7 Discussion

Lovelace (16) has fitted the K- and η -decay processes with a Veneziano model for $\pi\pi \to \pi\pi$ scattering continued off-shell to either the K or η mass. Thus, for example, from equations (1.5)

and (1.6) we obtain

$$M(\eta \to \pi^+ \pi^- \pi^0) = \langle \eta | \pi^0 \rangle_{em} (V(s,t) + V(s,u) - V(t,u)),$$

where $\langle \eta | \pi^0 \rangle_{em}$ describes the electromagnetic mixing of the η and the off-shell π^0. This model has the feature that it possesses Adler zeros (12) for either of the charged pions but none for the neutral one as the η does not lie on the ρ trajectory or any of its daughters.

The related decay $\eta \to 3\pi^0$ may be handled analogously and here the Veneziano form (V(t,u) + V(s,t) + V(s,u)) possesses no Adler zeros at all for any of the neutral pions.

Similar results were obtained for $K \to 3\pi$ using now the weak mixing of the kaon and the off-shell pion. It should be noted, however, that, as our results indicate, once one of the decays (K or η) has been fitted and the results used as a zero parameter prediction of the other decay, the new results are not quite in agreement with experiment.

Our results are thus in agreement with those of the Veneziano model in that when going from the K-decay to the η-decay we only change the mass and thus our two amplitudes will have the same structure of zeros.

The extrapolation off mass-shell from the K to the η is small and, a priori, we would expect them to have the same structure of zeros. The above discussion suggests that the η-decay may have a more complicated interaction structure than at present imagined. If the entire structure in the three-pion final state comes from final state interactions, while the interaction Hamiltonian merely determines the strength of the decay, then K

and $\eta \rightarrow 3\pi$ should be structurally the same, but having rates according to their weak and electromagnetic natures respectively. This simple expectation does not seem to be borne out at the present and would seem to indicate that at least some of the structure of the decay is intrinsic in the interaction Hamiltonian.

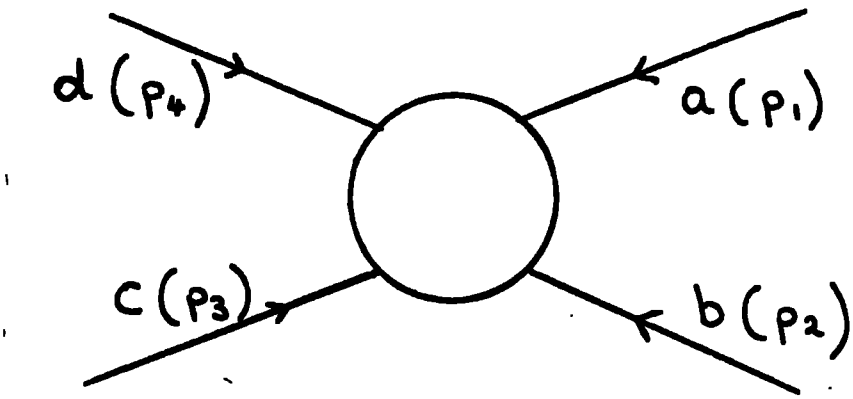

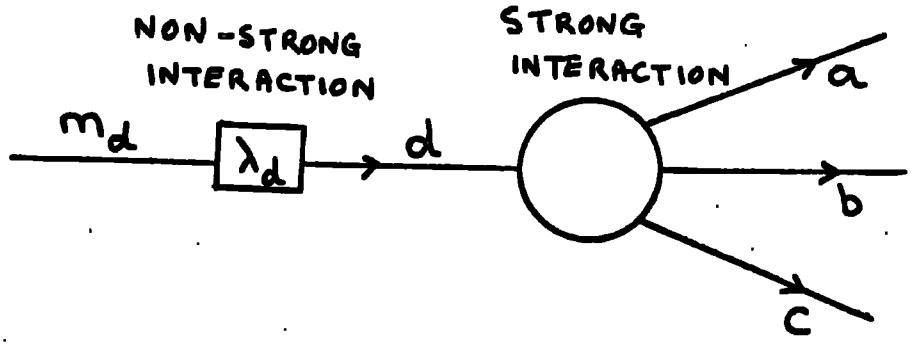

$$s = (p_4 - p_3)^2$$

$$t = (p_4 - p_2)^2$$

$$u = (p_4 - p_1)^2$$

Fig. 3.1 The pion pole contribution to the 3π decays of the $K(\eta)$ meson with λ being the weak (electromagnetic) coupling constant.

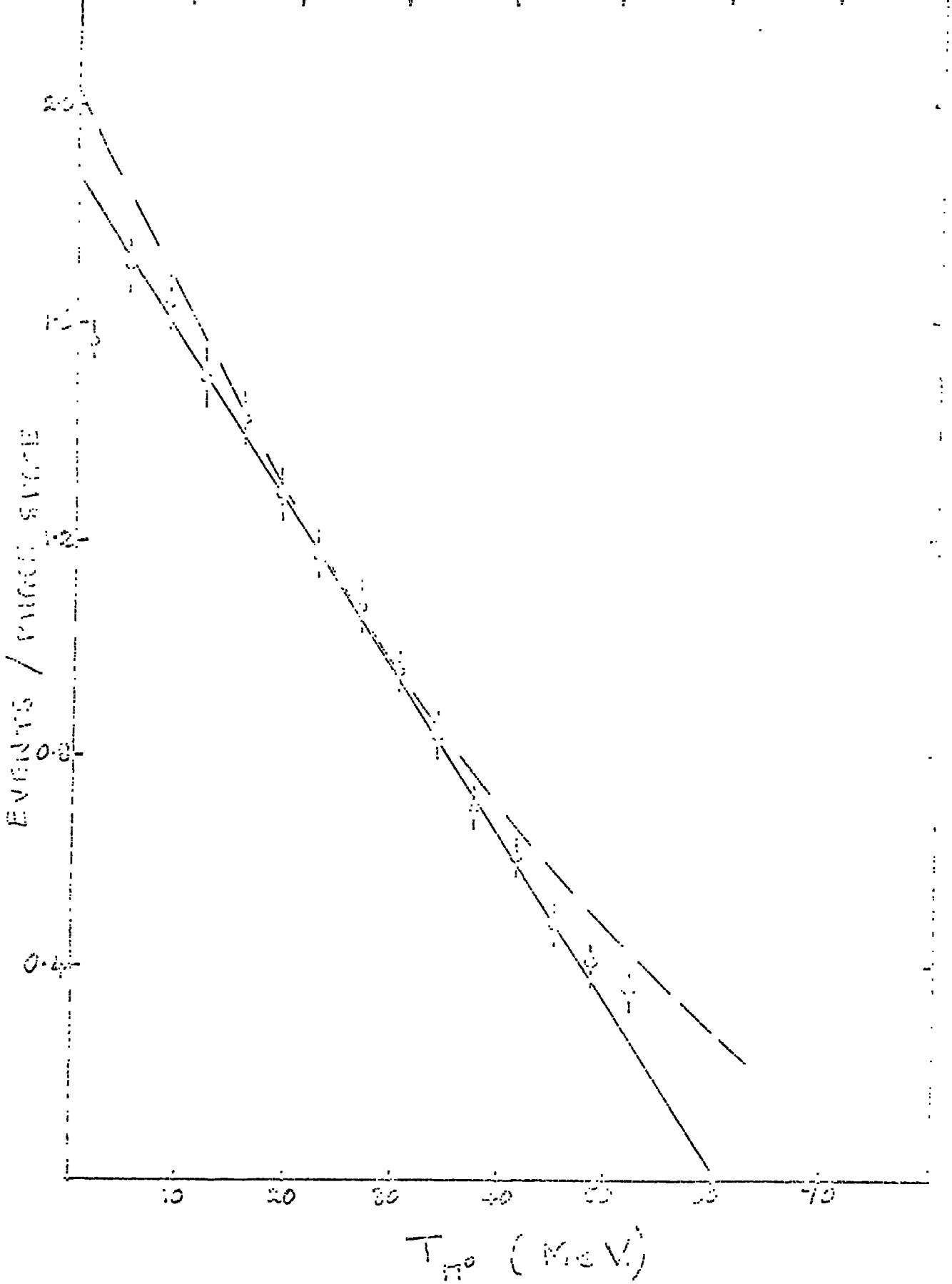

Fig. 3.2 The π^0 kinetic energy spectrum divided by phase space for $K^0 \rightarrow \pi^+ \pi^- \pi^0$. The data is from Ref.(70) with the solid line a linear fit and the dashed line showing quadratic and cubic effects.

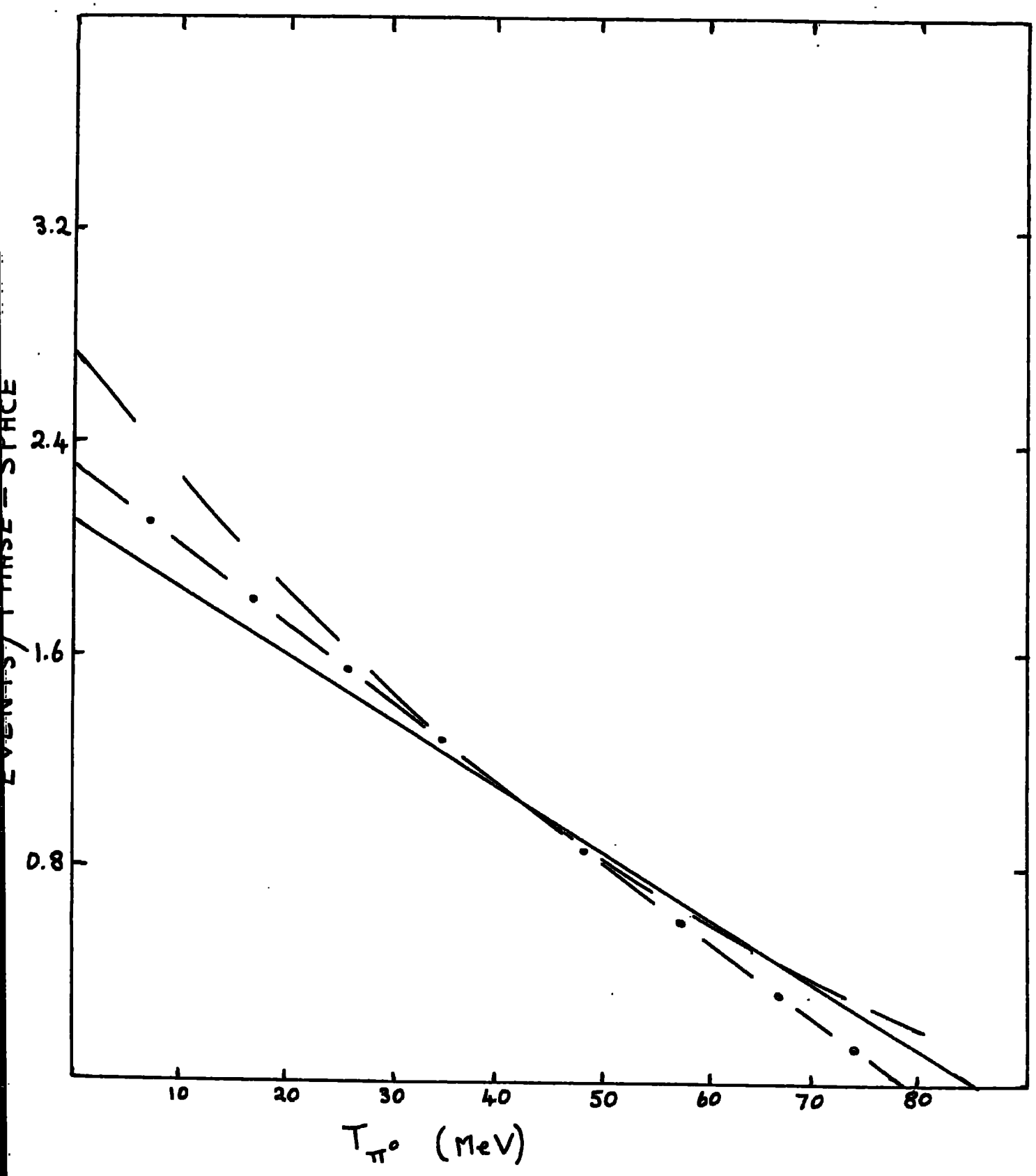

Fig. 3.3 The π^0 kinetic energy spectrum divided by the phase space for $\eta^0 \rightarrow \pi^+ \pi^- \pi^0$. The data (solid line) is from Ref.(74) with the linear fit (—·—·—·) and quadratic and cubic effects (— — — —) also shown.

CHAPTER 4

EFFECTIVE-RANGE EXPANSIONS FOR $\pi\pi$ AND πK SCATTERING

4.1 Introduction

In this chapter we investigate the effective-range expansions which enable us to analytically continue the $\pi\pi$ and πK current algebra models of Weinberg (10) and Griffith (11) above threshold, and thus enable us to do a phenomenological analysis of recent experimental data. The work is based on an article by the author (76).

We do not investigate any of the P-wave effects as the ρ is well fitted by the effective-range expansion (2.39), and from the shape of the phase-shifts the K* (892), can be similarly treated.

In the next section we review the work of Brown and Goble (55) in extending Weinberg's amplitudes for $\pi\pi$ scattering up to the resonance region, and how their analysis has been modified (77, 78) so as to make the I = 0 S-wave resonate near the ρ mass. Then we investigate how the work of Dilley (23) fits into the two extrapolation schemes. In section 3 we firstly extend the current algebra model of Griffith (11) for πK scattering to the resonance region, and then we constrain the I = $\frac{1}{2}$ S-wave to resonate, and compare our predicted phase-shifts with recent experimental data. Finally we compare our predictions with those of the Lovelace-Veneziano model (18).

4.2 Effective-range expansions for $\pi\pi$ scattering

A simple extrapolation of Weinberg's current algebra scattering amplitudes consistent with elastic unitarity has been proposed by Brown and Goble (55), and they make predictions for

the I = 0 and I = 2 S-wave phase-shifts up to energies around the kaon mass. The value they obtained for $\delta_0^0 - \delta_0^2$ at the kaon mass agrees well with that obtained from $K \to 2\pi$ decay rates. In addition the P-wave amplitude, when continued to higher energies via an effective-range expansion, with parameters fixed by requiring a resonance of the ρ mass, leads to a slightly modified version of the KSRF relation (51) determing the width of the in terms of its mass and the pion decay constant in good agreement with experiment.

The current algebra $\pi\pi$ amplitudes are given in Appendix D (D23 - 25) and can be written as

$$F_0^0(s) = (2s - \mu^2)\, a_0/7\mu^2, \qquad \text{(D23)}$$

$$F_1^1(s) = (s - 4\mu^2)\, a_1/4, \qquad \text{(D24)}$$

$$F_0^2(s) = (s - 2\mu^2)\, a_2/2\mu^2, \qquad \text{(D25)}$$

where a_0, a_1, a_2 are the scattering lengths.

We now write an once unsubtracted dispersion relation for the inverse amplitude with the only branch-cut being the right-hand unitarity cut which gives a contribution H(s) to the inverse amplitude, where H(s) is given by equation (2.4).

We now define $g_l^I(s)$ by

$$\left[A_l^I(s)\right]^{-1} = H(s) + g_l^I(s) \qquad (4.1)$$

so that $g_l^I(s)$ represents the contributions of the poles in the dispersion relation (2.3), and is a meromorphic function except for the inelastic unitarity cut along the positive real axis for $s > 16\mu^2$, and a cross-channel cut along the negative real axis ($s < 0$). We can write the ~~partial-wave~~ effective range expansion as

$$\rho(s)\ \text{ctg}\ \delta_l^I = (H(s) + i\rho(s)) + g_l^I(s) = \text{Re}\left[A_l^I(s)\right]^{-1},\ s > 4^2. \tag{4.2}$$

The current algebra S-wave amplitudes both vanish in the gap $0 \leq s \leq 4^2$ below the elastic threshold, and thus from (4.1) it is clear that $g_l^I(s)$ has a pole in this gap, and hence it is not possible to parameterise it as a finite polynomial in s. Accordingly we shall instead write the inverse function as a first order polynomial in s. We determine the coefficients of this expansion by fitting it to the current algebra amplitude at the point where the latter vanishes, and thus we obtain the same simple form for the unitarily corrected amplitude as from the Lovelace K-matrix method (18) (1.13), namely

$$A_0^I(s) = \frac{F_0^I(s)}{1 + H(s)\, F_0^I(s)} \tag{4.3}$$

The phase-shifts that follow from this assumption are shown as dashed lines on figure (4.1) where it can be seen that both phase-shifts are small with $\delta_0^0 \approx 30^\circ$ and $\delta_0^2 \approx -40^\circ$ at 700 MeV.

Enough data is now available to compare the S-wave phase-shifts obtained from Brown and Goble's method with experiment, as has been discussed in chapter 2. The predictions for δ_0^2 are too large, while the predictions for δ_0^0 are too small above the kaon mass as there is no σ resonance predicted, and if we believe the work of Weinberg on the algebraic realizations of chiral symmetry the ρ and σ masses are equal.

There have been several generalisations (77, 78) of Brown and Goble's procedure to improve the predictions for δ_0^0 in the region 500 - 1000 MeV. so as to include the σ as an S-wave resonance,

and we follow here the method of Greenberg (78) although all the methods are basically just different parameterisations for $g_o^I(s)$ so as to put in the σ. We give three parameterisations for $g_0^o(s)$:

$$\begin{aligned} 1) \quad g(s) &= (1/\alpha)/(1+ ck^2) + bk^2, \\ 2) \quad g(s) &= (1/\alpha + bk^2)/(1 + ck^2), \\ 3) \quad g(s) &= (1/\alpha)/(1 + ck^2) + b, \end{aligned} \tag{4.4}$$

where α is the scattering length, c is determined by the Adler zero in the I = 0 S-wave current algebra amplitude at $s = 0.5\mu^2$. The constant b, which can be thought of as giving some measure of the left-hand cut contribution to the amplitude, is determined by requiring that there is a resonance near the ρ mass and at the resonance position we have $\mathrm{ctg}\,\delta_o^o = 0$.

The amplitude $A_o^o(s)$ is now given by a generalised effective - range expansion and it matches the current algebra amplitude at threshold and the Adler zero. We can now use equation (4.2) to predict the phase shifts, and the width of the resonance is obtained by evaluating twice the difference in $\sqrt{s}$ of the phase-shifts at 45^o and 90^o.

The best fit to the data is shown on figure (4.1). This comes from model 1) for g(s) as the other two parameterisations result in a width greater than the resonance mass, and phase-shits smaller than the experimental values when s is greater than m_σ^2. The best fit comes from taking the resonance position to be at 730 MeV and then we predict the width of the σ to be 250 MeV.

An interesting feature of the amplitude in equation (4.2) is that

$$\lim_{s\to\infty} A_0^0(s) \sim 1/\ln s \qquad (4.5)$$

This is just the behaviour expected for $A_0^0(s)$ if the high-energy $\pi\pi$ scattering is dominated by Pomeranchuk exchange with a constant residue function and linear Regge trajectory.

- - - - - - - - - - - - - -

The technique used by Dilley (23) which has been mentioned earlier (see section (2.1)) gives predictions for the amplitudes in the region $s = 4\mu^2$ to $s = 8\mu^2$. We expand the invariant amplitude $A(s,t,u)$ in a power series in k_s, k_t and k_u which are defined by (24).

$$\begin{aligned} k_s &= \tfrac{1}{2}\sqrt{4\mu^2 - s}, \\ k_t &= \tfrac{1}{2}\sqrt{4\mu^2 - t}, \\ k_u &= \tfrac{1}{2}\sqrt{4\mu^2 - u}. \end{aligned} \qquad (4.6)$$

Thus below the physical $\pi\pi \to n\bar{n}$ threshold at $s = 4\mu^2$ the amplitude will be purely real and as we continue the amplitude above threshold some of the terms will develop imaginary parts. Next we impose elastic unitarity on the amplitude by defining

$$R^I(s) = \frac{\text{Im } A_0^I(s)}{\sqrt{(s-4\mu^2)/s}\; A_0^I(s)^2} \qquad (4.7)$$

where $R^I(s) = 1$ for exact elastic unitarity. We now define the root-mean-square deviation of $R^I(s)$ from unity in the interval $4\mu^2 \le s \le 8\mu^2$ as

$$\delta R^I(s) = \frac{1}{\sqrt{n}}\left(\sum_{i=1}^{n}\left(R^I(s_i) - 1\right)^2\right)^{\frac{1}{2}} \qquad (4.8)$$

where s_i are equally spaced points in the interval. We now vary the coefficients of the power series expansion so as to minimize

$\delta R^I(s)$. Fixing the S-wave scattering length $a_0 = 0.16$ we find the best fit gives $\delta_0^0 \approx 15^0$ and $\delta_0^2 \approx -5^0$ at $s = 8\mu^2$ (400 MeV.^{2}). This agrees with both the solutions, with (77, 78) and without (55), putting in the σ, but in this case we have not inserted any kinematic zero in the amplitude at the σ mass, so we can consider Dilley's type II solutions as having a non-resonant I = 0 S-wave.

4.3 Effective-range expansions for π K scattering

Having obtained a phenomenological description of the low-energy $\pi\pi$ data up to near 1 GeV we now extend our analysis and investigate the πK system which is similar to the $\pi\pi$ system in that there is a strong resonance in the I = $\frac{1}{2}$ P-wave, the K* (892), with a broad S-wave resonance lying somewhere near it. First of all we investigate the effect of unitarity corrections to the current algebra model in the same way as Brown and Goble (55) and then we analyse the effect of forcing the I = $\frac{1}{2}$ S-wave to contain a broad resonance.

We again write for the phase-shift

$$\frac{2k}{\sqrt{s}} \operatorname{ctg} \delta_0^I = H(s) + \frac{2ik}{\sqrt{s}} + g_0^I(s) = \mathrm{Re}\left[A_0^I(s)\right]^{-1}, \qquad (4.2)$$

where now we have unequal mass kinematics and

$$k^2 = (s - (m+\mu)^2)\ (s - (m-\mu)^2)/4s. \qquad (A12)$$

The function H(s) is chosen as before so as to enforce elastic unitarity and is given by a once subtracted dispersion relation for the inverse amplitude with the only branch-cut being along the right-hand unitarity cut in the complex s-plane

$$H(s) = \frac{s-(m+\mu)^2}{\pi}\int_{(m+\mu)^2}^{\infty} - \frac{2\,k(s')\,ds'}{\sqrt{s'}\,(s'-s)(s'-(m+\mu)^2)} \qquad (4.9)$$

The discontinuity of H(s) across the right-hand cut is $-2k/\sqrt{s}$ as required by unitarity, and it is well behaved asymptotically as

$$\lim_{s\to\infty} \text{Re } H(s) \sim \ln s. \qquad (4.10)$$

A subtraction is put in at threshold so as to force

$$H\,(s = (m+\mu)^2) = 0, \qquad (4.11)$$

and at threshold the amplitude is then given just by $g_0^I(s)$ which will give the correct scattering length.

The current algebra amplitudes of Griffith (11) can be written

$$F_0^{\frac{1}{2}}(s) = \frac{a_{\frac{1}{2}}}{4m\mu}\,(2s - 3k^2 - 2m^2 - 2\mu^2), \qquad (D47)$$

$$F_0^{\frac{3}{2}}(s) = \frac{a_{3/2}}{2m\mu}\,(s - m^2 - \mu^2), \qquad (D48)$$

where $a_{\frac{1}{2}}$ and $a_{3/2}$ are the scattering lengths. These amplitudes have zeros at $s = 11.95\mu^2$ for $F_0^{\frac{1}{2}}$ and $s = 13.45\mu^2$ for $F_0^{\frac{3}{2}}$, and by fitting a first order polynomial for $\left[g_0^I(s)\right]^{-1}$ to the current algebra amplitudes at the points where the latter vanish we again find the unitarized amplitude $A_0^I(s)$ is given by equation (4.3). The phase-shifts that this ansatz produces are shown as dashed lines in figures (4.2) and (4.3) with the scattering lengths given by current algebra as $a_{\frac{1}{2}} = -2a_{3/2} = 0.22$. Similar to the case the $I = \frac{3}{2}$ S-wave phase-shift is too big being -67° at

1250 MeV, whereas the $I = \frac{1}{2}$ S-wave shows no tendency to resonate and is too small, being 32° at 1250 MeV.

- - - - - - - - - - -

Ader et al. (25) have generalized the approach used by Dilley (23) to π K scattering. They give polynomial expansions for $A^{\pm}$ (s,t,u) in terms of the following variables

$$\begin{aligned} q_s &= \tfrac{1}{2}\sqrt{(m+\mu)^2 - s}, \\ q_t &= \tfrac{1}{2}\sqrt{4\mu^2 - t} \\ q_u &= \tfrac{1}{2}\sqrt{(m+\mu)^2 - u}, \end{aligned} \qquad (4.12)$$

They then impose elastic unitarity in the strip $((m+\mu)^2, (m+2\mu)^2)$ by defining

$$\delta R(s) = \sum_{i=1}^{n} \left((1 - R^{\frac{1}{2}}(s_i))^2 + (1 - R^{\frac{3}{2}}(s_i))^2 \right)^{\frac{1}{2}}$$

where

$$R^I(s) = \frac{\text{Im } A_0^I(s)}{2k/\sqrt{s}\,\left|A_0^I(s)\right|^2} \qquad (4.7)$$

and s_i are equally spaced in the interval. They obtain minimum values for $\delta R(s)$ for S-wave scattering lengths in the region

$$\begin{aligned} a_{\frac{1}{2}} &= 0.12 \pm 0.05, \\ a_{\frac{3}{2}} &= -0.085 \pm 0.04, \end{aligned} \qquad (4.13)$$

and the P-wave scattering length is given by a Breit-Wigner expression for the K* (892) with width 50 MeV.

Their predictions for the phase-shifts at 900 MeV are

$$\begin{aligned} \delta_0^{\frac{1}{2}} &= 30^{\circ} \pm 5^{\circ}, \\ \delta_0^{3/2} &= -25^{\circ} \pm 5^{\circ}. \end{aligned}$$

This agrees well with the non-resonant solutions shown in figures (4.2) and (4.3) in that the $I = \frac{1}{2}$ S-wave is too small whilst the $I = \frac{3}{2}$ S-wave is too large at 900 MeV.

- - - - - - - - - -

Before we consider the effect of making the $I = \frac{1}{2}$ S-wave resonate somewhere near the K* (892) it is interesting to see what the experimental results are.

$K\pi$ phase-shift analyses have recently been performed (79 - 81) using the reactions

$$K^+p \rightarrow K^+ \pi^- \Delta^{++} , \qquad (4.14)$$

$$K^+p \rightarrow K^0 \pi^0 \Delta^{++} , \qquad (4.15)$$

and we compare our predicted phase shifts with the data.

Trippe et al. (79) have performed a pole-extrapolation analysis of reactions (4.14) and (4.15) use Dürr - Pilkuhn form-factors and they showed that the observed moments of the $K\pi$ angular distribution have the properties of a slowly increasing $I = \frac{1}{2}$ S-wave phase-shift reaching 90^0 near 1100 MeV. They obtain a rough compatibility with the data by assuming a Breit-Wigner of mass 1100 MeV and width 400 MeV, although this does give incorrect threshold behaviour.

The Johns Hopkins group (80) have extrapolated the $d^2\sigma/dmdt\langle Y_l^0 \rangle$ quantities for both reactions to the pole, and performed an on-shell partial-wave analysis. They obtain an ambiguity in the phase-shifts similar to that in $\pi\pi$ (82) in that two solutions are obtained, one of which goes slowly through 90^0 at 1100 MeV, whilst the

other goes rapidly through 90^0 near the K*(892), but by comparing the extrapolated cross-section they prefer a resonance near 1100MeV.

A similar analysis to that of the Johns Hopkins group has been done by the Brussels - CERN - UCLA collaboration (81), with again an ambiguity in the phase-shifts, and one solution going rapidly through 90^0 at 900 MeV.

Yuta et al. (83) have analysed the K phase-shifts from

$$K^- p \rightarrow K^- \pi^+ n, \qquad (4.16)$$

and obtained S-wave phase-shifts in good agreement with those of references (80, 81) so we will only compare our predictions to those of the first two sets of data.

Following Greenberg (78) we make three parameterisations for $g_0^{\frac{1}{2}}(s)$ labelled 1) 2) 3) in figure (4.2)

$$\begin{aligned} 1) \quad & g(s) = (1/\alpha) \,/\, (1 + ck^2) + bk^2 \\ 2) \quad & g(s) = (1/\alpha + bk^2) \,/\, (1 + ck^2), \qquad (4.4) \\ 3) \quad & g(s) = (1/\alpha) \,/\, (1 + ck^2) + b, \end{aligned}$$

where α is the $I = \frac{1}{2}$ S-wave scattering length: and c is chosen to give the zero at the same point as the $I = \frac{1}{2}$ S-wave given by Griffith (11), while b is again chosen so as to give a resonance at $s = M^2$ by making ctg $\delta_0^{\frac{1}{2}}(s = M^2) = 0$.

We consider three values of the scattering length: $\alpha = 0.17$, 0.22 - Griffith's current algebra value, and $\alpha = 0.27$, so that we can test the sensitivity of our results. Setting M = 1100 MeV throughout the predicted widths of the resonance are given in table 1, and the resulting phase-shifts and their fit to the data are shown in figures (4.2) and (4.4). We find, similar to the $\pi\pi$ case the best fit to the data is with model 1) and $\alpha = 0.22$ although $\alpha = 0.17$ fits nearly as well. In general, a variation in α of 25% produces a variation in phase-shift at 900 MeV of 15%.

The position of the pole in g(s) is dependent on the way we extrapolate off mass-shell to the Adler zero, and this is not uniquely defined (section (2.4)). However, our predictions for the width are relatively insensitive to the exact position of the zero and a change in the position of the pole of 40% results in a change in the predicted width of less than 10%.

If we use the current algebra amplitude for $g_0^{\frac{1}{2}}(s)$

$$g_0^{\frac{1}{2}}(s) = \frac{4\,m\mu}{a_{\frac{1}{2}}^{1}\,(2s - 3k^2 - 2m^2 - 2\mu^2)} + bk^2 \qquad (4.17)$$

then we get phase-shifts in good agreement with model 1) and a predicted width of 450 MeV, which is not too surprising as the two parameterisations are constrained to be equal at three points: Adler zero, threshold and resonance position.

If we take the constant b as some contribution from the left-hand cut in a dispersion relation for the inverse amplitude, and assume that the $I = \frac{3}{2}$ S-wave has the same left-hand cut contribution i.e. we put

$$g_0^{3/2}(s) = \frac{2\,m\mu}{a_{3/2}\,(s - m^2 - \mu^2)} + bk^2 \qquad (4.18)$$

then we find the $I = \frac{3}{2}$ S-wave phase-shift is considerably reduced and for $a_{\frac{3}{2}} = -0.11$ we find $\delta_0^{3/2} = -25^\circ$ at 1250 MeV as is shown in figure (4.3). The corresponding value for $a_{\frac{3}{2}} = -0.085$ is $\delta_0^{3/2} = -19^\circ$.

4.4 Discussion

We can thus conclude that the current algebra amplitude for πK scattering when extrapolated above threshold by means of an

effective-range expansion which imposes elastic unitarity on the amplitude is compatible with experimental data for the S-waves in that:

(i) the $I = \frac{1}{2}$ S-wave is large, positive and resonates near 1100 MeV;

(ii) the $I = \frac{3}{2}$ S-wave is small and negative.

Our fit to the data of references (80, 81) is good even out to 1250 MeV although we are neglecting inelastic effects and contributions from the cross-channel on the left-hand cut are only approximated by the effective-range expansion for g(s). This suggests that these effects may be small up to 1250 MeV.

The two sets of data have ambiguities in their $I = \frac{1}{2}$ S-wave phase-shifts as discussed earlier, but the Johns Hopkins group (80) prefer a solution which is in good agreement with ours. It is interesting to note that Lovelace predicts a resonance under the K* (892) using a unitarised Veneziano model (18) (see figure (1.4)), as here the resonance is forced to be a daughter of the K* (892). If we make our model resonate at 900 MeV by altering b we get a predicted width for model 1) with $\alpha = 0.22$ of 130 MeV as against the 210 MeV predicted by Lovelace, and more in agreement with the rapidly varying phase-shifts indicated by the data.

In principle we can discriminate between the two solutions by measuring the $K^+\pi^-$ elastic cross-sections at the K* (892), but up to date the statistics have not been sufficiently accurate (84). However, the present results show no evidence for a narrow S-wave resonance on top of the K* (892), and if such an effect were present it should also be observed in the physical K* mass spectra; but no such effect has yet been reported.

Table 1

Predicted widths for scattering lengths α, and different models

α	1	2	3
0.17	325	375	420
0.22	470	525	575
0.27	520	575	635

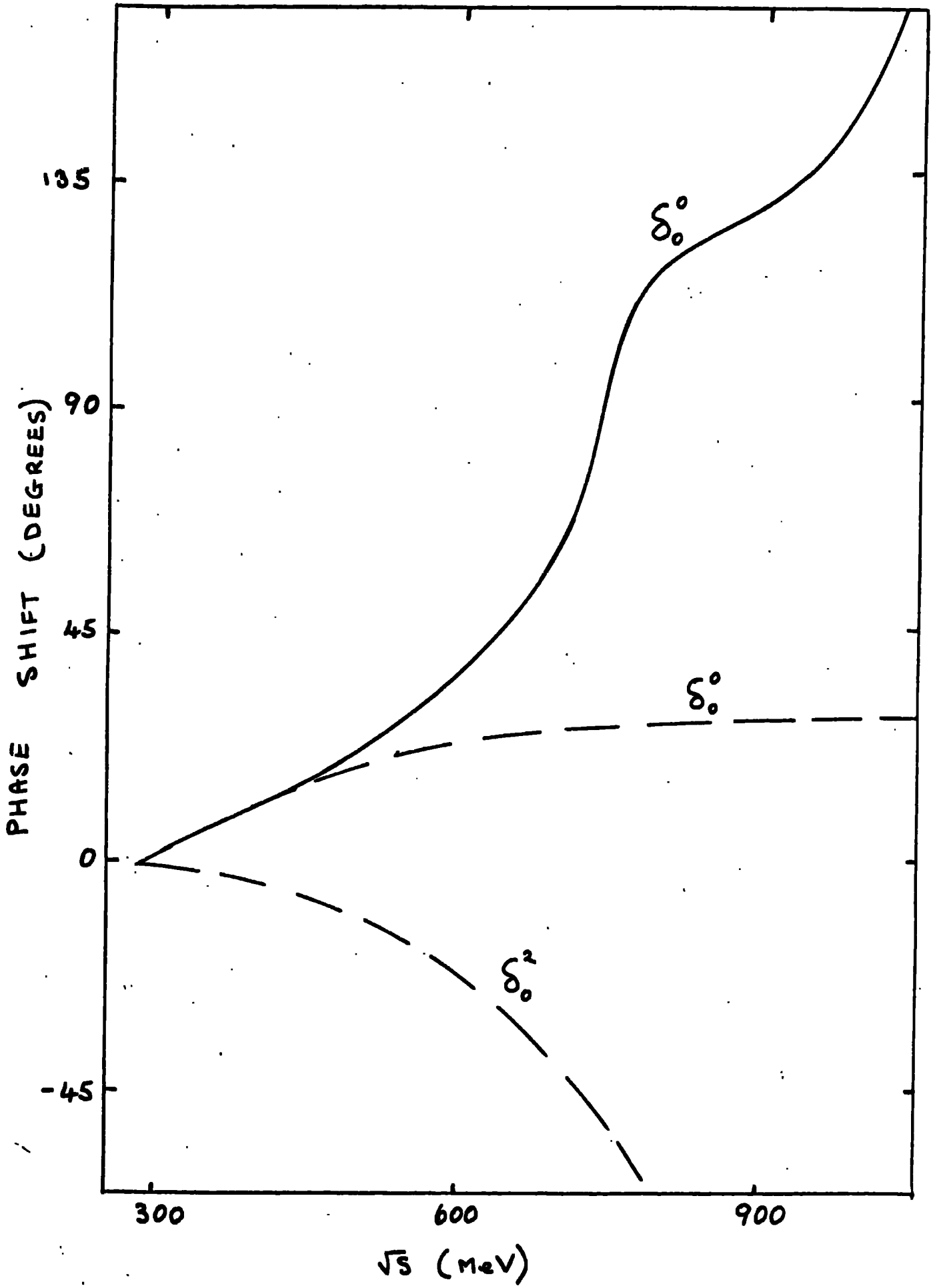

Fig. 4.I S-wave phase shifts given by Ref. (55) (dashed line) and by Ref. (78).

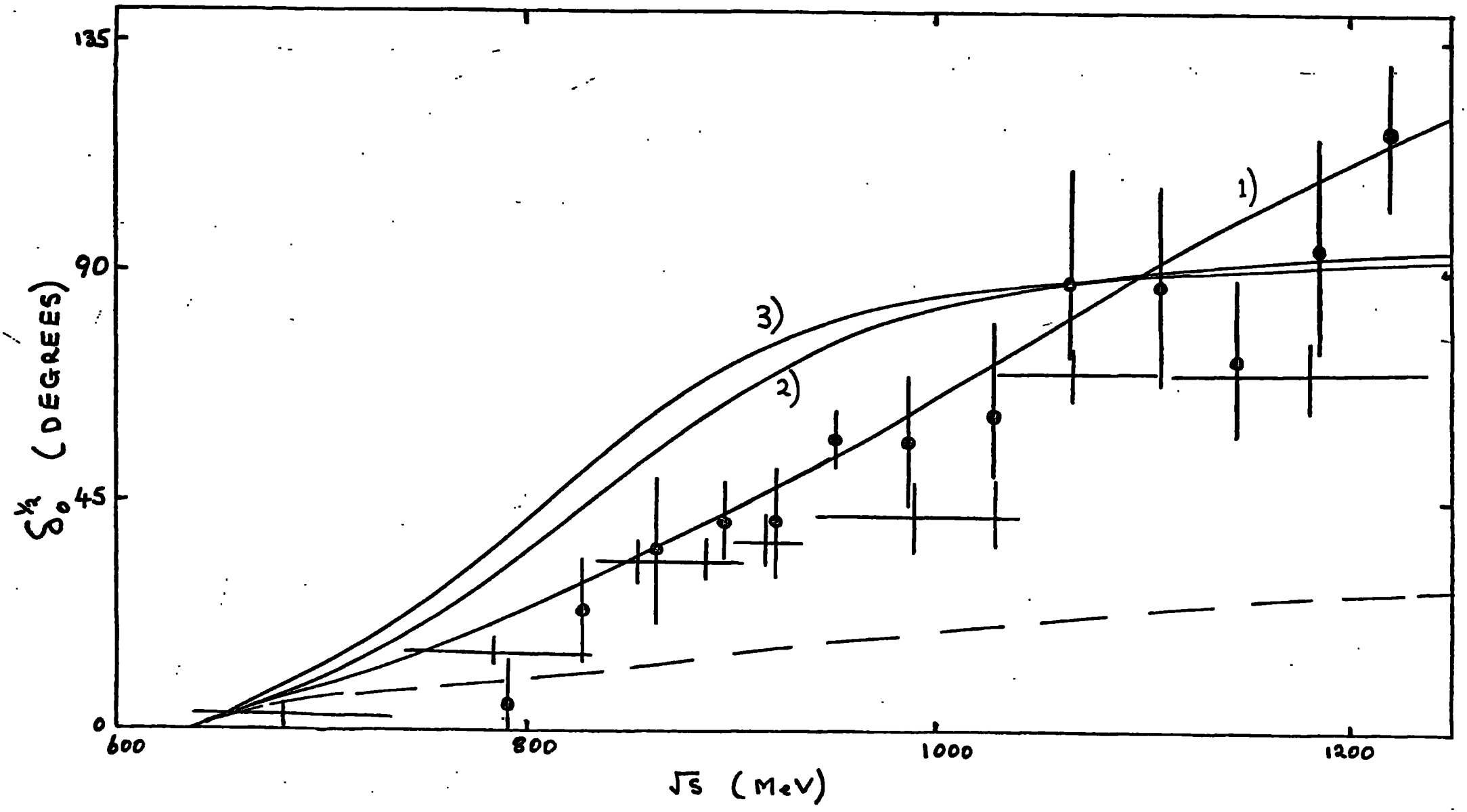

Fig . 4.2 The I = 1/2 S-wave phase shifts with $\alpha = 0.22$. The data is from Ref. (80) (|) and Ref. (81) (+) with the non-resonant effective range expansion also shown (dashed line) .

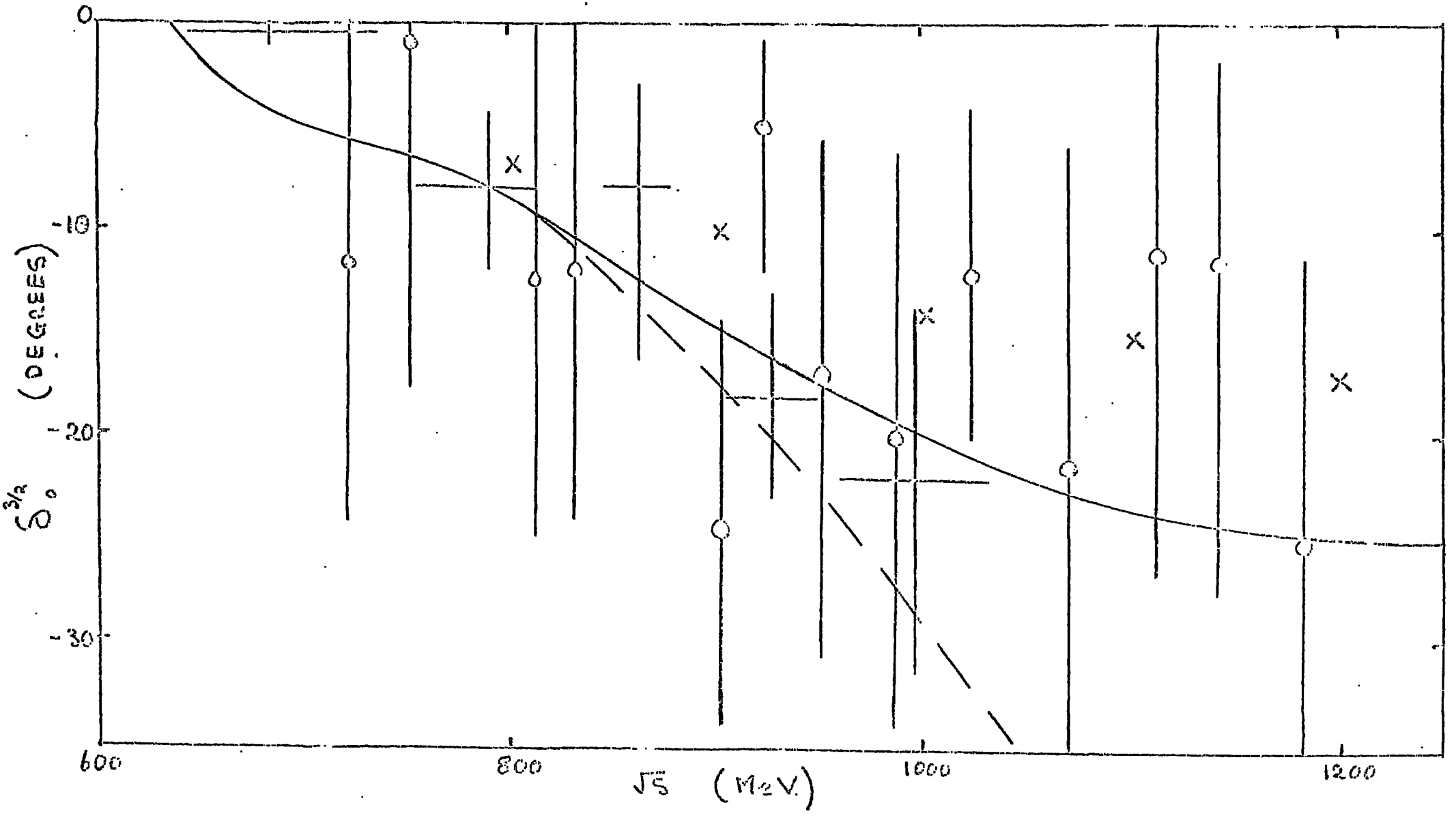

Fig. 4.3 The I = 3/2 S-wave phase shifts with $a^{3/2} = -0.11$. The data is from Ref. (80) (|), Ref. (81) (+), and Ref. (83) (×). The solution with a non-resonant I = 1/2 S-wave is shown as a dashed line.

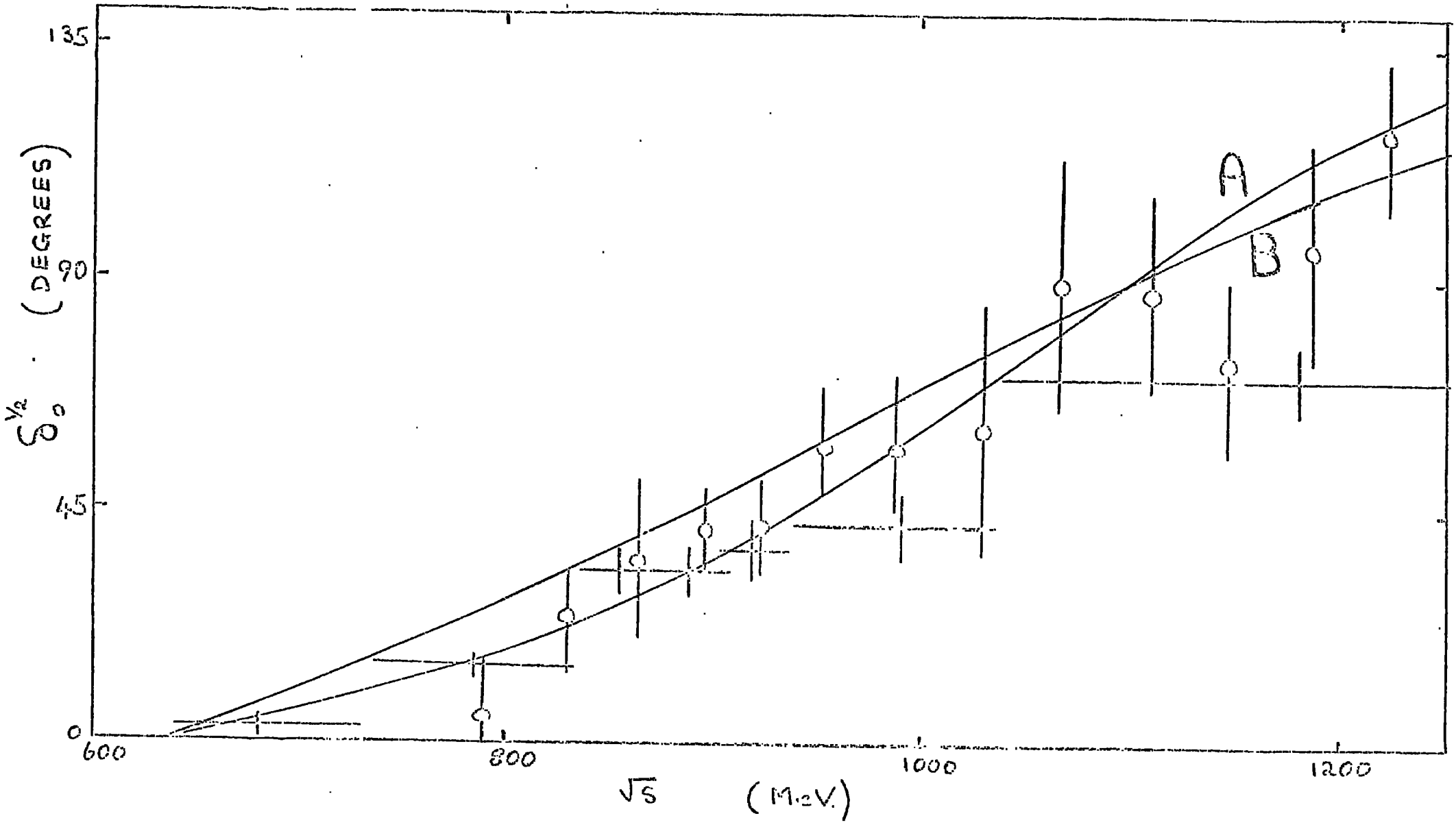

Fig. 4.4 The I = 1/2 S-wave phase shifts with $\alpha = 0.17$ (A) and $\alpha = 0.27$ (B). The data is as on Fig. 4.2.

CHAPTER 5

LOW-ENERGY $\pi\pi$ K SCATTERING

5.1 Introduction

Now that detailed experimental studies of $\pi K \to \pi\pi K$ scattering are becoming possible there is growing interest in theoretical predictions for this process. The model which is presented in this chapter is similar in construction to the one given in chapter 2. The basic assumption is made that the appropriate scattering amplitudes are smooth and simple functions of the energy-momentum variables on and near the mass-shell.

There are two dynamical assumptions:

(i) the existence of the K* (892) meson in the $I = \frac{1}{2}$ $l = 1$ amplitude;

(ii) the dominance of the $I = 1$ $l = 1$ $\pi\pi \to K\bar{K}$ amplitude by the ρ meson.

In addition we make physical assumptions similar to those we made for the $\pi\pi \to \pi\pi$ calculation in chapter 2.

(iii) only S- and P-waves contribute in the region of interest $\sqrt{s} \leq 1.3$ GeV;

(iv) the S-wave scattering lengths are small;

(v) elastic unitarity holds over the entire region of interest;

(vi) the contributions to the partial-wave series from the left-hand cut and circle cut can be evaluated directly from the crossed channel partial wave series.

The discussion of the validity of these expressions is the same as that given in chapter 2 and is reviewed briefly for the sake of completeness.

In making these assumptions we are aware that through analyticity and crossing both higher partial-waves and absorptive effects in the region $\sqrt{s} \leq 1.3$ GeV can influence the lower partial waves. These possibilities are discussed in the calculations.

The assumption of small S-wave scattering lengths is very restrictive but is well supported by current theoretical models (11, 18, 25, 29, 85, 86).

The sixth assumption is equivalent to disregarding the presence of third double spectral functions and in practice as our dispersion relations are subtracted, the results are insensitive to the distant left-hand cut. The assumption is necessary in order for us to obtain a closed system of equations.

In the next section we give the construction of the inverse amplitude dispersion relations for $l < 2$ and show how they are solved when expressed in terms of subtraction constants and zeros of the amplitude. A model for the amplitudes below threshold is then given and we see how this is constrained by analytic constraints and crossing sum rules similar to those used in previous chapters. Finally we discuss the numerical results we obtain.

5.2 Method

The partial wave amplitude $A_l^I(s)$ has the following singularities in the complex s-plane:

(i) a right-hand cut $(m+\mu)^2 \leq s < \infty$;

(ii) a left-hand cut $-\infty < s \leq (m-\mu)^2$;

(iii) a circle cut $|s| = m^2 - \mu^2$.

We define a function $G_l^I(s)$ by

$$G^I_l(s) = 1/(k^2(s)\ A^I_l(s)\ (s-s_0)),$$

and also we define $B^I_l(s) = (A^I_l(s))^{-1}$, then on the right hand cut elastic unitarity can be expressed as

$$\text{Im}\ B^I_l(s) = -2k(s) / \sqrt{s}.$$

In the complex s-plane very high energy scattering contributes through crossing around the point $s = 0$. Now $k^2 \to \infty$ as $s \to 0$ so these high energy contributions are suppressed and also the effect of unknown distant singularities is very much reduced. A subtraction is made as $s = s_0$ (which may depend on I and l) so as to further dampen the unknown large s behaviour of the amplitude.

A dispersion relation for $G^I_l(s)$ may be written (93)

$$B^I_l(s) = H(s) - H(s_0) + k^2(s)\, B^I_l(s_0)/k^2(s_0) + L^I_l(s) + C^I_l(s) + P^I_l(s). \qquad (5.1)$$

The elastic right-hand cut contribution can be evaluated in closed form independent of I and l to give

$$H(s) = \frac{-k^2(s)}{\pi} \int_{(m+\mu)^2}^{\infty} \frac{2k(s')\, ds'}{\sqrt{s'}\, k^2(s')\, (s'-s)},$$

$$= \frac{-2k(s)}{\pi\sqrt{s}} \log\left(\frac{s - m^2 - \mu^2 - 2k(s)\sqrt{s}}{2m\mu}\right) \qquad (5.2)$$

and similarly we have

$$H(s_0) = \frac{k^2(s)}{\pi} \frac{2}{k(s_0)\sqrt{s_0}} \tan^{-1}\left(\frac{2k(s_0)\ s_0}{s_0 - m^2 - \mu^2}\right)$$

when $(m-\mu)^2 < s_0 < (m+\mu)^2$.

The left-hand cut contribution is

$$L_l^I(s) = (s-s_o)\,\frac{k^2(s)}{\pi}\int_{-\infty}^{(m-\mu)^2}\frac{\mathrm{Im}\,B_l^I(s')\,ds'}{k^2(s')\,(s'-s)\,(s'-s_o)} \qquad (5.3)$$

and the contribution from the circle cut is

$$C_l^I(s) = (s-s_o)\,\frac{k^2(s)}{\pi}\int_{|s|=m^2-\mu^2}\frac{\Delta B_l^I(s')\,ds'}{k^2(s')\,(s'-s)\,(s'-s_o)} \qquad (5.4)$$

where $\Delta B_l^I(s)$ is given by

$$\Delta B_l^I(s) = \lim_{\varepsilon\to 0}\left(B_l^I((|s|+\varepsilon)e^{i\varphi}) - B_l^I((|s|-\varepsilon)\,e^{i\varphi})\right), \qquad (5.5)$$

where $|s| = m^2-\mu^2$ and $s = |s|\,e^{i\varphi}$.

Zeros of the amplitude at threshold ($k^2(s) = 0$) are given by the term $P_l^I(s)$.

The S-wave amplitude does not vanish when $k^2\to 0$ and k^2 has two zeros: at $s = (m-\mu)^2 = X$ and $s = (m+\mu)^2 = Y$ and we obtain

$$P_o^I(s) = k^2(s)\,(s-s_o)\left[\frac{-4Y}{(Y-X)\,(Y-s_o)\,A_o^I(Y)\,(Y-s)} - \frac{4X}{(X-Y)\,(X-s_o)\,(X-s)\,A_o^I(X)}\right] \qquad (5.6)$$

The P-wave amplitude vanishes when $k^2\to 0$ and thus $P_1^I(s)$ has contributions from two second order poles. If we have $A_1^I = \alpha k^2$ when $s = X$ and $A_1^I = \beta k^2$ when $s = Y$ then

$$P_1^I(s) = k^2(s)\,(s-s_o)\left[\frac{d}{ds'}\left(\frac{-16(s')^2}{(s'-Y)^2\alpha(s'-s)(s'-s_o)}\right)\Bigg|_{s'=X} + \frac{d}{ds'}\left(\frac{-16(s')^2}{(s'-X)^2\beta(s'-s)\,(s'-s_o)}\right)\Bigg|_{s'=Y}\right] \qquad (5.7)$$

The discontinuity across the crossed physical cut $0 \leq s \leq (m-\mu)^2$ is given in terms of the imaginary part of the physical πK scattering amplitude.

The circle cut discontinuity is given in terms of the absorptive part of the amplitudes for the t-channel process $\pi\pi \to K\bar{K}$.

All the processes discussed above contribute to the left hand cut $-\infty < s < 0$, but in addition there are many other contributions from, for example, the more massive intermediate states in the t-channel (4π, 6π, $K\bar{K}$ etc.) Some of these contribute also to the back of the circle cut ($s = \mu^2 - m^2$) e.g. $\pi\pi \to K\bar{K}$.

Thus for any value of s on the cut $-\infty < s \leq (m-\mu)^2$ we have by crossing

$$\mathrm{Im}\, A^I_l(s) = -\frac{1}{4k^2}\int_{\Sigma-s}^{c(s)} P_l\left(1+\frac{\Sigma-s-u}{2k^2}\right)\sum_{I'=\frac{1}{2}}^{\frac{3}{2}} \alpha_{II'}\sum_{l'=0}^{1}(2l'+1)\,P_{l'}\left(1+\frac{\Sigma-u-s}{2(\bar{k})^2}\right)\mathrm{Im}\, A^{I'}_{l'}(u)\,du$$

$$+\,\theta(-s)\frac{2}{4k^2}\int_{4\mu^2}^{-4k^2} P_l\left(1+\frac{t'}{2k^2}\right)\sum_{I'=0}^{1}\gamma_{II'}\sum_{l'=0}^{1}(2l'+1)\,P_{l'}\left(\frac{s+p^2+q^2}{2pq}\right)(pq)^{l'}\mathrm{Im}\, F^{I'}_{l'}(t')\,dt' \qquad (5.8)$$

where $(\bar{k})^2$ refers to the u-channel three momentum with

$$c(s) = (m^2-\mu^2)^2/s \quad \text{when } 0 < s \leq (m-\mu)^2,$$
$$= (m+\mu)^2 \quad \text{when } s \leq 0.$$

The second term in (5.8) includes the contribution from where the circle cut crosses the left-hand cut at $s = \mu^2 - m^2$.

On the circle cut we introduce a variable λ (93) defined by

$$S^{\pm}(\lambda) = 2\lambda + m^2+\mu^2 \pm 2i\sqrt{(\lambda+m^2)(-\lambda-\mu^2)},$$

so that

$$s^{\pm}(\lambda) = m^2 - \mu^2,$$
$$k^2(s^{\pm}) = \lambda \ .$$

The discontinuity of the scattering amplitude across the circle cut is given by

$$\Delta A^I_l(s_\pm(\lambda)) = \pm\frac{1}{4\lambda}\int_{4\mu^2}^{-4\lambda} P_l\left(1+\frac{t'}{2\lambda}\right)\sum_{I'=0}^{1}\gamma_{II'}\sum_{l'=0}^{1}2(2l'+1)(pq)^{l'}P_{l'}\left(\frac{s_\pm(\lambda)+p^2+q^2}{2pq}\right)\mathrm{Im}\,F^{I'}_{l'}(t')\,dt' \qquad (5.9)$$

The amplitudes on the circle cut are given by:

$$A^I_l(s^{\pm}) = CA^I_l(s) \pm i\,\Delta A^I_l(s), \qquad (5.10)$$
$$B^I_l(s^{\pm}) = CB^I_l(s) \mp i\,\Delta B^I_l(s), \qquad (5.11)$$

where the discontinuity of the inverse amplitude is required for the dispersion relation. It should be noted that the functions $CA^I_l(s)$ and $CB^I_l(s)$ are themselves complex functions.

For each value of $\Delta B^I_l(s)$ we calculate the contribution from the circle cut as follows.

We transform the integral over s to two integrals over λ ; one being the contribution of the cut from the lower half of the circle (s_-), and the other from the top half of the circle (s_+) and we obtain:

$$C^I_l(s) = (s-s_0)\,\frac{k^2(s)}{\pi}\left[\int_{-\mu^2}^{-m^2}\left(\frac{ds_+}{d\lambda}\right)\frac{\Delta B^I_l(s_+)}{\lambda\,(s_+-s)\,(s_+-s_0)}\,d\lambda + \int_{-m^2}^{-\mu^2}\left(\frac{ds_-}{d\lambda}\right)\frac{\Delta B^I_l(s_-)}{\lambda\,(s_--s)\,(s_--s_0)}\,d\lambda\right]$$

Although $\Delta B^I_l(s^{\pm})$ is a complex function, it is a real analytic function in that

$$\Delta B_\ell^I(s+) \quad = \quad -\Delta B_\ell^{I*} \quad (s_-),$$

and so for s real we obtain $C_\ell^I(s)$ also real.

We evaluate $\Delta B_\ell^I(s^\pm)$ using the following iterative procedure:

(i) first time through we put $\Delta B_\ell^I(s) = 0$ and then using the value of $CB_\ell^I(s)$ obtained by evaluating $B_\ell^I(s)$ on the circle cut from equation (5.1) we have $B_\ell^I(s^\pm)$ from (5.11);

(ii) we invert $B_\ell^I(s^\pm)$ to get $A_\ell^I(s^\pm)$ and from the knowledge of $\Delta A_\ell^I(s^\pm)$ we calculate $CA_\ell^I(s^\pm)$ from (5.10);

(iii) the second time through the programme we have new values for $\Delta A_\ell^I(s^\pm)$ and $CB_\ell^I(s^\pm)$ and we use these with the previous estimate for $CA_\ell^I(s)$ to calculate $\Delta B_\ell^I(s)$;

(iv) on the n^{th} time through we use the values of $\Delta A_\ell^I(s)$ and $CB_\ell^I(s)$ from the n^{th} iteration and the value of $CA_\ell^I(s)$ from the $(n-1)^{th}$ iteration to calculate $\Delta B_\ell^I(s)$.

It should be noted that the n^{th} iteration for $CB_\ell^I(s)$ uses the value of $\Delta B_\ell^I(s)$ from the $(n-1)^{th}$ iteration for $C_\ell^I(s)$ and also the $(n-1)^{th}$ value of $ImB_\ell^I(s)$ when evaluating $L_\ell^I(s)$.

The unitarity condition for $F_\ell^I(t)$ requires that it has the same phase as the pion-pion amplitude for $4\mu^2 \leq t \leq 16\mu^2$. Then the quantity $F_\ell^I(t)\, D_\ell^I(t)$ where $D_\ell^I(t)$ has the phase exp $(-i\delta_\ell^I(\pi\pi \rightarrow \pi\pi))$ has the following singularities in the t-plane:

(i) the right-hand cut $16\mu^2 \leq t < \infty$;

(ii) the left-hand cut $-\infty < t \leq 0$.

We write the following once-subtracted dispersion relation for $F_\ell^I(t)$

$$D^I_l(t)\, F^I_l(t) = \frac{(t-t_o)}{\pi} \int_{-\infty}^{0} \frac{\mathrm{Im}F^I_l(t')\, D^I_l(t')\, dt'}{(t'-t)(t'-t_o)} + F^I_l(t_o) D^I_l(t_o), \tag{5.12}$$

where the right-hand cut is neglected, assuming that four-pion and other higher mass intermediate states contribute very little in the low-energy region. These small effects are absorbed into the subtraction constants which are:

(i) for $I = 0$ $l = 0$, $t_o = 0.5\mu^2$, and if we assume a linear off mass-shell extrapolation from the Adler zero (12) then we have $D^0_0(0.5\mu^2) = 0$;

(ii) for $I = 1$ $l = 1$, $t_o = 4\mu^2$ and hence $D^1_1(4\mu^2) = 0$ as this is at the physical $\pi\pi$ threshold.

On the left-hand cut the discontinuity is given by

$$\mathrm{Im}\, F^I_l(t) = -\int_{(m+\mu)^2}^{(p_-+q_-)^2} \frac{1}{8(p-q_-)^{l+1}} P_l\left(\frac{s'+p^2+q^2}{2pq}\right) \sum_{I'=\frac{1}{2}}^{3/2} \beta_{II'} \sum_{l'=0}^{l} (2l'+1) P_{l'}\left(1+\frac{t}{2k^2}\right) \mathrm{Im}\, A^{I'}_{l'}(s')\, ds' \tag{5.13}$$

where $(p_-)^2 = -p^2$ and $(q_-)^2 = -q^2$ as on the left-hand cut $t<0$.

Note that the Legendre expansion on the right-hand side is valid only for $t > -32\mu^2$, so the dispersion integral (5.12) is cut off at $t = -32\mu^2$ and the contribution of the rest of the left-hand cut absorbed into the subtraction terms. The sensitivity of our results to these subtraction terms is discussed later.

In order for us to be able physically to do the integrals we have to introduce a cut-off ($s = \Lambda$) in the left-hand cut integral. This is chosen to be $s = -32\mu^2$ as the Legendre expansion for

$A^I_l(s)$ is only valid up to this point. For $s < \Lambda$ we assume

$$\text{Im } B^I_l(s) = \text{Im } B^I_l(\Lambda)\,(s/\Lambda)^{\alpha}.$$

The results for the phase-shifts for $\sqrt{s} < 1.3$ GeV are insensitive to the precise value of Λ and α provided $\Lambda < -32\mu^2$ and $\alpha \leq 0$. For all the results quoted here $\alpha = 0$.

There are now four partial waves in the model and the amplitudes are calculated interatively as follows:

(i) we specify s_0 and from our sub-threshold models for πK and $\pi\pi$ we have predictions for $B^I_l(s_0)$, $P^I_l(s)$, $D^I_l(t)$;

(ii) for the first iteration we put $L^I_l(s) = 0 = C^I_l(s)$ and calculate $H(s)$, $H(s_0)$ and then calculate $B^I_l(s)$ from the cut-off point Λ to a point on the right-hand cut where we believe elastic unitarity still holds ($\sqrt{s} \approx 1.3$ GeV). This also gives a prediction for $B^I_l(s)$ on the circle cut;

(iii) use these values of $B^I_l(s)$ to get values of $A^I_l(s)$ between $-32\mu^2$ and $70\mu^2$ (1210 MeV^2);

(iv) use (5.13) to get $\text{Im}F^I_l(t)$ with t on the left-hand cut;

(v) use (5.12) to obtain a prediction for $\text{Im}F^I_l(t)$ with $t > 4\mu^2$;

(vi) with this new prediction for $\text{Im}F^I_l(t)$ we calculate $\text{Im}A^I_l(s)$ on the left-hand cut (5.8), and $\text{Re}A^I_l(s)$ on the left-hand cut comes from the dispersion relation (5.1). These then give a better estimate for $\text{Im}B^I_l(s)$ on the left-hand cut;

(vii) we obtain a new estimate for $\Delta A^I_l(s\pm)$ from $\text{Im}F^I_l(t)$ in (5.9) and using the estimate for $CB^I_l(s)$ from (5.1) we get a better estimate for $\Delta B^I_l(s)$ as previously explained;

(viii) now recalculate $B^I_l(s)$ with the improved estimates for $L^I_l(s)$ and $C^I_l(s)$;

(ix) go to (iii) and cycle to convergence.

This procedure is basically a generalisation of that used in the original application of the inverse amplitude method, and its convergence has been proved.

5.3 Sub-threshold amplitudes

In this section the π K isospin amplitudes are constructed from suitably crossing-symmetric polynomials in the usual s,t,u variables. Terms up to quadratic are included and the absence of prominent isospin $\frac{3}{2}$ resonances is incorporated in a conventional way. The polynomials are chosen so that amplitudes obey the Adler consistency condition (12). Also on mass-shell ρ dominance of the I = 1 ℓ = 1 $\pi\pi \to K\bar{K}$ amplitude imposes further constraints on the polynomials in terms of the ρ mass and width. Our final constraint equations come from using the second order current algebra results of Griffith (11) (Appendix D).

The conventional way to express the assumption that the isospin $\frac{3}{2}$ channel contains no resonances is to assert that the dependence of $A^{3/2}(s,t,u)$ on s as an independent variable may be neglected in comparison with its dependence on t and u. Then if we introduce a function H(t,u) (87) where

$$H(t,u) = a+bt+cu+dt^2+eu^2+ftu,$$

$$\text{then } A^{3/2}(s,t,u) = H(t,u). \tag{5.14}$$

The charge symmetry of A^+ and A^- (A39) requires

$$A^-(s,t,u) = H(t,s) - H(t,u), \tag{5.15}$$

with

$$A^{\frac{1}{2}}(s,t,u) = \tfrac{3}{2} H(t,s) - \tfrac{1}{2} H(t,u). \tag{5.16}$$

If we now invoke ρ dominance of A^- we can write (5.15) as

$$A^-(s,t,u) = \frac{g(s-u)}{M^2 - t} \tag{5.17}$$

where $M = m_\rho$ and g is the product of its $\pi\pi\pi$ and $K\bar{K}$ coupling constants.

By expanding (5.17) and equating its coefficients at $t = 0$ with those of (5.15) we have

$$c + e\Sigma = g/M^2, \tag{5.18}$$

$$f - e = g/M^4 \tag{5.19}$$

The coupling constant g is evaluated as follows:

We rewrite (5.17) as:

$$A^- = 6\left[\frac{2}{3}\ pqg\ \frac{1}{M^2-t}\right]\frac{s-u}{4\ pq},$$

$$= 2(2l+1)\left[\frac{2}{3}\ pqg\ \frac{1}{M^2-t}\right]P_l(\cos\varphi), \quad l=1 \tag{5.20}$$

and comparing with the amplitude for $\pi\pi \to \rho \to \pi\pi$ namely

$$6\left[\frac{2}{3}\ q^2\ \frac{\gamma_\rho^2}{8\pi}\ \frac{1}{M^2-t}\right]\frac{s-u}{4q^2},$$

$$= 2(2l+1)\left[\frac{2}{3}\ q^2\ \frac{\gamma_\rho^2}{8\pi}\ \frac{1}{M^2-t}\right]P_l(\cos\theta_t),\ l=1 \tag{5.21}$$

where γ_ρ is the $\rho\pi\pi$ coupling constant. Assuming universality of the ρ coupling (88) we see that at t=0 we obtain

$$g = \frac{\mu}{2m} \times \frac{\gamma_\rho^2}{4\pi} \tag{5.22}$$

The decay rate formula $$\Gamma = \frac{2z^3}{3M^2}\ \frac{\gamma_\rho^2}{4\pi} \tag{5.23}$$

where $4z^2 = (M^2 - 4\mu^2)$ leads to the numerical result $\gamma_\rho^2/4\pi = 2.3$ and thus

$$g = 0.32 \tag{5.24}$$

We obtain further constraints on our parameters by considering the results of Griffith (11) which have been discussed in Appendix D. Pion - PCAC implies that if $s = u = m^2$, $t = \mu^2$ then $A^{3/2}(s,t,u) = 0$

$$a+b\mu^2 + cm^2 + d\mu^4 + em^4 + f\mu^2m^2 = 0 \qquad (5.25)$$

Kaon-PCAC implies that if $s=u=\mu^2$, $t=m^2$ then $A^{3/2}(s,t,u) = 0$

$$a + bm^2 + c\mu^2 + dm^4 + e\mu^4 + f\mu^2 m^2 = 0 \qquad (5.26)$$

If we take two pions off-shell such that $s \to m^2 + 2p.q$, $t = 0$, $u \to m^2 - 2p.q$ then (D39 - D41) gives

$$a + cm^2 + em^4 = -\mu^2/f_\pi f_k\, 64\pi, \qquad (5.27)$$

$$2c + 4em^2 = 1/f_\pi^2 \pi\, 32 . \qquad (5.28)$$

If we take two kaons off-shell such that $s \to \mu^2 + 2p.q$, $t = 0$, $u \to \mu^2 - 2p.q$ then (D42 - D44) gives

$$a + c\mu^2 + e\mu^4 = -m^2/f\, f_k\, 64\pi, \qquad (5.29)$$

$$2c + 4e\mu^2 = -1/f^2_k\, 32\pi, \qquad (5.30)$$

and thus from (5.27) and (5.29) we have

$$\frac{a + cm^2 + em^4}{a + c\mu^2 + e\mu^4} = \frac{\mu 2}{m^2} \qquad (5.31)$$

If we project out the S-wave from $A^{3/2}(s,t,u)$ and define the scattering length $a_{3/2}$ as the value of the amplitude at threshold $(s = (m+\mu)^2)$ then we have

$$a_{3/2} = a + c(m-\mu)^2 + e(m-\mu)^4, \qquad (5.32)$$

and from (5.18) (5.31) (5.32) we have

$$e = (a_{3/2} + 2\mu mg/M^2) / 5m^2\mu^2, \qquad (5.33)$$

$$f = e + g/M^4 \qquad (5.19)$$

$$c = g/M^2 - e\Sigma \qquad (5.18)$$

$$a = a_{3/2} - c(m-\mu)^2 - e(m-\mu)^4, \qquad (5.32)$$

$$d = (c(\mu^4 - m^4) + e(\mu^6 - m^6) + (a+fm^2\mu^2)(\mu^2 - m^2))/(\mu^4 m^2 - m^4\mu^2), \quad (5.34)$$

$$b = -a - cm^2 - d\mu^4 - em^4 - fm^2\mu^2. \quad (5.35)$$

The model for the $\pi\pi \to \pi\pi$ amplitude in the region $4\mu^2 \leq t \leq 16\mu^2$ is given as follows:

Both amplitudes are made to obey elastic unitarity as $\mathrm{Im}\left[A^I_l(s)\right]^{-1} = -2k/\sqrt{s}$.

a) The $I = 0$ $l = 0$ amplitude is parameterised as an effective-range expansion for the σ resonance as

$$A^0_0(s) = 1/(1/a_0 + bk^2 + ck^4 + dk^6 - 2ik/\sqrt{s}), \quad (5.36)$$

where a_0 is the scattering length (= 0.16) and the other three parameters are evaluated by fixing where the phase-shift is 45°, 90° and 135° to give a σ resonance at 700 MeV with a width of 250 MeV.

b) The $I = 1$ $l = 1$ amplitude is assumed to be given by (2.39) with $a_1 = 0.035\mu^{-2}$, M = 765 MeV and Γ = 120 MeV.

5.4 Analyticity constraints and sum rules

Whilst the inverse amplidue method is a convenient way of implementing unitarity it does suffer from the two theoretical drawbacks that it may in fact lead to important violations of both crossing symmetry and unitarity. The discussion of these violations has been given in section (2.3).

We can minimize these violations by imposing constraints on our amplitudes. These crossing sum rules and analyticity constraints are generalisations of those given earlier by Roskies et al. (7) and by Martin et al. (5). We use the analyticity constraints as checks on our starting models for the iteration scheme to make sure they correspond to physical amplitudes (the crossing sum

rules are automatically satisfied); and then we use both sets of constraints to test the amplitudes we have generated and check that they correspond to a physical set of amplitudes.

In the rest of this section we firstly give the crossing sum rules and then the analyticity constraints, and finally discuss some phenomenological constraints.

Crossing sum rules

These have been derived by Basdevant (89) and are a generalisation of the $\pi\pi$ crossing sum rules derived by Roskies (7), although Basdevant also derives the $\pi\pi$ sum rules using a simpler technique that the polynomial expressions of Roskies.

If we denote $\int_{(m-\mu)^2}^{(m+\mu)^2} f(s)\,ds$ by $\langle f \rangle$ then the three sum rules which do not involve D-waves are:

$$\langle k^2 (A_0^{\frac{1}{2}} - A_0^{3/2}) \rangle = 0 \qquad (5.37)$$

$$\langle k^4 (A_0^{\frac{1}{2}} - A_0^{3/2}) \rangle = \langle k^4 (A_1^{\frac{1}{2}} - A_1^{3/2}) \rangle \qquad (5.38)$$

$$\langle k^2 (s - k^2 - m^2 - \mu^2)(A_0^{\frac{1}{2}} + 2A_0^{3/2}) \rangle = - \langle k^4 (A_1^{\frac{1}{2}} + 2A_1^{3/2}) \rangle \qquad (5.39)$$

Analyticity constraints

These have been derived by Ader et al. (90) using the earlier techniques developed by Martin (5). The ones which we use to test our model are the following:

$$a_{3/2} \geq F_0^0(0)/\sqrt{6} + \frac{3}{2} F_1^1(0), \qquad (5.40)$$

$$a_{\frac{1}{2}} \geq F_0^0(0)/\sqrt{6} - 3 F_1^1(0), \qquad (5.41)$$

$$\frac{d}{dt} F_0^0(t)\Big|_{t=0} \leq \frac{\sqrt{6}}{2} (a_1^{\frac{1}{2}} + 2a_1^{3/2}). \qquad (5.42)$$

If $m^2 - \mu^2 = X$, $(4\mu^2 - t)/(4m^2 - t) = P$ and $\int_0^{4\mu^2} F(t)dt = \langle F(t) \rangle$ then the other constraints are:

$$A_0^{3/2}(x) + 2A_0^{\frac{1}{2}}(x) \leq 3 \langle (F_0^0(t)/\sqrt{6} + \tfrac{3}{2} P F_1^1(t)) \rangle / 4\mu^2, \quad (5.43)$$

$$A_0^{3/2}(x) - A_1^{3/2}(x) + 2(A_0^{\frac{1}{2}}(x) - A_1^{\frac{1}{2}}(x)) \leq 3 \langle (F_0^0(t)/\sqrt{6} + \tfrac{3}{2} P F_1^1(t)) t \rangle / 8\mu^4, \quad (5.44)$$

$$(3\mu - 2m) A_0^{\frac{1}{2}}(x) + (6\mu + 2m) A_0^{3/2}(x) \leq 3 \langle (F_0^0(t) \sqrt{\tfrac{3}{2}} - 3m/\mu P F_1^1(t)) \rangle / 4\mu \quad (5.45)$$

$$(3\mu - 2m)(A_0^{\frac{1}{2}}(x) - A_1^{\frac{1}{2}}(x)) + (6\mu + 2m)(A_0^{3/2}(x) - A_1^{3/2}(x)) \leq 3 \langle (F_0^0(t) \sqrt{\tfrac{3}{2}} - 3m/\mu P F_1^1(t)) t \rangle / 8\mu^3. \quad (5.46)$$

In addition to the above constraints we also impose several phenomenological constraints (79 - 81, 83) on our amplitudes.

(i) both the P-waves have no zeros below threshold as the Adler zeros only manifest themselves in the S-waves. For the simple linear current algebra model of Griffith (11) this constraint is trivially satisfied but in our model it is non-trivial that the P-waves have no zeros below threshold, both on input and output from the iteration scheme.

(ii) the $I = \frac{1}{2}$ P-wave scattering length is forced to be positive as we know the $I = \frac{1}{2}$ $l = 1$ phase-shift is positive above threshold as this partial wave contains the K*(892) resonance;

(iii) the $I = \frac{3}{2}$ S-wave phase-shift is experimentally small and negative in the region we are interested in;

(iv) the $I = \frac{3}{2}$ P-wave is experimentally consistent with zero and a unitarized Veneziano model (18) predicts its value to be less than 5° up to 1.4 GeV.

5.5 Results

The subtraction-point s_0 is fixed at the value $15\mu^2$ in all but the $I = \frac{1}{2}$ P-wave where the K*(892) meson is inserted through a subtraction at $s_0 = m_{K^*}^2 = (892\ \text{MeV})^2$ with $B_1^{\frac{1}{2}}(m_{K^*}^2) = 0$.

The choice of subthreshold subtraction point is made well away from the physical branch point at $s = (m+\mu)^2 = 20.5\mu^2$. This is because in the $\pi\pi$ system a large $I = 0$ S-wave phase-shift near threshold can affect the adequacy of the polynomial model and lead to significant errors in an extrapolation to the S-wave thresholds. Choosing the subtraction well away from threshold then allows consistent solutions containing a large isoscalar interaction as well as the possibility of others. We believe a similar argument holds for πK scattering.

The range of values chosen for the one parameter in the model is $a_{3/2} = -0.08 \pm 0.03$ and for each value of this scattering length we require, both an input and output from the iteration

(i) the crossing sum rules (89) are satisfied;

(ii) the analyticity constraints are satisfied;

(iii) the iteration converges i.e. the amplitudes do not oscillate from one iteration to another but are stable and are in agreement within 20% at the end of the fifth iteration, and within 2% at the end of the tenth and final iteration;

(iv) the phenomenological constraints are satisfied.

We find the constraints and sum rules are not as difficult to satisfy as they were in the $\pi\pi \to \pi\pi$ model discussed earlier. This is because we have no constraints relating amplitudes above

threshold to those below threshold, and hence no positivity constraints on higher partial waves (in our case $\lambda \geq 2$) which were obtained in the $\pi\pi$ case via crossing.

We find we are able to satisfy all the constraints and sum rules for $-0.05 \geq a_{3/2} \geq -0.66$.

Current algebra predictions for the S-wave scattering lengths have been made by Cronin (85) ($a_{\frac{1}{2}} = 0.13 \pm 0.02$, $a_{3/2} = -0.07 \pm 0.01$) and by Griffith (11) ($a_{\frac{1}{2}} = 0.22$, $a_{3/2} = -0.11$). Lovelace (18) predicts $a_{\frac{1}{2}} = 0.21$ and $a_{3/2} = -0.097$ from his unitarised Veneziano model, while Moffat et al. (29) using a Regge pole model have $a_{\frac{1}{2}} = 0.15$ and $a_{3/2} = -0.06$ (note that we do not use his more recent results of 0.13 and -0.078 as this model gives wrong predictions for a_2 when applied to $\pi\pi$ scattering). These earlier predictions give no consistent predictions for $a_{3/2}$ and so we present our results as a band of predicted phase-shifts with the extremums given by $a_{3/2} = 0.055$ (when we predict $a_{\frac{1}{2}} = 0.16$) and $a_{3/2} = -0.066$ ($a_{\frac{1}{2}} = 0.17$). The phase-shifts are shown in figure (5.1).

The main features of the results are as follows:

(i) A large $I = \frac{3}{2}$ S-wave passing through 90^0 near 1100 MeV of the "down-up" type with a width between 180 and 220 MeV and in reasonable agreement with the experimental data discussed in chapter 4. This is in contrast with the results of Moffatt (29) and Lovelace (18) who assume the mass spectrum and are thus forced to have a resonance near the K*(892) and thus the only predictive power of such models in this energy region is for the width of the Even here there is a wide difference in their predictions with Moffat's solution being of the "down-up" type with a predicted width of 60MeV, while Lovelace's is more of the "up-down" type with a

width of 210 MeV. It should be noted that experiment predicts a narrow resonance (width $\approx$ 50 MeV) if the resonance position is near the K*(892) whilst predicting a broad resonance (width $>$ 150 MeV) if the amplitude resonates near 1100MeV.

(ii) The $I = \frac{3}{2}$ S-wave is small, negative and falls to about -3° to -5° at 1.2 GeV.

(iii) The $I = \frac{1}{2}$ P-wave resonates near the K*(892) mass and the predicted width is 30 - 40 MeV in reasonable agreement with the experimental value of 50 MeV. The scattering length is predicted to lie in the range $0.013\mu^{-2}$ - $0.015\mu^{-2}$.

(iv) The $I = \frac{3}{2}$ P-wave is negative ($a_1^{3/2}$ lies in the range $-0.003\mu^{-2}$ - $-0.005\mu^{-2}$) and is compatible with zero up to 1.2 GeV.

Our solutions are stable as can be seen from figure (5.1) and if we decrease the magnitude of $a_{3/2}$ by 15% the $\delta_0^{\frac{1}{2}}$ decreases by 20% at 1.2 GeV and $\left|\delta_0^{3/2}\right|$ decreases by 30% whilst the P-waves stay the same.

If we alter s_0 or $a_{3/2}$ so that $\delta_0^{\frac{1}{2}}$ decreases and becomes non-resonant then we find, in analogy with our $\pi\pi$ calculations, that $\left|\delta_0^{3/2}\right|$ increases e.g. these exist solutions (which are non-physical because either they do not satisfy the sum rules or the P-waves develop sub-threshold zeros) where $\delta_0^{\frac{1}{2}} = 65^{\circ}$ and $\delta_0^{3/2} = -62^{\circ}$ at 1.2 GeV.

All the solutions we investigated have zeros in $A_0^{\frac{1}{2}}$ and $A_0^{3/2}$ for $(m-\mu)^2 \leq s \leq (m+\mu)^2$ ($s_{\frac{1}{2}}$ and $s_{\frac{3}{2}}$ respectively). These may be identified as on-shell manifestations of the Adler zeros demanded by PCAC - not because they are at the positions given in the Griffith model (11) ($s_{\frac{1}{2}} \approx 11.95\mu^2$, $s_{\frac{3}{2}} \approx 13.45\mu^2$) but because they

satisfy the sum rule:

$$3\, s_{\frac{1}{2}} \;+\; 5\, s_{\frac{3}{2}} \;=\; 100\mu^2. \qquad (5.47)$$

This is a generalisation of the sum rule derived by Pennington and Pond (27) for $\pi\pi$ scattering. Note that this sum rule is not exact (even though the current algebra results satisfy it to 0.1%) as the ratio m/μ is irrational and the zeros even in the Griffith model are at irrational points. The sum rule is based on the quadratic extrapolation off-shell of our model, and thus contains the results of Griffith using linear extrapolation as a subset.

The actual zeros we predict lie close to the current algebra results and are:

$$s_{\frac{1}{2}} \;=\; 11.99\mu^2, \quad s_{\frac{3}{2}} \;=\; 13.34\mu^2. \qquad (5.48)$$

One of the main reasons for using a quadratic model is so that we are able to get a prediction for the ratio f_K/f_π which in all linear models is forced to be unity whereas experiment says the ratio is 1.18 ± 0.08. From equations (5.28) and (5.30) we have

$$\frac{c + 2em^2}{c + 2e\mu^2} \;=\; \frac{f_K^2}{f_\mu^2}$$

and for $a_{3/2} = -0.066$ this gives

$$f_K \;=\; 1.225\; f_\pi\,. \qquad (5.49)$$

Also from (5.30) we have

$$c + 2e\mu^2 \;=\; 1/64\pi f_K^2\,,$$

which gives $$f_K \;=\; 119 \text{ MeV}, \qquad (5.50)$$

and from (5.49) or (5.28) this gives

$$f_{\pi\pi} = 97 \text{ MeV}. \qquad (5.51)$$

The value for $f_{\pi\pi}$ is an agreement with experiment ($f_\pi \approx 95$ MeV) and the ratio f_K/f_π is in excellent agreement with that predicted recently by Wambach and Schulke (86) ($f_K/f_\pi = 1.23$) from PCAC corrections to K_{l3} decay.

Our predictions for f_K are very sensitive to the particular value of $a^{\cdot}_{3/2}$ chosen, and the above is the best solution. For $a^{\cdot}_{3/2} = -0.055$ we predict $f_K/f_\pi = 2.0$ with $f_{\pi\pi} = 98$ MeV and $f_K = 198$ MeV.

The amplitudes below threshold are shown in figure (5.2). We find the input and output amplitudes lie within 1% of each other and so only the input amplitudes are shown with $a^{\cdot}_{3/2} = -0.066$. It is perhaps not too surprising that the amplitudes agree with each other as the S-wave amplitudes are constrained to be equal at four points: the two thresholds $s = (m-\mu)^2$, $s = (m+\mu)^2$, the Adler point, and the subtraction point. The P-wave amplitudes are small below threshold and of course vanish at the two thresholds.

The left-hand cut contributions to the amplitude are small and stable. If we alter the behaviour on the distant left-hand cut by putting $\alpha = -1$ then this only alters the phase-shifts by less than 10%. If we also alter the $\pi\pi \to \pi\pi$ amplitudes used in the calculation of the t-channel amplitudes by, say, making the σ resonate at 500 MeV or putting $a_1 = 0.04\mu^{-2}$ then again the phase-shifts are altered by less than 10%.

We have assumed that elastic unitarity holds up to 1.2 GeV. Previous analyses indicate that they are small up to 1100 MeV (91) but in the K** (1420) region the inelasticity is known to be approximately 50% (92). We have also ignored the inelasticity in the $\pi\pi \to K\bar{K}$ amplitudes at the $K\bar{K}$ threshold when the $I = 0$ $l = 0$ $\pi\pi$ phase-shift rises from near 90^0 to near 180^0 in the region 950 - 990 MeV. This sharp behaviour is very difficult to impose on a smooth function (see chapter 2), but from our previous discussion we believe the effect in the $\pi K \to \pi K$ amplitudes would not be significant.

5.6 Conclusion

We have presented a sub-threshold model for πK scattering which is a generalisation of earlier current algebra models. We find the ratio f_K/f_π is in good agreement with experiment, and a sum rule for the on-shell manifestations of the Adler zeros is predicted. This sum rule, while it cannot be exact, should be obeyed to within 1% by all future linear and quadratic sub-threshold models for πK scattering.

We have extended these amplitudes above the physical πK threshold while at the same time making sure the left-hand cut and circle cut contributions are treated carefully. The amplitudes are also constrained to obey the analyticity and crossing constraints, both on input and output from the iteration procedure, and thus we may reasonably expect them to correspond to physical partial-wave amplitudes.

Inelastic effects have been ignored in both the s- and t-channels but we may reasonably expect them to be small up to 1200 MeV and the effects on the amplitudes to be correspondingly small and of the order of 10%.

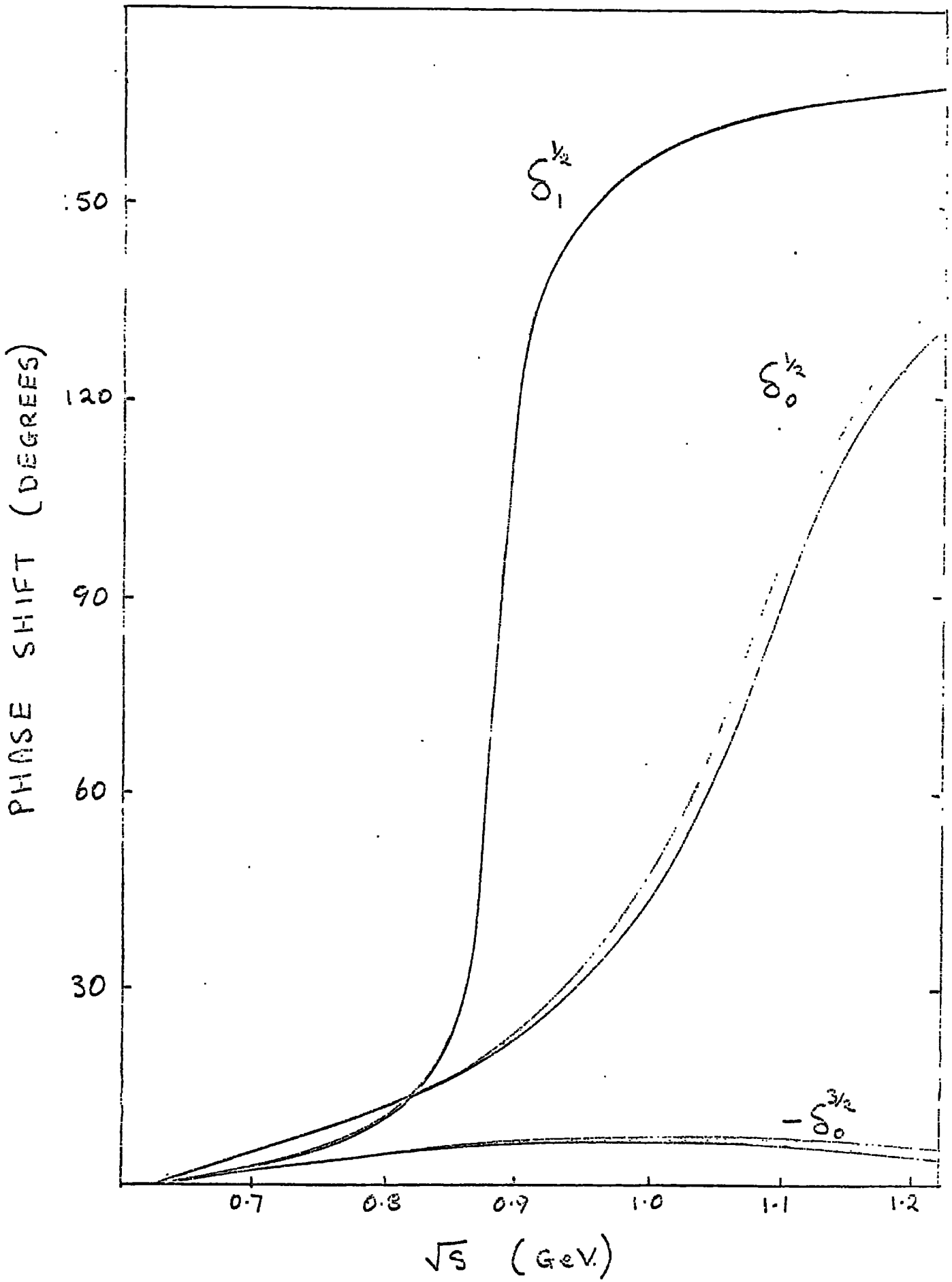

Fig. 5.I Range of solutions for S- and P- waves satisfying the constraints and sum rules .

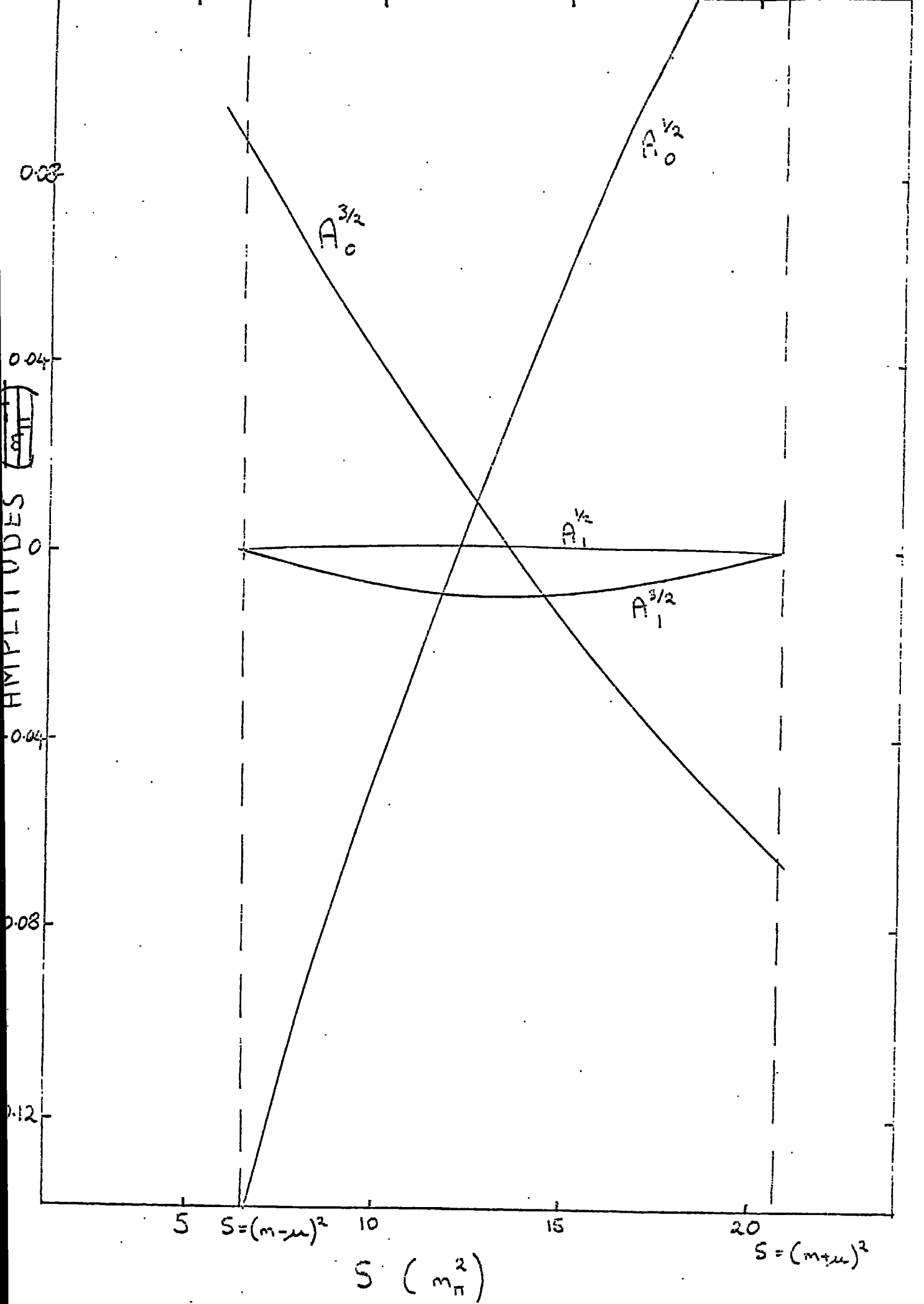

Fig. 5.2 Polynomial and calculated amplitudes in the sub-threshold region.

CHAPTER 6

THE PROBLEM OF THE η AND CONCLUDING REMARKS

We have seen that the ideas of current algebra plus ρ dominance of the $I = 1$ $l = 1$ partial-wave amplitude and the satisfaction of rigorous sum rules and analyticity constraints have led us to resonant $I = 0$ or $I = \frac{1}{2}$ S-waves for both $\pi\pi$ and πK scattering with particles σ (or ε) and κ resulting. Both of these new particles have $J^P = 0^+$ and it is interesting to consider them as members of the SU(3) 0^+ octet which is directly related to the SU(3) nonet of pseudoscalar mesons with $J^P = 0^-$. The obvious member of the 0^+ octet corresponding to the η would be the $\delta(962)$ as the strong decay

$$\delta \rightarrow \pi\eta$$

has been observed, with the $\pi_N(1016)$ then being interpreted as the $K\bar{K}$ decay mode of the $\delta(962)$.

The non-leptonic decay $\eta \rightarrow 3\pi$ could not be fitted quite as well as the $K \rightarrow 3\pi$ decay and we noted Sutherland's paradox (65) that if we assume a linear matrix element for the decay then current algebra predicts the decay is forbidden. Further evidence for the unusual behaviour of the η in the interaction of pseudoscalar mesons comes from considering the simplest Veneziano formula for $\pi\eta \rightarrow \pi\eta$ scattering which has the form

$$A(s,t,u) \propto V_{A_2 f}(s,t) + V_{A_2 A_2}(s,u) + V_{f A_2}(t,u), \qquad (6.1)$$

and which ensures correct signatures for the A_2 and f (degenerate with the ρ and ω). Imposing the Adler zero an each term in the usual way, whether in the soft-pion limit ($s = m_\eta^2 = u$, $t = \mu^2$), or in the soft-η limit ($s = \mu^2 = u$, $t = m_\eta^2$) gives

$$1 - \alpha_\rho(\mu^2) - \alpha_\rho(m_\eta^2) = 0, \qquad (6.2)$$

and thus from equation (1.8) $m_\eta = \mu$.

Much discussion has been devoted to this prediction and many cures have been proposed but nothing very satisfactory, has emerged.

In addition Osborn (94) has noticed that already at the soft - meson level amplitudes involving η's have a qualitatively different off-shell extrapolation from the ones for $\pi\pi$ and πK. The $\pi\eta \to \pi\eta$ amplitude is

$$A(s,t,u, q_1^2, p_1^2, q_2^2, p_2^2) = \frac{1}{3f_\eta^2} (s+t+u-3\mu^2 - \frac{(m_\eta^2 - \mu^2)}{m_\eta^2} (p_1^2 + p_2^2)), \quad (6.3)$$

where the q's and p's are pion and η momenta. Thus explicit dependence on the p's is indicated and if this is replaced by the on-shell value the Adler zero is not present (i.e. this new off-shell form is irrelevant for current algebra). Maybe therefore the off-shell extrapolation of equation (6.1) is quatitatively different from that of equations (D21) and (D45, D46). This would also be a solution to Sutherland's paradox.

In conclusion we have found that pions and kaons have a very similar structure above and below threshold with a similar extrapolation off-shell to the Adler zero; whilst the η, although being a member of the same SU(3) nonet and thus a priori we would expect it to have a similar structure, has a very different current algebra amplitude and hence any extrapolation off-shell may be dubious. It is thus very tentatively that we associate the $\delta(962)$ with the η in the same way as we have associated the σ and κ with the π and K respectively.

APPENDIX A

Kinematics.

We define the usual Mandelstam variables s,t,u by:

$$s = (p_1 + p_2)^2 = (p_3 + p_4)^2 \quad \text{(A1)}$$

$$t = (p_1 + p_3)^2 = (p_2 + p_4)^2 \quad \text{(A2)}$$

$$u = (p_1 + p_4)^2 = (p_2 + p_3)^2 \quad \text{(A3)}$$

where p_1, p_2, and $-p_3$, $-p_4$ denote the four-momenta of the initial and final particles respectively. Conservation of four-momenta requires that

$$s + t + u = \sum_{i=1}^{4} m_i^2 \quad \text{(A4)}$$

where m_i is the mass of the ith particle.

For $\pi\pi \to \pi\pi$ in terms of the three-momentum k and the centre of mass scattering angle θ_s we have in the s channel

$$\cos\theta_s = 1 + \frac{2t}{s - 4\mu^2} = -1 - \frac{2u}{s - 4\mu^2} \quad \text{(A5)}$$

$$4k^2 = s - 4\mu^2 \quad \text{(A6)}$$

where μ is the pion mass and the s channel physical region is $s \geq 4\mu^2$, $|\cos\theta_s| \leq 1$.

Similarly in the t channel we have:

$$\cos\theta_t = 1 + \frac{2s}{t-4\mu^2} = \frac{s - u}{t-4\mu^2} \quad \text{(A7)}$$

and in the u channel

$$\cos\theta_u = -1 - \frac{2s}{u - 4\mu^2} \quad \text{(A8)}$$

For $\pi K \to \pi K$ we define m to be the kaon mass and we have:

$$s = m^2 + \mu^2 + 2k^2 + 2\sqrt{(k^2 + m^2)(k^2 + \mu^2)} \quad (A9)$$

$$t = -2k^2 (1 - \cos\theta_s) \quad (A10)$$

$$u = 2m^2 + 2\mu^2 - s + 2k^2 (1 - \cos\theta_s) \quad (A11)$$

where now $k^2 = (s - (m + \mu)^2)(s - (m - \mu)^2)/4s$ (A12)

The final set of kinematics we will require is for the $K\bar{K}$ system where we have:

$$s = -p^2 - q^2 + 2pq \cos\varphi \quad (A13)$$

$$t = 2(p^2 + q^2 + m^2 + \mu^2) \quad (A14)$$

$$u = -p^2 - q^2 - 2pq \cos\varphi \quad (A15)$$

where $4p^2 = t - 4m^2$ (A16)

$$4q^2 = t - 4\mu^2 \quad (A17)$$

and φ is the centre of mass scattering angle and is given by

$$\cos\varphi = \frac{s-u}{4pq} \quad (A18)$$

and we define $\sum = 2m^2 + 2\mu^2$ (A19)

<u>$\pi\pi$ crossing matrix</u>

Since isospin is conserved and the three values I = 0, 1, 2 can occur we expect three independent invariant functions of s,t, and u. These can be conveniently written as:

$$A(s,t,u)\,\delta_{ab}\,\delta_{cd} + B(s,t,u)\,\delta_{ac}\,\delta_{bd} + C(s,t,u) \times \delta_{ad}\,\delta_{bc} \quad (A20)$$

where a, b, c, d are the isospin labels of the four external particles. Crossing symmetry leads at once to the relations

$$A(s,t,u) = B(t,s,u) = C(u,t,s) \qquad \text{(A21)}$$

$$B(s,t,u) = C(s,u,t)$$

The three isospin amplitudes are now given as:

$$A^0 = 3A + B + C \qquad \text{(A22)}$$

$$A^1 = B - C \qquad \text{(A23)}$$

$$A^2 = B + C \qquad \text{(A24)}$$

If we take $A^I(s,t,u)$ as the s channel isospin amplitudes then the t channel isospin amplitudes $A^I(t,s,u)$ are given by

$$A^I(t,s,u) = \sum_{I'=0}^{2} \beta_{II'} A^{I'}(s,t,u) \qquad \text{(A25)}$$

where the crossing matrix is:

$$\beta_{II'} = \begin{pmatrix} \frac{1}{3} & 1 & \frac{5}{3} \\ \frac{1}{3} & \frac{1}{2} & -\frac{5}{6} \\ \frac{1}{3} & -\frac{1}{2} & \frac{1}{6} \end{pmatrix} \qquad \text{(A26)}$$

and the u channel isospin amplitudes are given by

$$A^I(u,t,s) = \sum_{I'=0}^{2} (-1)^{I+I'} \beta_{II'} A^{I'}(s,t,u) \qquad \text{(A27)}$$

Partial wave amplitudes

The s channel partial wave amplitude for isospin I and angular momentum l, $A^I_l(s)$ is defined by

$$A^I_l(s) = \frac{1}{4} \int_{-1}^{+1} A^I(s,t)\, P_l(\cos\theta_s)\, d(\cos\theta_s) \qquad \text{(A28)}$$

and hence

$$A^I(s, \cos\theta_s) = 2 \sum_{l=0}^{\infty} (2l+1)\, P_l(\cos\theta_s)\, A^I_l(s) \qquad \text{(A29)}$$

We include the extra factor of "2" as from Bose statistics we must have $I + l$ even and hence we only have half the usual number of partial waves.

Unitarity for the partial wave amplitude can be expressed as:

$$\mathrm{Im}A_l^I(s) \geq \frac{2k}{\sqrt{s}} \left| A_l^I(s) \right|^2 \qquad \text{(A30)}$$

where the equality holds in the region of elastic scattering $4\mu^2 \leq s \leq 16\mu^2$. Alternatively we can express the amplitude as

$$A_l^I(s) = \frac{\sqrt{s}}{2ik} \left(\eta_l^I e^{2i\delta_l^I} - 1 \right) \qquad \text{(A31)}$$

where δ_l^I is the phase shift and η_l^I the inelasticity parameter. We note that for elastic scattering $\eta_l^I = 1$.

From the above expression (A31) we can now calculate the total, elastic, and inelastic cross-sections for each partial wave amplitude and we find:

$$\sigma_{\mathrm{TOT}}{}_l^I = 2\pi (2l+1) (1 - \eta_l^I \cos 2\delta_l^I)/k^2 \qquad \text{(A32)}$$

$$\sigma_{\mathrm{ELASTIC}}{}_l^I = \pi(2l+1) \left| \eta_l^I \exp(2\delta_l^I) - 1 \right|^2/k^2 \qquad \text{(A33)}$$

$$\sigma_{\mathrm{INEL}}{}_l^I = \pi(2l+1) (1 - (\eta_l^I)^2)/k^2 \qquad \text{(A34)}$$

<u>πK crossing matrices</u>

The scattering amplitude is defined by

$$S_{ab} = \delta_{ab} + i(2\pi)^4 8\pi \delta^4(p_b - p_a) A_{ab}/16 \times (P_{o1} P_{o2} P_{o3} P_{o4})^{\frac{1}{2}} \qquad \text{(A35)}$$

where in the isospin space of the kaon A_{ab} is given by

$$A_{ab} = \delta_{ab} A^+ + \tfrac{1}{2}\left[\tau_a, \tau_b\right] A^- \qquad \text{(A36)}$$

where τ_a, τ_b are Pauli spinor matrices.

Crossing requires that the same scattering amplitude $A_{\pm}(s,t,u)$ when continued to appropiate values of the variables s,t,u describes all the three channels.

$$\pi K \to \pi K \quad (s), \quad \pi\pi \to K\bar{K} \quad (t), \quad \pi\bar{K} \to \pi\bar{K} \quad (u)$$

The eigenstates of total isotopic spin $I = \frac{1}{2}, \frac{3}{2}$ in the s-channel are:

$$A^{\frac{1}{2}} = A^{+} + 2A^{-} \tag{A37}$$

$$A^{\frac{3}{2}} = A^{+} - A^{-} \tag{A38}$$

when two pions are exchanged from (A36) we have

$$A^{\pm}(s,t,u) = \pm A^{\pm}(u,s,t) \tag{A39}$$

and so the s-u crossing matrix is defined by

$$A^{I}(s,t,u) = \sum_{J'=\frac{1}{2}}^{3/2} \alpha_{IJ'} A^{J'}(u,t,s) \tag{A40}$$

where

$$\alpha_{IJ'} = \begin{pmatrix} -\frac{1}{3} & \frac{4}{3} \\ \frac{2}{3} & \frac{1}{3} \end{pmatrix} \tag{A41}$$

In the t channel the eigenstates of isospin are $I = 0$ or $I = 1$ where

$$F^{0} = \sqrt{6}A^{+} \tag{A42}$$

$$F^{1} = 2A^{-} \tag{A43}$$

and the t-s crossing matrix is defined by

$$F^{I}(t,s,u) = \sum_{I'=\frac{1}{2}}^{3/2} \beta_{IJ'} A^{I'}(s,t,u) \tag{A44}$$

with

$$\beta_{IJ'} = \begin{pmatrix} \frac{\sqrt{6}}{3} & \frac{2\sqrt{6}}{3} \\ \frac{2}{3} & -\frac{2}{3} \end{pmatrix} \tag{A45}$$

and we also introduce the s-t crossing matrix defined as

$$\gamma_{IJ'} = (\beta_{IJ'})^{-1} \tag{A46}$$

$$= \begin{pmatrix} \frac{1}{\sqrt{6}} & 1 \\ \frac{1}{\sqrt{6}} & -\frac{1}{2} \end{pmatrix}$$

Partial wave amplitudes

The t channel partial wave amplitudes are defined by

$$F^I_l(t) = \frac{1}{4(pq)^l} \int_{-1}^{1} F^I(t, \cos\phi)\, P_l(\cos\phi)\, d(\cos\phi) \qquad \text{(A47)}$$

and hence

$$F^I(t, \cos\phi) = 2 \sum_{l=0}^{\infty} (2l+1)\, P_l(\cos\phi)\, (pq)^l\, F^I_l(t) \qquad \text{(A48)}$$

and as we have Bose statistics $I + l$ is even for each partial wave amplitide.

APPENDIX B

Experiment

The spinless nature of pions and kaons makes them relatively easy to find experimentally but extracting $\pi\pi$ and πK amplitudes and phase shifts is very difficult as we do not have any pion targets, although with the new intersecting storage rings it is hoped we may soon observe $\pi\pi$ and πK interactions on their own. The experimental technique used at the moment is to make use of the pions that exist in the virtual meson cloud which surrounds the target proton. One assumes that the processes shown in figure (1.1) actually occur and these may be used to study $X\pi$ scattering where the beam particle X scatters on the virtual pion yielding

$$Xp \rightarrow X \pi^{+} n \qquad \text{(B1)}$$

$$Xp \rightarrow X \pi^{-} \Delta^{++} \qquad \text{(B2)}$$

and it is a crucial assumption of all $X\pi$ data that one pion exchange dominates the class of charge exchange reactions depicted in figure (1.1)

Goebel, Chew and Low (3) suggested that cross-sections for a beam particle scattering on a real pion may be extracted from observed differential cross-sections for pion production processes. In the suggested procedure the differential cross-section in t for the exchanged pion is analytically continued into the unphysical region to the value of t which corresponds to the mass of a real pion (with the usual metric $t = \mu^2$). Although this procedure has been refined over the years by putting in complicated form factors and absorptive terms the extrapolation is still subject to errors even with very accurate data near t=0.

The ambiguity in the phase shift for $\pi\pi \to \pi\pi$ comes from this experimental technique as values for the isospin zero S-wave phase shift δ_0^0 come from studying the S - P interference term in the reaction

$$\pi^- p \to n \pi^- \pi^+ \qquad \text{(B3)}$$

as in this reaction we measure (neglecting δ_0^2)

$$\sin \delta_1^1 \sin \delta_0^0 \cos (\delta_1^1 - \delta_0^0) \qquad \text{(B4)}$$

so that the ambiguity

$$\delta_0^0 \to \pi/2 + \delta_1^1 - \delta_0^0 \qquad \text{(B5)}$$

results which is the famous "up-down" ambiguity. In principle this ambiguity may be resolved by measuring all the interactions between the different charge states of the dipion system but as yet the data is not sufficiently good. The present experimental data for $\pi\pi \to \pi\pi$ is shown in figure (1.2) where the ambiguities can be clearly seen.

APPENDIX C

Analyticity constraints

The constraints are based on the following consequences of axiomatic field theory:

(i) Crossing symmetry.

(ii) Analyticity domain and the existence of fixed t dispersion relations for $-28\mu^2 \leq t \leq 4\mu^2$.

(iii) Convergence of partial wave expansions for the amplitude or its absorptive part in the Lehmann - Martin ellipse.

(iv) Asymptotic bounds e.g. Froissart bound.

(v) From (iv) there are at most two subtractions in fixed t dispersion relations for $-28\mu^2 \leq t \leq 4\mu^2$ and the Froissart - Gribov integral converges in that region for $\lambda \geq 2$.

We will derive below some of the earliest constraints found by Jin and Martin (5) as these illustrate some of the techniques used in deriving the more powerful constraints that have been discovered recently. From now on we will assume the usual metric and put $\mu^2 = 1$.

We consider the completely symmetric $\pi^0 \pi^0 \to \pi^0 \pi^0$ amplitude

$$F^{00}(s,t,u) = \tfrac{1}{3} A^0(s,t,u) + \tfrac{2}{3} A^2(s,t,u)$$

$$= A(s,t,u) + B(s,t,u) + C(s,t,u) \qquad (C1)$$

The S-wave is given by

$$f_0^{00}(s) = \frac{1}{s-4} \int_{4-s}^{0} F^{00}(s,t,u)\, dt \qquad (C2)$$

By crossing we have

$$F^{00}(4, 0, 0) = F^{00}(0,4,0) \qquad (C3)$$

and hence

$$f_0^{00}(4) = \sum_{l \text{ EVEN}}^{\infty} (2l+1)\, f_l^{00}(0) \qquad (C4)$$

for $0 \leq s \leq 4$ and $l \geq 2$ the Froissart - Gribov projection is

$$f_l^{00} = \frac{2}{4-s} \int_4^{\infty} Q_l\left(\frac{2t}{s-4} - 1\right) \mathrm{Im}\, F^{00}(s,t,u)\, dt \qquad (C5)$$

where Q_l is a Legendre function of the second kind.

Now $\mathrm{Im}F^{00}(s,t,u) > 0$ in this region because of unitarity and thus we have

$$f_l^{00}(s) \geq 0 \qquad l \geq 2 \qquad (C6)$$

and this gives the inequality

$$f_0^{00}(4) \geq f_0^{00}(0) \qquad (C7)$$

- - - - - - - - - - - - - - - -

At $s = 0$ (C2) gives

$$f_0^{00}(0) = \frac{1}{4} \int_0^4 F^{00}(0,t,4-t)\, dt \qquad (C8)$$

if we use $t \leftrightarrow u$ crossing we can rewrite this as

$$f^{00}(0) = \tfrac{1}{2} \int_2^4 F^{00}(0,t,4-t)\, dt \qquad (C9)$$

$$= \tfrac{1}{2} \int_2^4 \left(f_0^{00}(s) + \sum_{l=2}^{\infty} (2l+1)\, f_l^{00}(s)\right) ds \qquad (C10)$$

but from (C5) $f_l^{00} \geq 0$ for $l \geq 2$ and $|s| \leq 4$, and hence

$$f_0^{00}(0) \geq \tfrac{1}{2} \int_2^4 f_0^{00}(s)\, ds \qquad (C11)$$

- - - - - - - - - - - - - - - -

Now we change variables and consider the function $F^{00}(s, \cos\theta)$. This function is analytic in a cut plane with a positive discontinuity across the right hand cut. The Froissart-Gribov projection gives

$$F^{00}(s, \cos\theta) = f_0^{00}(s) + \frac{1}{\pi} \sum_{l \text{ EVEN} \geq 2}^{\infty} (2l+1)\, P_l(\cos\theta)$$

$$\times \int_{z_0}^{\infty} \mathrm{Im}\, F^{oo}(s,z)\, Q_\ell(z)\, dz \qquad (C12)$$

with $z_0 = 8/(s-4) - 1$. Using the Darboux - Christoffel formula

$$\sum_{\ell\ \mathrm{EVEN} \geq L} (2\ell+1)\, P_\ell(x)\, Q_\ell(z) = L\, \frac{zQ_{L-1}(z)P_L(x) - xP_{L-1}(x)Q_L(z)}{z^2 - x^2} \qquad (C13)$$

we get

$$F^{oo}(s\ \cos\theta) = f_o^{oo}(s) + \frac{2}{\pi} \times \int_{z_0}^{\infty} \frac{(zQ_1(z)\, P_2(c\cos\theta) - c\cos\theta\, P_1(c\cos\theta)\, Q_2(z))\mathrm{Im}F^{oo}(s,z)dz}{z^2 - \cos^2\theta} \qquad (C14)$$

for $\left|c\cos\theta\right| < \frac{1}{\sqrt{3}}$ we have $P_2(c\cos\theta) < 0$ and hence because of the positivity of $\mathrm{Im}\, F^{oo}(s,z)$ we have

$$F^{oo}(s, \cos\theta = \tfrac{1}{\sqrt{3}}) < f_o^{oo}(s) \qquad (C15)$$

and at s=0 $$F^{oo}(0,\ t = 2 + \tfrac{2}{\sqrt{3}}) < f_o^{oo}(0) \qquad (C16)$$

and hence the chain of inequalities

$$f_o^{oo}(0) > F(s=0,\ t = 2 + \tfrac{2}{\sqrt{3}}) > f_o^{oo}(2 + \tfrac{2}{\sqrt{3}}) \qquad (C17)$$

gives $$f_o^{oo}(0) > f_o^{oo}(2 + \tfrac{2}{\sqrt{3}}) \qquad (C18)$$

- - - - - - - - - - - -

(C12) can be rewritten as

$$F^{oo}(s,t,u) = f_o^{oo}(s) + \frac{1}{\pi} \int_4^{\infty} \mathrm{Im}F^{oo}(s,x,u) \left[\frac{1}{x-t} + \frac{1}{x-u} - \frac{2}{(4-s)} \log\left(\frac{x}{x+s-4}\right)\right] dx \qquad (C19)$$

This is crossing symmetric in $t \leftrightarrow u$ but not necessarily in $s \longleftrightarrow u$.

To do this we impose

$$\frac{d}{ds} F^{oo}(s,t,\ 4-s-t) = 0 \quad \text{for } s=u \text{ i.e. } t=4-2s \qquad (C20)$$

this gives $$\frac{d}{ds} f_o^{oo}(s) + \frac{1}{\pi}\int_4^\infty \frac{d}{ds}\, \mathrm{Im}F^{oo}(s,x,u)\left[\frac{1}{x-4+2s} + \frac{1}{x-s} - \frac{2}{4-s}\log\left(\frac{x}{x+s-4}\right)\right]dx$$

$$= \frac{-1}{\pi}\int_4^\infty \mathrm{Im}F^{oo}(s,x,u)\left[\frac{-1}{(x-s)^2} - \frac{2}{(4-s)^2}\log\left(\frac{x}{x+s-4}\right) + \frac{2}{(4-s)}\,\frac{1}{(x+s-4)}\right]dx \qquad (C21)$$

This is interesting in itself as it shows that knowledge of the absorptive part fixes the S-wave up to a constant.

The bracket in the first integral of (C21) is > 0 for $0 \leq s \leq 0.62$ (C.22)

The bracket in the second integral of (C21) is >0 for $0 \leq s \leq 1.6$ (C23)

from (C14) the bracket in the first integral of (C21) is <0 for $0.69 \leq s \leq 1.76$ (C24)

and it can be shown that the bracket in the second integral is < 0 for $1.7 < s < 4$ (C25)

From (C22 - C25) we conclude $\frac{df_o^{oo}}{ds}(s) > 0$ for $1.7 < s < 1.76$ (C26)

- - - - - - - - - - - -

As can be seen the derivation of these constraints soon becomes rather complicated and for the rest of this thesis any constraint will will be stated without proof.

Crossing sum rules

Necessary and sufficient conditions for a set of partial wave amplitudes to belong to a crossing symmetric amplitude have been obtained by Balachandran and Nuyts (6) and further exploited by Roskies et al. (7) and by Basdevant et al.(8). We will derive here

the five crossing sum rules relating just the S and P waves in scattering using the method of Basdevant et al. as with their technique it is easy to see how to generalize the results to π K scattering.

We denote by M^+ (M^-) an amplitude symmetric (antisymmetric) under s–u exchange. If we denote by g^+ (g^-) a polynomial in s, t, and u symmetric (antisymmetric) under s–u exchange and define these four functions in the Mandelstam triangle D $0 < s < 4\mu^2$ $0 < t < 4\mu^2$, $0 < u < 4\mu^2$ then we have:

$$\iint_D ds\ dt\ M^+(s,t,u)\ g^-(s,t,u) = 0 \qquad (C27)$$

$$\iint_D ds\ dt\ M^-(s,t,u)\ g^+(s,t,u) = 0 \qquad (C28)$$

In terms of the invariant amplitudes A, B, C and the s channel isospin amplitudes we can define

$$M^- = A(s,t,u) - C(s,t,u) = (2A^0 + 3A^1 - 5A^2)/6 \qquad (C29)$$

and

$$M^+ = A(s,t,u) + B(s,t,u) + C(s,t,u) = (A^0 + 2A^2)/3 \qquad (C30)$$

If we let g^- = s–u then we obtain the sum rule

$$\iint_D ds\ dt\ (s-u)\ (A^0 + 2A^2) = 0 \qquad (C31)$$

now $$s - u = s - (4-s- (1 - \cos\theta)(4-s)/2)$$

$$= \frac{3s - 4}{2} - \cos\theta\ \frac{(4-s)}{2} \qquad (C32)$$

with

$$dt = \frac{(4-s)}{2}\ d(\cos\theta) \equiv \frac{(4-s)}{2}\ dz \qquad (C33)$$

If we change the integration over t to an integration over $\cos\theta(z)$ the limits of the integration become –1 and +1

$$\int_0^4 ds \int_{-1}^{1} dz\ (4-s)\left(\frac{(3s-4)}{2} - z\frac{(4-s)}{2}\right)\ (A^0+2A^2) = 0 \qquad (C34)$$

projecting aut the partial waves from (C34) we get

$$\int_0^4 (3s-4)\ (4-s)\ (A_o^0(s) + 2A_o^2(s)\ )\ ds \quad = \quad 0 \qquad \text{(C35)}$$

- - - - - - - - - - - - - - - -

Using (C28) with $g^+ = 1$ we obtain

$$\iint_D ds\ \ dt\ (2A^0 - 5A^2 + 3A^1) \quad = \quad 0 \qquad \text{(C36)}$$

and this reduces to

$$\int_0^4 (4-s)\ (2A_o^0(s) - 5A_o^2(s))\ ds \quad = \quad 0 \qquad \text{(C37)}$$

- - - - - - - - - - - - - - - -

If we put $g^+ = t$ we now get

$$\int_0^4 ds \int_{-1}^{+1} dz\ (4-s)^2\ (1-z)\ (2A^0 - 5A^2 + 3A^1) = 0 \qquad \text{(C38)}$$

and this gives

$$\int_0^4 ds\ \ (4-s)^2\ (2A_o^0(s) - 5A_o^2(s)) = 3 \int_o^4 (4-s)^2\ A_1^1(s)\ ds \qquad \text{(C39)}$$

- - - - - - - - - - - - - - - -

If $g^+ = (s-u)^2 - t^2$ then this reduces to $(2s-4)^2 + 2t(2s-4)$ and we have

$$\int_0^4 ds \int_{-1}^{+1} dz(4-s)\ ((2s-4)^2+(2s-4)(4-s)(1-z))\ \times$$
$$(2A^0 - 5A^2 + 3A^1) \quad = \quad 0 \qquad \text{(C40)}$$

$$\int_0^4 ds\ (4-s)\ ((2s-4)^2 + (2s-4)(4-s))(2A_0^0 - 5A_0^2)$$
$$= \int_0^4 (4-s)^2\ 3A_1^1\ (2s-4)ds \qquad \text{(C41)}$$

$$\int_0^4 ds\ s(s-2)\ (4-s)\ (2A_0^0 - 5A_0^2) = \int_0^4 3(s-2)(4-s)^2\ A_1^1\ ds \qquad \text{(C42)}$$

From (C42) and (C39) we have

$$\int_0^4 s(4-s)^2\ (2A_0^0(s) - 5A_0^2(s)ds \quad = \quad -3 \int_o^4 s(4-s)^2 A_1^1(s)\ ds \qquad \text{(C43)}$$

- - - - - - - - - - - - - - - -

The fifth sum rule is obtained by making g^+ a fourth order symmetric combination of s and u, and then subtracting various powers of t to eliminate P- and D-waves, and finally reduces to

$$g^+ = 2s^2(4-s) - 2s(3s-4)t \qquad \text{(C44)}$$

which gives the sum rule:

$$\int_0^4 s(4-s)^3\ (2A_0^0(s) - 5A_0^2(s))ds = -3\int_0^4 s(4-s)^2(3s-4)\ A_1^1(s)ds \quad (C45)$$

- - - - - - - - - - - - - -

These crossing constraints are obviously necessary for crossing symmetry but it has been shown by obtaining the sum rules by expanding the amplitudes in terms of a complete set of functions that they are also sufficient conditions; and also a group theoretic derivation of their sufficiency has been given(9).

Note that as we go to higher partial waves the number of sum rules increases rapidly e.g. There are two sum rules for the S-wave alone, three for the S- and P-waves, but ten for S-, P- and D-waves.

APPENDIX D

Soft-meson theory

PCAC and the Adler condition

We consider an axial-vector $A_i^\mu(x)$ with Lorentz indices (μ=0, 1, 2, 3) and SU(3) indices i (i = 1, 8). The divergence D_i is given by

$$D_i(x) = \partial_\mu A_i^\mu(x) \tag{D1}$$

We do not consider the divergence of vector currents V_i as $\partial_\mu V_i^\mu = 0$ i.e. charge is conserved. If we now consider the fourier transformed quantities

$$D_i(q) = -iq_\mu A_i^\mu(q) \tag{D2}$$

and go to the rest frame then only the time component remains

$$D_i(q) = -iq_o A_i^o(q) \tag{D3}$$

But in the rest frame only spin zero particles can couple to the time component and hence the matrix element of D between two states $|a\rangle$ and $|b\rangle$ will have poles in q^2 whenever q^2 is equal to the mass of the meson which can couple. i.e. for i = 1, 2, 3 the pion pole will couple, and i = 4,5 will have the kaon pole.

The hypothesis that D_1, D_2, D_3 are dominated by the pion pole is called PCAC and explicitly is

$$\langle b \mid D_i(q) \mid a \rangle \approx f_\pi \frac{(\text{amp. for } a \to b + \pi)}{\mu^2 - q^2} \tag{D4}$$

where f_π is the decay amplitude for $\pi \to e\nu$

$$\langle 0 \mid \partial_\mu A_a^\mu(0) \mid \pi_{qb} \rangle = f_\pi \mu^2 \delta_{ab} (2q^o)^{-\frac{1}{2}} (2\pi)^{-3/2} \tag{D5}$$

We get a similar result for kaon PCAC

$$\langle 0 \mid \partial_\mu A_a^\mu(0) \mid K_{qb} \rangle = f_k m^2 \delta_{ab} (2q^o)^{-\frac{1}{2}} (2\pi)^{-3/2} \tag{D6}$$

The Adler consistency conditions follow simply from this as from D(2) we have

$$\langle b \mid D_i(q) \mid a \rangle \approx q_\mu \langle b \mid A_i^\mu(q) \mid a \rangle \qquad (D7)$$

and in the limit $q_\mu \to 0$, $\langle b \mid A_i^\mu(q) \mid a \rangle \not\to \infty$ as the dipion system foes not have any poles below threshold and we obtain

$$\lim_{q_\mu \to 0} \langle b \mid D_i(q) \mid a \rangle = 0 \qquad (D8)$$

then using (D4) we have

$$\text{amp. for } a \to b + \text{soft } \pi = 0 \qquad (D9)$$

Thus for any process where one or more of the external particles is a pion or kaon the whole amplitude must vanish when we take one of the mesons off mass-shell and put its four-momentum to zero.

The current algebra $\pi\pi$ and π K scattering amplitudes necessitate the introduction of a new scalar particle, the σ (or ε) meson. The existence of this particle was first proposed by Schwinger (13) as a way of interpreting the high mass of the muon, and further developed by Gell-Mann and Levy in their "σ-model" (14) to explain the Goldberger-Treiman relation for the rate of charged pion decay.

Weinberg's $\pi\pi$ model

We define the off-mass-shell invariant $\pi\pi$ amplitude $\langle f, qb \mid M \mid i, ka \rangle$ by

$$\iint d^4x d^4y \langle f \mid T\{ \partial_\mu A_b^\mu(x), \partial_\nu A_a^\nu(y) \} \mid i \rangle e^{-iqx} e^{iky}$$
$$= 2i\delta^4(p_f + q - p_i - k) \frac{f_\pi^2 \mu^4 \langle f, qb \mid M \mid i, ka \rangle}{(q^2 + \mu^2)(k^2 + \mu^2)(4E_i E_f)^{\frac{1}{2}}} \qquad (D10)$$

where k_μ, q_μ are the initial and final pion four-momenta, a and b are the initial and final pion isospin indices, i and f are the initial and final target particles, and the T bracket indicates a time ordered product.

Weinberg now proves a theorem that as q_μ and k_μ vanish

together the connected part of M approaches

$$\langle f,\ qb \mid M \mid i,\ ka \rangle \to M^{o}_{fb,\ ia} - \frac{p\cdot q}{16\mu\pi f_\pi^2} (T_\pi)_{ba} \cdot (T_t)_{fi}$$

$$+ \text{poles} + O(qq,\ qk,\ kk) \qquad \text{(D11)}$$

where M^o is a constant proportional to $\langle f \mid \sigma_{ab}(0) \mid i \rangle$ with $p_f = p_i = p$ and the "σ-term" is defined to be

$$i\,\sigma_{ab}(x)\,\delta^4(x-y) = \delta(x^o - y^o)\left[A^o_b(x),\ \partial_\mu A^\mu_a(y)\right] \qquad \text{(D12)}$$

and is assumed to be purely isoscalar (I=0). T_π and T_t are the pion and target isospin matrices with $(T_{\pi_c})_{ba} = i\varepsilon_{abc}$.

Crossing symmetry, isospin conservation and Bose statistics require that the expansion of the off mass-shell amplitude to second order in momenta is of the form

$$\langle ld,\ qb \mid M \mid pc,\ ka \rangle = \delta_{ab}\,\delta_{cd}\,(A + B(s+u) + Ct) +$$

$$\delta_{ad}\,\delta_{cb}\,(A + B(s+t) + Cu) + \delta_{ac}\,\delta_{bd}\,(A + B(u+t) + Cs) \qquad \text{(D13)}$$

with $\quad s = (p+k)^2,\ t = (k-q)^2,\ \quad u = (p-q)^2 \qquad \text{(D14)}$

The Adler condition shows that

$$A + \mu^2(2B + C) = 0 \qquad \text{(D15)}$$

When $q_\mu \to 0$ and $k_\mu \to 0$ we have $s \to \mu^2 + 2p\cdot q$ $\quad t \to 0$ $\quad u \to \mu^2 - 2p\cdot q$ with

$$\langle ld,\ qb \mid M \mid pc\ \ ka \rangle \to M^{o}_{db,\ ca} \frac{-p\cdot q}{16\mu\pi f_\pi^2}\ i\,\varepsilon_{abx}\ i\,\varepsilon_{cdx}$$

$$= M^{o}_{db,\ ca} - \frac{p\cdot q}{\mu 16\pi f_\pi^2}\ (\delta_{da}\,\delta_{bc} - \delta_{bd}\,\delta_{ac}) \qquad \text{(D16)}$$

thus equating the coefficient of $(p.q)$ in (D16) and (D13) we have

$$-B+C = 1/32\pi\mu f_\pi^2 \qquad \text{(D17)}$$

and also: $M^{o}_{db,\ ca} = \delta_{ab}\,\delta_{cd}\,(A + 2^2 B) + (\delta_{ad}\,\delta_{bc} + \delta_{bd}\,\delta_{ac})$

$$(A + \mu^2 C + \mu^2 B). \qquad \text{(D18)}$$

We want $M^{o}_{db,\ ca}$ to be an isoscalar and so only depend on $\delta_{ab}\,\delta_{cd}$ and thus

$$A + \mu^2 C + \mu^2 B = 0 \qquad \text{(D19)}$$

from (D15, 17, 19) we have $B = 0$, $A = -\mu^2 C$, $C = 1/32\pi\mu f_\pi^2$ (D20)

with $M_{db,\,ca} = (\delta_{ab}\delta_{cd}(t-\mu^2) + \delta_{ad}\delta_{cb}(u-\mu^2) + \delta_{ac}\delta_{bd}$

$(s-\mu^2)) / 32\pi\mu f_\pi^2$ (D21)

From (A20) the s-channel isospin amplitudes can now be defined

$$A^0(s,t,u) = (2s-\mu^2) / 32\pi\mu f_\pi^2 \quad \text{(D23)}$$

$$A^1(s,t,u) = (s-4\mu^2) / 96\pi\mu f_\pi^2 \quad \text{(D24)}$$

$$A^2(s,t,u) = (2\mu^2 - s) / 32\pi\mu f_\pi^2 \quad \text{(D25)}$$

The scattering lengths are defined as the following:

$$a_0 = A^0(s = 4\mu^2,\ t = 0,\ u = 0) \quad \text{(D26)}$$

$$a_1(s-4\mu^2)/4 = A^1(s=4\mu^2,\ t = 0,\ u = 0) \quad \text{(D27)}$$

$$a_2 = A^2(s = 4\mu^2,\ t = 0,\ u = 0) \quad \text{(D28)}$$

If we now define a quantity L by the Godlberger-Treiman relation

$$L = \mu/8\pi f_\pi^2 \quad \text{(D29)}$$

and put in the experimental value for $f_\pi = 95$MeV. then we have

$$L = 0.087\mu^{-1} \quad \text{(D30)}$$

with $a_0 = \frac{7L}{4} = .15\mu^{-1}$, $a_1 = \frac{L}{3^2} = .03\mu^{-3}$ $a_2 = -\frac{L}{2} = -.04\mu^{-1}$ (D31)

and the following sum rules:

$$2a_0 - 5a_2 = 18\mu^2 a_1 \quad \text{(D32)}$$

$$L = 3\mu^2 a_1 \quad \text{(D33)}$$

Griffith's K model

We consider the process:

$$\pi(q) + K(p) \rightarrow \pi(q') + K(p') \quad \text{(D34)}$$

and we define the s-channel isospin amplitudes in terms of t-channel amplitudes with definite charge parity $\pm$ by crossing (A37, 38). We write linear expansions for $A^{\pm}(s,t,u,\ q^2,\ q'^2,\ p^2,\ p'^2)$:

$$A^+ = A + B(s+u) + Ct + D(p^2 + p'^2) \quad \text{(D35)}$$

$$A^- = A'(s-u) \quad \text{(D36)}$$

and we now consider various low energy limitsfor $A_2^3(s,t,u,\ q^2\ q'^2,\ p^2,\ p'^2)$. $q \rightarrow 0$ or $q' \rightarrow 0$ (soft-pion Adler zeros)

$$A^{\frac{3}{2}}(m^2, \mu^2, m^2, 0, \mu^2, m^2, m^2) = 0 = A + 2m^2(B+D) + \mu^2 C \qquad (D37)$$

$p \to 0$ or $p' \to 0$ (soft-kaon Adler zeros)

$$A^{\frac{3}{2}}(\mu^2, m^2, \mu^2, \mu^2, \mu^2, 0, m^2) = 0 = A + 2\mu^2 B + m^2(C+D) \qquad (D38)$$

Using a generalization of the technique of Weinberg for the "σ term" we have a "π term" for π k scattering:

$q \to 0$ and $q' \to 0$ $\quad s \to m^2 + 2p.q$, $t \to 0$, $u \to m^2 - 2p.q$

$$A^{\frac{3}{2}}(m^2 + 2p.q, 0, m^2 - 2p.q, 0, 0, m^2, m^2) = A + 2m^2(B+D) + 4p.q\, A' \qquad (D39)$$

where
$$A + 2m^2(B+D) = -\mu^2/f_\pi f_k 64\pi\mu \qquad (D40)$$
$$A' = 1/128\pi\mu f_\pi^2 \qquad (D41)$$

Similarly when $p \to 0$ and $p' \to 0$ $\quad s \to \mu^2 + 2p.q$, $t \to 0$, $u \to \mu^2 - 2p.q$

$$A^{\frac{3}{2}}(\mu^2 + 2p.q, 0, \mu^2 - 2p.q, u^2, \mu^2, 0, 0) = A + 2B\mu^2 + 4p.qA' \qquad (D42)$$

where
$$A + 2B\mu^2 = -m^2/f_\pi f_k 64\pi\mu \qquad (D43)$$
$$A' = 1/128\pi\mu f_k^2 \qquad (D44)$$

From (D41, 44) $f_\pi = f_k = f$ and (D37 - 44) give

$$A = B = C/2 = 1/128\pi\mu f^2, \quad D=0, \quad A = (-m^2 - \mu^2)/64\pi\mu f^2$$

and this gives:

$$A^+ = (s+u+2t - 2m^2 - 2\mu^2)/128\pi\mu f^2 \qquad (D45)$$
$$A^- = (s-u)/128\pi\mu f^2 \qquad (D46)$$

and hence we finally obtain using (A37, 38)

$$A^{\frac{1}{2}}(s,t,u) = (3s+3t - 4m^2 - 4\mu^2)/128\pi\mu f^2 \qquad (D47)$$
$$A^{\frac{3}{2}}(s,t,u) = (2m^2 + 2\mu^2 - 2s)/128\pi\mu f^2 \qquad (D48)$$

The S-wave scattering lengths are defined to be the value of the amplitudes at the threshold $s = (m+\mu)^2$, $t = 0$, $u = (m-\mu)^2$ and hence
$$-2a3/2 = a_{\frac{1}{2}} = m\mu/16\pi\mu f^2 \qquad (D49)$$

and putting in the experimental value for $f = f_\pi = 95$ MeV. we have

$$-2a3/2 = a_{\frac{1}{2}} = 0.16\mu^{-1} \qquad (D50)$$

REFERENCES

(1) W. Heisenberg, Zeits. f. Physik 120, 513 (1943).

(2) A.D. Martin and T.D. Spearman, Phys. Rev. 136, B1480 (1964).

(3) C. Goebel, Phys. Rev. Letters 1, 337 (1958);
G.F. Chew and F.E. Low, Phys. Rev. 113, 1640 (1959).

(4) G.F. Chew and S. Mandelstam, Phys. Rev. 119, 467 (1960).

(5) A. Martin and Y.S. Jin, Phys. Rev. 135, B1369 (1964);
A. Martin, Nuovo Cimento 47A, 265 (1967).

(6) A.P. Balachandran and J. Nuyts, Phys. Rev. 172, 1821 (1968).

(7) R. Roskies, Nuovo Cimento 65A, 467 (1970).

(8) J.L. Basdevant, G. Cohen-Tannoudji and A. Morel, Nuovo Cimento 64A, 585 (1969).

(9) C.S. Cooper and M.R. Pennington, J. Math. Phys. 12, 1509 (1971).

(10) S. Weinberg, Phys. Rev. Letters 17, 616 (1966).

(11) R.W. Griffith, Phys. Rev. 176, 1705 (1968).

(12) S.L. Adler, Phys. Rev. 137, B1022 (1965);
Phys. Rev. 139, B1638 (1965).

(13) J. Schwinger, Ann. Phys. 2, 407 (1957).

(14) M. Gell-Mann and M. Levy, Nuovo Cimento 16, 705 (1960).

(15) G. Veneziano, Nuovo Cimento 57A, 190 (1968).

(16) C. Lovelace, Phys. Letters 28B, 264 (1968).

(17) S. Weinberg, Phys. Rev. Letters 18, 507 (1967);
M.I.T. preprint (1968).

(18) C. Lovelace, Proc. Conf. on $\pi\pi$ and $K\pi$ Interactions (Eds. F. Loeffler, E. Malamud) Argonne Report 1969, page 562.

(19) K. Kang, Lettere al Nuovo Cimento 3, 576 (1970);

K. Kang, M. Lacombe, R. Vinh Mau, Phys. Rev. D4, 3005 (1971);

R. Baier, H. Kuhnelt, F. Widder, Lettere al Nuovo Cimento 3, 594 (1970).

(20) Proc. Conf. on $\pi\pi$ and $K\pi$ Interactions (Eds. F. Loeffler, E. Malamud) Argonne Report (1969);

P.E. Schlein, Proc. International School of Subnuclear Physics (Ed.A. Zichichi) (1970).

(21) D. Morgan and J. Pisut, Springer Tracts in Modern Physics, Vol. 55 page 1 (Springer Verlag, Berlin, 1970);

J.L. Petersen, Phys. Reports 2C, 155 (1971).

(22) D. Atkinson, Nucl. Phys. B 7, 375 (1968); B8, 377 (1968); B13, 415 (1969);

J. Kupsch, Nucl. Phys. B11, 573 (1969); B12, 155 (1969); Nuovo Cimento 66A, 202 (1970).

(23) J.P. Dilley, Nucl. Phys. B25, 227 (1970).

(24) J. Iliopoulos, Nuovo Cimento 52A, 192 (1967).

(25) J.P. Ader, C. Meyers and B. Bonnier, Bordeaux Preprint PTB - 46 (1972).

G.F. Chew, S. Mandelstam and H.P. Noyes, Phys. Rev. 119, 478 (1960).

(27) P. Pennington and P. Pond, Nuovo Cimento 3A, 548 (1971).

(28) E.P. Tryon, Phys. Rev. D4, 1202; 1216; 1221; (1971).

(29) J.W. Moffat, Phys. Rev. D3, 1222 (1971);

P. Curry, I.O. Moen, J.W. Moffat and V.G. Snell, Phys. Rev. D3, 1233 (1971).

(30) J.B. Carrotte and R.C. Johnson Phys. Rev. D2, 1945 (1970); Ann. Phys (1972) in press.

(31) G. Wanders, Springer Tracts in Modern Physics, Vol. 57, page 22(Springer Verlag, Berlin, 1971).

(32) R. Arnowitt et al., Phys. Rev. Letters 20, 475 (1968);
C. Lovelace, ref. (18).

(33) R.C. Arnold, Phys. Rev.Letters 14, 657 (1965);
J. Finkelstein, Phys. Rev. Letters 22, 362 (1969).

(34) J.W. Moffat, Phys. Rev. 121,926 (1961).

(35) M.R. Pennington and P. Pond Lettere al. Nuovo Cimento 2, 1086 (1971).

The model of Brown and Goble ref. (55) also violates some of the five Roskies sum rules.

(36) A.K. Common, Nuovo Cimento 53A, 946 (1968).

(37) G. Auberson, O. Brander, G. Mahoux and A. Martin Nuovo Cimento 65A 743 (1970);
G. Auberson, Nuovo Cimento 68A, 281 (1970).

(38) M.R. Pennington, Nucl. Phys. B24, 317 (1970);
M.R. Pennington, and A.K. Common, University of Kent preprint (1971).

(39) H.C. Yen and R. Roskies, Phys. Rev. D4, 1873 (1971).

(40) R.C. Joynson and R.H. Graham, Phys. Rev. 188, 2362 (1969);
G. Auberson, O. Piguet and G. Wanders, Phys. Letters 28B, 41 (1968).

(41) Martin, ref. (5);

(41) Common, ref. (36);
Auberson, ref. (37).

(42) F. Widder, Universitat Graz Preprint (1971);
F. Widder and H. Kuhnelt, Universitat Graz preprint (1971).

(43) A. Wanders, Private Communication;
M.R. Pennington, Private Communication.

(44) L.J. Gutay, F.T. Meire and J.H. Scharenguivel, Phys. Rev. Letters 23, 431 (1969).

(45) D. Cline, K.J. Braun and V.R. Scherer, Nucl. Phys. B18, 77 (1970).

(46) M.G. Olsson, University of Wisconsin preprint COO - 270 (1970).

(47) D. Morgan and G. Shaw, Phys. Rev. D2, 520 (1970).

(48) M.G. Olsson, Phys. Rev. 162, 1338 (1967).

(49) M.G. Olsson, University of Wisconsin preprint COO - 282 (1970).

(50) R.C. Johnson, Nucl. Phys. B 23, 247 (1970).

(51) K. Kawarbayashi and M. Suzuki, Phys. Rev. Letters 16, 255 (1966);

Riazuddin and Fayyazuddin, Phys. Rev. 147, 1071 (1966).

(52) G. Shaw, Phys, Letters 28B, 44 (1968).

(53) T.F. Hoang, Nuovo Cimento 64A, 55 (1969).

(54) B.Y. Oh et al., Phys. Rev. Letters 23, 331 (1969).

(55) L.S. Brown and R.L. Goble, Phys. Rev. Letters 20, 346 (1968).

(56) J.C. Le Guillou, A. Morel and H. Navelet, Nuovo Cimento 5A, 659 (1971).

(57) S.M. Flatte et al., Phys. Letters 36B, 152(1971); 38B, 232 (1972).

(58) D. Morgan, Paper submitted to Bologna Conf. on Meson Resonances, (1971).

(59) J.P. Baton, G. Laurens and J. Reignier, Phys. Letters 33B, 528 (1970).

(60) J.S.M. Flatté, Paper presented at Bologna Conf. on Meson Resonances, (1971).

(61) H. Dietl, Paper presented at Bologna Conf. on Meson Resonances, (1971).

(62) G.W. Bennett and R.C. Johnson Phys. Letters 36B, 483 (1971).

(63) E.P. Tryon, Phys. Letters 38B, 527 (1972).

(64) B.R. Holstein, Phys. Rev. 183, 1228 (1969); and refs. therein.

(65) D.G. Sutherland, Phys. Letters 23, 384 (1966).

(66) S. Weinberg, Phys. Rev. Letters 4, 87 (1960).

(67) C. Kacser, Phys. Rev. 130, 355 (1963).

R. Arnowitt, M.H. Friedman, P. Nath and P.Pond Nuovo Cimento 4A, 765 (1971).

(68) P. Pond, Westfield College preprint (1971).

(69) P.G. Murray, Proc. Daresbury Study Weekend no.2 DNPL/R9, (1971).

(70) M.G. Albrow et al., Phys. Letters 33B, 516 (1970).

(71) C.D. Buchanan et al., Phys. Letters 33B, 623 (1970).

(72) W.T. Ford et al., Phys. Letters 38B, 335 (1972).

(73) T.S. Mast et al., Phys. Rev. 183, 1200 (1969).

(74) A.M. Cnops et al., Phys. Letters 27B, 113 (1968).

(75) Holstein, ref. (64)

Sutherland, ref. (65);

J.S. Bell and D.G.Sutherland, Nucl. Phys. B4, 315 (1968);

B.H. Kellett, Nucl. Phys. B21, 413 (1970).

(76) J.B. Carrotte, Lettere al Nuovo Cimento 2, 503 (1971).

(77) A. Neveu and J. Scherk, Orsay preprint (1969);

L.S. Brown and R.L. Goble, Unvversity of Washington preprint (1969).

(78) D.F. Greenberg, Phys. Rev. 184, 1934 (1969).

(79) T.G. Trippe et al., Phys. Letters 28B, 203 (1968).

(80) P. Antich et al., Nucl. Phys. B32, 381 (1971).

(81) H.H. Bingham et al., Nucl. Phys. B41, 1 (1972).

(82) L.J. Gutay et al., Phys. Rev. Letters 18, 142 (1967).

(83) H. Yuta et al., Phys. Rev. Letters 26, 1502 (1971).

(84) P.E. Schlein, Ref. (20).

(85) J.A. Cronin, Phys. Rev. 161, 1483 (1967).

(86)	L. Schulke and U.M. Wambach,	Ruhr Universitat, Bochum, preprint TP11/44 (1971);
	U.M. Wambach,	Ruhr Universitat, Bochum, preprint TP11/52 (1971).
(87)	R.C. Johnson,	J. Phys. A: Gen. Phys. 4, 883 (1971).
(88)	J.J. Sakurai,	Ann. Phys. 11, 1 (1960).
(89)	J.L. Basdevant et al.,	ref. (8).
(90)	J.P. Ader, A. Villani and A.H. Zimerman,	Nuovo Cimento 5A, 258 (1971).
(91)	P.E. Schlein,	Meson Spectroscopy (Eds. C. Baltay and A.H. Rosenfeld) pg. 161 (Benjamin, 1968).
(92)	M. Aguilar - Benitez et al.,	Phys. Rev. Letters 25, 1362 (1970).
(93)	M. Huq,	Nuovo Cimento 41A, 48 (1966).
(94)	H. Osborn,	Nucl. Phys. B15, 501 (1970).